Analysis of the Functional Role of Nucleoporin Nup214 in Nuclear Transport and Other Cellular Processes

Inauguraldissertation

zur Erlangung der Würde eines Doktors der Philosophie

vorgelegt der

Philosophisch-Naturwissenschaftlichen Fakultät

der Universität Basel

von

Sara Maria Paulillo

aus São Paulo, Brasilien

Basel, 2006

Genehmigt von der Philosophisch-Naturwissenschaftlichen Fakultät auf Antrag von

Prof. Dr. Ueli Aebi

PD Dr. Birthe Fahrenkrog

Prof. Dr. Olga Mayans

Prof. Dr. Urs Greber

Basel, den 21. November 2006

Prof. Dr. Hans-Peter Hauri

Dekan der Philosophisch-Naturwissenschaftlichen Fakultät

Copyright Declaration

I declare that I wrote this thesis, **Analysis of The Functional Role of Nucleoporin Nup214 in Nuclear Transport and Other Cellular Processes**, with the help indicated and only handed it into the Faculty of Science of the University of Basel and to no other faculty and no other university.

Sara Maria Paulillo

"The more I study nature, the more I stand amazed at the work of the Creator."

Louis Pasteur

Contents

List of Abbreviations

ABL1	v-abl Abelson murine leukemia viral oncogene homolog 1
Ad2	adenovirus type 2
AFM	atomic force microscope
AL	annulate lamellae
AML	acute myelogenous leukemia
ATL	adult T-cell leukemia
ATP	adenosine triphosphate
AUL	acute undifferentiated leukemia
BAPTA	(1,2-bis(o-aminophenoxy)ethane-N,N,N',N'-tetraacetic acid)
CAS	cellular apoptosis susceptibility protein
CML	chronic myelogenous leukemia
COPI	coatomer protein I
CRM1	chromosome region maintenance 1 protein
cryo-EM	cryo-electron microscopy
Da	Dalton
Dbp5	DEAD box protein 5
DDX10	DEAD (Asp-Glu-Ala-Asp) box polypeptide 10
DMEM	dulbecco's modified Eagle's medium
DNA	deoxyribonucleic acid
DRAQ	deep red anthraquinone
DTT	dithiothreitol
EDTA	ethylenediaminetetraacetic acid
EGTA	ethylene glycol tetraacetic acid
EM	electron microscope/y
FCS	fetal calf serum
FG	phenylalanine-glycine
GFP	green fluorescent protein
GlcNAc	N-acetylglucosamine
gp	glycoprotein
GTP	guanosine triphosphate
HEK-293	human embryonic kidney 293 cells
HeLa	Henrietta Lacks' cervical cancer cells
HEPES	4-(2-hydroxyethyl)-1-piperazineethanesulfonic acid
His	histidine
HIV	human immunodeficiency virus
HL-60	human acute myeloid leukemia cells
hnRNP	heterogeneous ribonucleoprotein
HOX	homeotic complex

IBB	importin-binding
IgG	immunoglobulin G
immuno-EM	immuno-electron microscopy
IPTG	isopropyl-β-D-thiogalactopyranoside
KCl	potassium chloride
LSB	low salt buffer
MAPK	mitogen-activated protein kinase
mbo	members only
MDS	myelodysplastic syndrome
MEM	minimum essential medium
$MgCl_2$	magnesium chloride
Mlp	myosin like protein
NAPs	nucleosome assembly proteins
NE	nuclear envelope
NEBD	nuclear envelope breakdown
NES	nuclear export signal
NF-kB	nuclear factor kappa B
NTA	nitrilotriacetic acid
NLS	nuclear localization signal
NPC	nuclear pore complex
NTD	N-terminal domain
NTF2	nuclear transport factor 2
Nup	nucleoporin
NXF1	nuclear RNA export factor 1
O-GlcNAc	O-linked beta-N-acetylglucosamine
PMSF	phenylmethylsulphonylfluoride
POT	protection of telomere
RanBP	Ran binding protein
RanGAP	Ran GTPase activating protein
RanGDP	Ran guanosine diphosphate (GDP)-bound form
RanGEF	Ran guanine nucleotide exchange factor
RanGTP	Ran guanosine triphosphate (GTP)-bound form
Rap1	repressor activator protein 1
RCC1	regulator of chromosome condensation
RNA	ribonucleic acid
RNP	ribonucleoprotein
Sal1	Sal-like 1
SDS-PAGE	sodium dodecyl sulfate polyacrylamide gel electrophoresis
SEM	scanning electron microscope
SERCA	sarco/endoplasmic reticulum Ca^{2+}-ATPase

Smad	mothers against decapentaplegic homolog
Stat	signal transducer and activator of transcription
SUMO	small ubiquitin-related modifier
SV	Simian vacuolating virus
T-ALL	T-cell acute lymphoblastic leukemia
TGF-β	transforming growth factor-β
TIN	TRF1-interacting nuclear factor 2
TNF-α	tumor necrosis factor-alpha
TOP1	topoisomerase (DNA) I
TPP1	tripeptyl-peptidase I precursor
TRF	telomere repeat-binding factor
TTP	tristetraprolin
Ubc9	ubiquitin-conjugating enzyme 9
ViPEr	visual programming environment
WGA	wheat germ agglutinin
WPP	tryptophan-proline-proline
XPO	exportin

List of Figures

List of Tables

Chapter 1. Introduction

The Nuclear Pore Complex from Higher Eukaryotes to Plants

The nuclear pore complex: from higher eukaryotes to plants

Sara M. Paulillo and Birthe Fahrenkrog*

M.E. Müller Institute for Structural Biology, Biozentrum, University of Basel, Klingelbergstrasse 70, 4056 Basel, Switzerland

*corresponding author: birthe.fahrenkrog@unibas.ch

Summary

Nuclear pore complexes (NPCs) provide the sole gateway between the cytoplasm and nucleus of eukaryotic cells and they act as mediator of all macromolecular exchange between these distinct subcellular compartments. Whereas the structure of the plant NPC has been studied already decades ago by distinct electron microscopy approaches, the characterization of its molecular components, the nucleoporins, has still remained largely elusive. In this review, we will focus on recent progress that has been made regarding the molecular composition of the plant NPC as well as on its role in nucleocytoplasmic transport and other processes, such as host-pathogen signaling in plants. In addition, we will discuss recent findings on the vertebrate nucleoporins that appear to be absent in the plant NPC and their implications in cell organization related processes and diseases.

1.1 Introduction

The nuclear envelope (NE) separates the cytoplasmic and nuclear compartments in eukaryotic cells. The double membrane of the NE, which is continuous with the endoplasmic reticulum, is perforated by nuclear pore complexes (NPCs). NPCs are large multi-protein complexes that facilitate bidirectional translocation of proteins, RNAs, and small molecules between the nucleus and the cytoplasm of eukaryotic cells (Fahrenkrog and Aebi 2003; Fahrenkrog et al. 2004). The NPC structure has been studied extensively by distinct electron microscopy (EM) and electron tomography approaches in a number of species, such as *Xenopus laevis* oocyte nuclei, *Saccharomyces cerevisiae*, *Caenorhabditis elegans, Dictyostelium discoideum* as well as plants (Franke 1970; Severs and Jordan 1975; Rout et al. 2000; Pante and Kann 2002; Fahrenkrog and Aebi 2003; Stoffler et al. 2003; Beck et al. 2004). Together these studies have revealed that the overall structure of the NPC is evolutionary conserved, although the linear dimensions of the NPC might vary from species to species. The main function of the NPC is mediating bidirectional trafficking and exchange of proteins, RNAs, and/or even large macromolecular complexes, such as ribosomes, between the nucleus and cytoplasm of eukaryotic cells and it is doing so with outstanding efficiency. Cargoes are delivered to and transported through the NPC by an interaction between transport receptors and nuclear pore complex proteins (nucleoporins) that are characterized by the presence of phenylalanine-glycine (FG) repeat regions (Fried and Kutay 2003; Pemberton and Paschal 2005). Directionality of nucleocytoplasmic transport pathways is thereby primarily regulated by the small GTPase Ran due to a chemical gradient of RanGTP between the nucleus and cytoplasm.

1.2 Nuclear pore complex structure

The NPC structure has been studied extensively and in detail by distinct EM and electron tomography studies in a variety of species (Franke 1970; Roberts and Northcote 1970; Severs and Jordan 1975; Hinshaw et al. 1992; Akey and Radermacher 1993; Goldberg and Allen 1993; Rout et al. 2000; Stoffler et al. 2003; Beck et al. 2004), which led to a consensus model of the 3D NPC architecture (Fig. 1.1). Accordingly, the NPC comprises an eight-fold symmetric central framework that is anchored in the NE, being continuous with the cytoplasmic as well as the nuclear ring moiety. From the cytoplasmic ring moiety, eight filaments emerge towards the cytoplasm, whereas the nuclear ring moiety anchors eight

filaments that join to a distal ring thereby forming the so-called nuclear basket. Enclosed by the central framework is the central pore, which has a depth of ~90 nm and a diameter of ~40 nm. The central pore mediates all trafficking between the nucleus and the cytoplasm and it enables transport of macromolecules with diameters of up to 39 nm (Pante and Kann 2002). A controversially discussed NPC feature is the nature of the central plug (Fahrenkrog and Aebi 2003; Fahrenkrog et al. 2004). Based on 2-D electron micrographs, the central plug was supposed to be situated within the central pore and to be a *bona fide* stationary component of the NPC (Stoffler et al. 1999). However, studies using atomic force microscopy (AFM) as well as cryo-EM have showed that the central plug most likely corresponds to cargo in transit through the central pore and/or the distal ring of the nuclear basket (Bustamante et al. 2000; Danker and Oberleithner 2000; Stoffler et al. 2003).

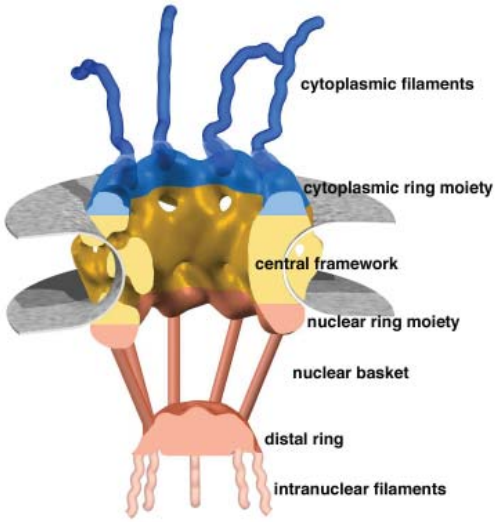

Figure 1.1: Schematic representation of the 3-D architecture of the nuclear pore complex (NPC). The NPC is composed of the central framework that is continuous with a cytoplasmic and a nuclear ring moiety. The cytoplasmic ring moiety is decorated by the cytoplasmic filaments, whereas the nuclear ring moiety is capped by a nuclear basket. This figure was modeled and prepared by D. Stoffler using ViPEr, a Visual Programming Environment, that was developed by D. Stoffler and M. Sanner at The Scripps Research Institute, La Jolla, California, USA. The model is based on a reconstruction of native NPCs embedded in thick amorphous ice (Stoffler et al. 2003) .

The overall 3D-structure of the NPC seems to be conserved in plants as well, as to be judged from thin-sectioning EM (Franke 1970; Roberts and Northcote 1970; Severs and Jordan 1975). However, high-resolution EM studies of the plant NPC architecture have yet to come. Based on thin-sectioning and freeze-fracture EM, the plant NPC exhibits the typical eightfold radial symmetry of the central framework, as well as the nuclear basket and cytoplasmic fibrils (Severs and Jordan 1975; Heese-Peck et al. 1995). In its linear dimensions, the plant NPC appears to be very close to *Xenopus* NPCs and as such about 15% larger than the yeast NPC (Roberts and Northcote 1970; Yang et al. 1998; Stoffler et al. 2003) (Fig. 1.2). However, some differences observed in linear dimensions might arise from different sample preparation techniques used.

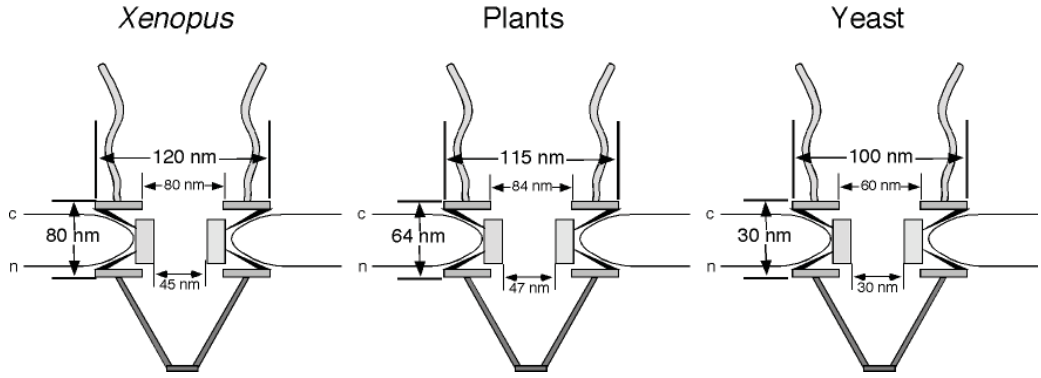

Figure 1.2: Schematic comparison of nuclear pore complex dimensions in *Xenopus* oocytes, plants and yeast.

1.3 The NPC molecular architecture

The NPC has a molecular mass of ~125 MDa in vertebrates and it is composed of about 30 different proteins called nucleoporins (Rout et al. 2000; Cronshaw et al. 2002). Due to the eightfold rotational symmetry of the central framework of the NPC (Maul 1971), nucleoporins are present in eight copies per NPC or in multiple of eight (Rout et al. 2000; Rabut et al. 2004). Immunogold-EM demonstrated that most of the nucleoporins are located on both, the nuclear and the cytoplasmic face of the NPC, whereas only a few locate to either the cytoplasmic or the nuclear face of the NPC (Rout et al. 2000). Based on secondary structure prediction, the symmetric nucleoporins have been grouped into three classes (Devos et al. 2006): nucleoporins belonging to the transmembrane group, which contains transmembrane α-helices and a cadherin-fold. These nucleoporins seem to form the outermost group of nucleoporins and are thought to help anchoring the NPC in the NE. The second class of symmetric nucleoporins comprises nucleoporins harboring the conserved sequence motif of FG-repeats in combination with a coiled-coil fold that may contribute to

the formation of the NPC's central framework. The third group of nucleoporins contain β-propeller and α-solenoid folds and these nucleoporins localize towards the inside of the NPC (Devos et al. 2006).

FG-repeat domains are found in about one third of the symmetric and asymmetric nucleoporins and they are thought to mediate the main interaction between soluble transport receptors and the NPC. Based on biophysical measurements, the FG-repeat domains of yeast nucleoporins were found to be natively unfolded, i.e. having no or only little secondary structure (Denning et al. 2002; Denning et al. 2003). This notion is further supported by immuno-EM studies on the two vertebrate FG-repeat nucleoporins Nup153 and Nup214 that showed that FG-repeat domains are flexible and mobile within the NPC (Fahrenkrog et al. 2002; Paulillo et al. 2005). AFM studies on recombinantly expressed FG-repeat domains of human Nup153 further revealed that this domain in fact is an extended molecule with a length of ~180 nm resembling an unfolded polypeptide chain (Lim and Aebi 2005). Moreover, the location of the FG-repeat domains of Nup153 and Nup214 is linked to the transport state of the NPC, further supporting their role in nucleocytoplasmic transport (Paulillo et al. 2005). However, systematic deletion of FG-repeat regions in yeast nucleoporins showed that yeast NPCs are able to compensate the loss of about 50% of their FG-repeats with only little effect on the efficiency of distinct nucleocytoplasmic transport pathways (Strawn et al. 2004; Zeitler and Weis 2004), indicating that FG-repeats are highly redundant within the NPC and/or that other interaction sites for transport receptors exist within the NPC.

1.4 Nucleoporin subcomplexes

Biochemical and genetic interactions among nucleoporins have shown that nucleoporins are often organized in subcomplexes that interact with each other to form the NPC. Much progress has been made in the past few years in elucidating the composition of distinct subcomplexes and their localization within the NPC (Fig. 1.3). How individual subcomplexes interact with each other to form the NPC, however, is only poorly understood. One well-studied and conserved subcomplex is the vertebrate Nup107-160 complex and its yeast homologue the Nup84p complex. The Nup107-160 complex is composed of nine nucleoporins and it resides on both sides of the central framework of the NPC (Belgareh et al. 2001; Krull et al. 2004). The Nup107-160 complex seems to represent the core element of the central framework, since depletion of any member of this NPC subcomplex in nuclear reconstitution assays led to the assembly of NPC-free nuclei, suggesting that the Nup107-160 complex is essential for NPC assembly (Harel et al. 2003; Walther et al. 2003). Nup155 and the pore membrane protein POM121 have been found to be essential for NE formation and NPC assembly as well (Antonin et al. 2005; Franz et al. 2005). Nup155 is part of a less

well-characterized NPC subcomplex that also localizes to both sides of the central framework (see (Lim 2006)). How the Nup107-160 complex and the Nup155 complex interact with each other to act in NPC assembly, however, remains to be elucidated.

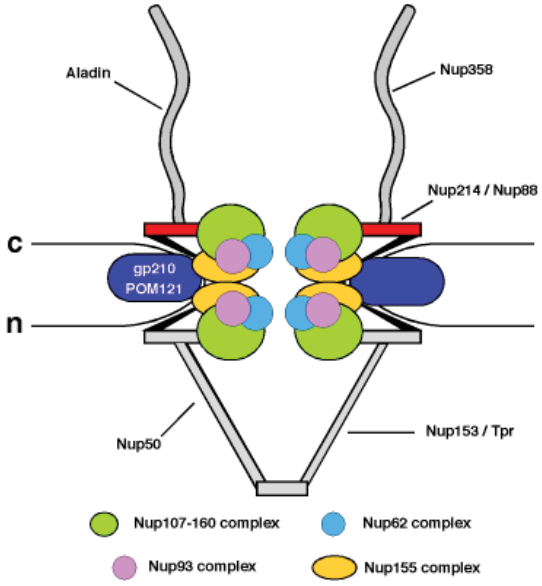

Figure 1.3: Schematic representation of nucleoporin and nucleoporin subcomplex localization within the vertebrate NPC. Nup107-160 complex: Nup107, Nup160, Nup133, Nup96, Nup75, Nup43, Nup37, Seh1, Sec 13; Nup155 complex: Nup155, Nup98, Nup170; Nup93 complex: Nup93, Nup205, Nup188, Nup35; Nup62 complex: Nup62, Nup58, Nup54, Nup45. c, cytoplasm; n, nucleus.

Another well-characterized subcomplex of the NPC is the Nup62 complex, which is composed of four nucleoporins (Dabauvalle et al. 1990; Finlay et al. 1991; Kita et al. 1993; Guan et al. 1995; Hu et al. 1996). All four nucleoporins of this subcomplex contain FG-repeats within their amino acid sequence and appear to be located near the central pore of the NPC, symmetrically on both sides (Guan et al. 1995). Therefore, this NPC subcomplex is thought to play a critical role in nuclear import as well as export (Hu et al. 1996; Levesque et al. 2006).

1.5 Vertebrate nucleoporins

1.5.1 Nup358

Nup358 (also named RanBP2) is a huge nucleoporin that is thought to be the major constituent of the cytoplasmic filaments of the NPCs (Yokoyama et al. 1995; Walther et al. 2002). Association of Nup358 with the NPC appears to be dependent on the presence of Nup214 and Nup88, since all three nucleoporins co-immunoprecipitated as a subcomplex. However, the absence of Nup358 did not affect the localization of Nup214 and Nup88 (Bernad et al. 2004).

Based on its primary sequence, Nup358 exhibits the most variable structural organization of all known nucleoporins: an N-terminal leucine-rich region, four potential Ran binding sites (i.e. Ran-binding protein 1 homologous domains) flanked by characteristic FXFG or FG repeats, eight zinc finger motifs of the Cys_2-Cys_2 type, and a C-terminal cyclophilin A domain (Wu et al. 1995). Due to the presence of FG-repeats within its amino acid sequence, Nup358 has been shown to provide binding sites for transport receptors of bulk mRNA export such as NXF1-p15, and the GTPase-activating protein for Ran, RanGAP1 (Saitoh et al. 1998; Bachi et al. 2000). Moreover, importin-β was also reported to associate with Nup358 in *Xenopus* egg extracts (Saitoh et al. 1996) and HeLa cell extracts (Chi et al. 1996). Finally, in addition to the binding sites provided by the FG-repeats of Nup358, its zinc fingers associate with high specificity to the nuclear export factor, exportin-1 (CRM1) (Singh et al. 1999).

During mitosis, Nup358 is located to both spindle microtubules and kinetochores, and the small ubiquitin-related modifier protein SUMO-1-dependent association of Nup358 with RanGAP1 guarantees proper kinetochore organization and function (Joseph et al. 2002; Salina et al. 2003; Joseph et al. 2004).

The interaction of Nup358 with RanGAP1 is modulated by the essential protein SUMO1 (Melchior 2000) and recent experiments have highlighted the involvement of Nup358 in the SUMOylation process (Pichler et al. 2002). Pichler et al. investigated SUMO1 intranuclear localization in order to elucidate the basis of SUMO1 modifications of targeted NLS-containing proteins and found that Nup358 has an E3 ligase-like activity (Pichler et al. 2002). Although the 30-kDa catalytic domain of Nup358 involved in SUMOylation does not contain the typical RING-finger motif and does not show homology to ubiquitin E3 ligases, this catalytic domain was reported to stably bind to Ubc9 (Ubiquitin-like protein SUMO-1 conjugating enzyme) (Pichler et al. 2004). It was recently demonstrated that Nup358 C-terminal domain can bind to SUMO-1 modified RanGAP1 and to Ubc9 simultaneously, indicating that Ubc9 could act to tether RanGAP1 to Nup358 (Matunis et al. 1998; Zhang

et al. 2002). Although SUMO modification is believed to be a predominantly nuclear event, SUMO modification and demodification of proteins can occur at the NPC (Zhang et al. 2002). These findings confer to Nup358 unexpected roles, such as SUMOylation of particular cargoes by a conjugation/deconjugation process of proteins during transport. Although SUMOylation may be mechanistically involved in the translocation of cargoes through the NPC, the E3 ligase activity of Nup358 remains unclear. Additional studies are needed to elucidate if Nup358 E3 activity is required for RanGAP1 SUMO conjugation, or if its action is merely restricted to maintain a stable complex at the NPC (Reverter and Lima 2005).

1.5.2 Nup153

Nup153, one of the most extensively studied nucleoporins in vertebrates, is asymmetrically located to the nucleoplasmic side of the NPC. The N-terminal domain of Nup153 comprises a M9-like nuclear localization signal (NLS), a RNA-binding domain and information for NPC targeting (Bastos et al. 1996; Enarson et al. 1998; Nakielny et al. 1999; Dimaano et al. 2001). Nup153's central domain contains four zinc fingers (of the Cys_2-Cys_2 type) that interacts with DNA, RanGDP and the COPI complex (Sukegawa and Blobel 1993; Nakielny et al. 1999; Liu et al. 2003). The C-terminal highly mobile FG-repeat domain of Nup153 binds to CRM1, transportin and importin-β (Sukegawa and Blobel 1993; Shah et al. 1998; Nakielny et al. 1999; Ben-Efraim and Gerace 2001; Denning et al. 2003).

Immuno-EM studies of the vertebrate nucleoporin Nup153 indicated that its N-terminal domain is anchored to the nuclear rim of the NPC, whereas its zinc-finger domain was found at the distal ring (Fahrenkrog et al. 2002). The Nup 153 C-terminal domain topology demonstrated a high degree of mobility and structural flexibility, since this epitope could be detected at the nuclear basket and near or at the cytoplasmic ring of the NPC (Fahrenkrog et al. 2002). Several interacting partners were attributed to Nup153, among which are protein and RNA transport receptors, transcription factors, cellular regulation proteins and proteases, DNA, RNA, the Nup107-160 complex and Tpr, lamin B, and the membrane-remodeling complex, COPI (reviewed in (Ball and Ullman 2005)).

Three members of the COPI coatomer complex (β, β' and α) were reported to specifically associate with Nup153's zinc finger region (Liu et al. 2003) as well as with the zinc finger domain of Nup358 (Prunuske et al. 2006). The interaction of Nup153 and COPI plays a role in the division of eukaryotic cells leading to nuclear envelope disassembly in a stepwise process. This process known as nuclear envelope breakdown (NEBD) involves dispersal of the nuclear membrane as well as disassemble of the NPCs, which break into small subunits (Prunuske et al. 2006). Nup153, in turn, is an active modulator of this process, although

more careful mechanistic studies are still needed in order to elucidate COPI recruitment of Nup153 zinc fingers (Prunuske et al. 2006).

1.5.3 Nup88

Nup88 is a nucleoporin found in a subcomplex with the oncogenic nucleoporin Nup214 at the cytoplasmic face of the NPC. Nup88 was found to be highly overexpressed in distinct aggressive human tumours, which typically show a high degree of metastasis (Martinez et al. 1999; Gould et al. 2000; Agudo et al. 2004).

Uv et al. reported that the *Drosophila* homologue of the mammalian Nup88, named members only (*mbo*), might regulate the nuclear translocation of the Rel family transcription factors Dorsal and Dif (Uv et al. 2000). The selective requirement of DNup88, however, does not affect the nuclear transport of several other proteins and RNA export (Uv et al. 2000).

Further studies on the defect in nuclear accumulation of Rel proteins in *Drosophila* revealed that the continuous shuttling in and out of the nucleus requires DCRM1. Moreover, Nup88 was described to tether CRM1 to the NPC and therefore is assumed as a nuclear export attenuator for NES-mediated nuclear export (Roth et al. 2003). Finally, a recent article by Samakovlis and co-workers claims that the concentration levels of Nup88 in complex with Nup214 control CRM1 recruitment to the NPC (Xylourgidis et al. 2006).

Nup88 is also involved in the regulation of human huntingtin transport, the major determinant protein of Huntington's neurodegenerative disorder (Takano and Gusella 2002). Interestingly, the NF-kB/Rel/dorsal family of transcription factors are candidates for association with huntingtin to form complexes for its nuclear import, which is Nup88-dependent (Takano and Gusella 2002), suggesting that Nup88 alone (or in complex with Nup214) plays a transport-independent role in such diseases.

1.5.4 Nup214

1.5.4.1 Structural characteristics, organization and interacting partners

The vertebrate nucleoporin Nup214 is another component of the NPC's cytoplasmic face, more specifically located at the cytoplasmic ring moiety of the NPC. It has been

previously shown that Nup 214 and Nup88 form a stable complex (Bastos et al. 1997; Fornerod et al. 1997; Matsuoka et al. 1999), which is required for the docking of Nup214 to the NPC (Roth et al. 2003; Bernad et al. 2004).

Based on its amino acid sequence, Nup214 is organized in three distinct domains: (i) an N-terminal domain, which is predicted to be organized into a β-propeller fold similarly to its yeast homologue Nup159p (Weirich et al. 2004) and which carries a WD40 domain, (ii) a central domain that contains a leucine zipper motif and two predicted coiled-coil segments and (iii) a C-terminal domain that harbors 6 FxFG motifs and 36 FG dipeptid motifs (Fornerod et al. 1995).

Dbp5, a DEAD box helicase involved in mRNA transport, was found to interact with the N-terminal domain of Nup214. Izaurralde and co-workers showed that hDbp5 is recruited to the NPC via a conserved and stable interaction with Nup214 (Schmitt et al. 1999). Moreover, mutated hDbp5 was microinjected into *Xenopus* nuclei, which resulted in a inhibition of nuclear exit of mRNAs (Schmitt et al. 1999). When part of the N-terminal domain of Nup214's yeast homologue Nup159p is deleted, polyadenylated RNA accumulates in the yeast nuclei and growth becomes temperature-sensitive (Del Priore et al. 1997). This indicates that the N-terminal domain of Nup159p is required for Dbp5 docking to the NPC, but an overexpression of Dbp5 can compensate the absence of the N-terminus of Nup159p (Weirich et al. 2004). Although the means by which the complex Dbp5-Nup159 is formed is not known, two possible non-mutually exclusive models were presented. First, the N-terminal domain of Nup159p might be involved in Dbp5p nuclear import, and, second, Nup159p N-terminal domain is required for Dbp5 release from cytoplasmic RNAs (Weirich et al. 2004).

Although the sequence similarity between Nup214 and Nup159p is quite low, they might be functional homologues, and FG repeat motifs serve as docking sites for different cargoes. The export receptor for leucine-rich nuclear export signals hCRM1 binds to Nup214 FG-repeat domain to form a stable complex, which localizes to the NE. The docking of CRM1 to the NE by Nup214 acts as a terminal-binding site in NES-dependent hCRM1-mediated nuclear export (Fornerod et al. 1996; Bernad et al. 2004). In this context, Nup214 is involved in the disassembly of CRM1 export complex as well as CRM1 recycling (Askjaer et al. 1999). It was proposed in earlier studies that the stable association of Nup214 and CRM1 might be efficiently released in a terminal step of export by an interaction with RanBP1 (Ran Binding Protein 1) and/or with Ran binding domains of Nup358 (Kehlenbach et al. 1999). Further studies, however, revealed RanGAP as the candidate to act catalytically in the release of export complexes from Nup214 (Hutten and Kehlenbach 2006).

Although the release of CRM1 from Nup214 in the final steps of nuclear export is

still unclear, the formation of a very stable complex containing Nup214, CRM1, RanGTP, and an export substrate is central to CRM1-mediated nuclear export (Hutten and Kehlenbach 2006). Thus, the role of Nup214 in CRM1-mediated transport is specific and essential for proper export of cargoes.

Some of Nup214-CRM1 transport mediated processes include the shuttling of the unphosphorylated signal transducer and activator of transcription factor, Stat1 between the nucleus and cytoplasm and the export of the HIV Rev protein in human cells (Zolotukhin and Felber 1999; Marg et al. 2004). Nup214 is also target for the export factor TAP, which plays a role in the export of viral RNAs, and may bridge the interaction between specific RNP export substrates and the NPC (Katahira et al. 1999; Bachi et al. 2000).

Similarly to the export factor TAP, Smad transcription factors bear hydrophobic patches in their C-terminal domain, referred to as the "hydrophobic corridor" which are recognized by FG-repeat nucleoporins such as Nup214 (Xu et al. 2002; Xu et al. 2003). Smad proteins are transcription factors that act as mediators of the TGF-β (transforming growth factor-β) receptor signals. It was shown that Nup214 associates with various members of the Smad family, such as Smad2, Smad3 and Smad4 (Xu et al. 2002; Xu et al. 2003). The export of the transcription factor Smad4 is CRM1 mediated, whereas the FG-repeat domain of the nucleoporins Nup214 and Nup153 are able to interact in a karyopherin-independent manner with Smad transcription factors (Xu et al. 2003). Interestingly, the direct contact of Smad4 with FG-containing nucleoporins appears to happen via a domain distinct from the hydrophobic corridor in Smad2 and Smad3 (Xu et al. 2003).

Matsubayashi et al. reported a distinct pathway for nuclear import of MAPK (Mitogen-Activated Protein Kinase), in which MAPK is able to bind directly to the FG-repeat region of Nup214. Similarly, the zinc finger-containing protein tristetraprolin (TTP), which is implicated in the regulation of TNF-α (Tumor Necrosis Factor-α) production in mice, was shown to directly bind the FG-repeats of Nup214 (Matsubayashi et al. 2001; Carman and Nadler 2004). These importin-β-independent interactions might play a role in the regulation of protein localization in the cell.

During cell cycle Nup214 is posttranslationally modified by *O*-linked *N*-acetylglucosamines (*O*-Glc*N*Ac) at levels that remain constant, whereas its phosphorylation occurs during mitosis (Macaulay et al. 1995; Miller et al. 1999). NPCs devoid of N-acetylglucosamine-bearing nucleoporins show normal morphology, but are defective for import of a reporter substrate carrying an NLS (Finlay and Forbes 1990). The function and regulation of glycosylation and phosphorylation of nucleoporins has remained largely elusive.

1.5.4.2 Nup214 and leukemia

Nup214 as well as its associated nucleoporin Nup88 are vastly related to or directly implicated in cancer. Nup214 was initially identified in a chromosomal translocation product associated with a subtype of acute myeloid leukemia (von Lindern et al. 1992).

In these translocations (see Table 1.1), the C-terminal domain of Nup214, except its last six amino acids, is fused to the SET protein (von Lindern et al. 1992).

Human *SET* encodes a 39 kDa predominantly nuclear phosphoprotein, which shows a high homology to the nucleosome assembly proteins (NAPs) that play a role in chromatin remodeling (von Lindern et al. 1992; Adachi et al. 1994; Miyaji-Yamaguchi et al. 1999). SET was also reported to interact with several other proteins, suggesting a role in mRNA stabilization, chromosome remodeling, apoptosis, cell cycle and transcriptional regulation (Li et al. 1996; Estanyol et al. 1999; Compagnone et al. 2000; Morita et al. 2000; Canela et al. 2003; Fan et al. 2003).

Genes	Translocations	Leukemias
DEK	t(6;9)(p23;q34)	AML
SET	t(9;9)(q34;q34)	AUL
ABL1	Episomal amplicon	T-ALL

Table 1.1. Nup214 translocations in leukemia. AUL, acute undifferentiated leukemia; AML, acute myelogenous leukemia; T-ALL, T-cell acute lymphoblastic leukemia.

SET is present in the same chromosomal region as Nup214 and the resulting product of the *SET-NUP214* translocation is a chimeric protein of 155 kDa. A forced expression of SET and SET-Nup214 inhibits cell proliferation, induces differentiation and subsequently, cell cycle arrest in the human U937T promonocytic cell line (Boer et al. 1998; Kandilci et al. 2004). Overexpression of SET-Nup214 in human cells disrupted the nuclear export of

NES-proteins, suggesting that SET-Nup214 causes aberrant localization of hCRM1 (Saito et al. 2004).

The human DEK is a phosphoprotein (Fornerod et al. 1995) with several phosphorylation sites of which most are clustered in the carboxy-terminal region (Kappes et al. 2004) and the great majority of DEK is bound to chromatin (Kappes et al. 2001). DEK-Nup214 fusion proteins were discovered in patients with AML, which subtype is characterized by a specific (6;9) (p23;q34) chromosomal translocation. This chromosomal translocation results in most of the DEK coding sequence being fused to a C-terminal fragment of NUP214 (von Lindern et al., 1990). Overexpression of DEK-Nup214 in myeloid precursor cells, resulted in cell cycle arrest (Boer et al. 1998). Moreover, Nup214 overexpression arrests cells in G_0 and its depletion leads to cell cycle arrest in G_2, undeniably indicating that Nup214 is essential for proper cell cycle progression (Boer et al. 1998).

DEK and SET do not show any sequence similarities except that they both contain highly acidic regions and coiled-coil domains (Miyaji-Yamaguchi et al. 1999; Hussey and Dobrovic 2002). However, the nature of DEK-NUP214 translocation is very similar to the one found in SET-NUP214 translocation, where both complete sequences are fused to the C-terminal domain of Nup214, which associates with hCRM1 (von Lindern et al. 1992; Fornerod et al. 1995; Fornerod et al. 1996). Moreover, the central region of Nup214 seems to be partially lost, since these fusion proteins failed to associate with Nup88 (Fornerod et al. 1996).

DEK-Nup214 and SET-Nup214 were reported to localize exclusively in the nucleus, which resulted in a relocation of the carboxyterminal domain of Nup214 from the NPC to the nucleoplasm (Fornerod et al. 1995).

As Nup214 is essential for CRM1-dependent NES-mediated nucleocytoplasmic transport of target proteins, the sequestration of CRM1 to the nucleus in DEK-Nup214 and SET-Nup214 cells impairs the shuttling of tumor suppressors or oncogenes between the nucleus and the cytoplasm, which may affect their functions (Brunet et al. 2002; Joseph and Moll 2003).

Recently, a third NUP214-related chromosomal rearrangement has been described leading to T-ALL (T-cell acute lymphoblastic leukemia) (Graux et al. 2004). In this translocation, the N-terminal domain of Nup214 was found to be fused to the kinase domain of the tyrosine kinase ABL1, leading to the expression of an activated tyrosine kinase (Graux et al. 2004). Interestingly, *NUP214-ABL1* fusions retain the N-terminal domain of NUP214, including the coiled-coil domains that might allow its oligomerization and further phosphorylation (Graux et al. 2004).

1.5.4.3 Nup214 and viruses

Contrary to most RNA viruses, DNA viruses require the nuclear replication machinery of the cell to replicate their own genome, and thus must enter the nucleus of the host cell. Viruses can undergo substantial uncoating in the cytoplasm before translocation into the nucleus and some can disassemble within the NPC (Whittaker et al. 2000).

The NPC acts a barrier for viruses to import their high molecular weight nucleoprotein complex into the nucleus. The central pore of the NPC can expand up to ~39 nm in diameter to allow cargo-complexes, proteins or particles to translocate the NPC (Pante and Kann 2002), however, the diameters of many viruses known to replicate in the nucleus are much larger.

Like other DNA viruses, adenovirus capsids disassemble at the NPC prior to import of the viral genome into the nucleus since their protein capsids size varies from 60-90 nm in diameter (Whittaker et al. 2000). The genomes of adenoviruses consist of nonenveloped linear, double-stranded DNA of 30-38 kbp. Adenovirus virions associate with microtubules for directional transport towards the NPC followed by an association with the FG-repeats of the nucleoporin Nup214 prior delivering their DNA to the nucleoplasm (reviewed in (Greber and Way 2006)).

Nup214 acts as the docking site of Ad2 (Adenovirus type 2) capsids, and this association does not require additional cytosolic import factors (Trotman et al. 2001). The uncoating of NPC-docked adenoviral capsids and subsequent genome translocation to the nucleus is facilitated by the nuclear histone H1, which, in turn attracts the heterodimer importin-β/importin7 leading thus to capsid disassembly (Trotman et al. 2001). Although the translocation of Ad2 DNA through the NPC remains unknown, it was reported that the export factor CRM1 acts as a positional indicator of the nucleus for the adenovirus (Strunze et al. 2005). Moreover, CRM1 was reported to be crucial to the detachment of adenoviruses from the microtubules and required for Ad2 nuclear import (Strunze et al. 2005).

One of the best-understood retroviral RNA export pathways is the one utilized by human immunodeficiency virus type 1 (HIV-1) Rev, which is the HIV encoded regulatory protein responsible for the export of the Rev-responsive element containing viral RNA (Zolotukhin and Felber 1999).

Several peripheral nucleoporins, including Nup214, are thought to participate in Rev-mediated RNA export by a direct interaction with FG-repeat domains (Stutz et al. 1996).

Truncated forms of Nup214 can inhibit Rev function (Bogerd et al. 1998), furthermore,

the FG-containing repeat domain of Nup214 can inhibit Rev-mediated expression of viral proteins (Zolotukhin and Felber 1999). Rev NES was shown to directly interact with human CRM1, therefore a depletion of Nup214 FG-repeats impair the ability of CRM1 to bind Rev (Bogerd et al. 1998).

1.6 Nucleoporins and NPC composition in plants

Although the ultrastructure of the plant NPC has been described some decades ago (Franke 1970; Roberts and Northcote 1970; Severs and Jordan 1975), surprisingly little is known about its molecular composition. Only few *Arabidopsis thaliana* nucleoporins have been characterized hitherto. In a protein-protein BLAST search, Rose et al. identified four putative *Arabidopsis* nucleoporins that share 30 to 40% of identity and similarity with the human nucleoporins gp210, Nup98, Tpr, and Nup155, respectively (Rose et al. 2004).

1.6.1 gp210

gp210 is a transmembrane nucleoporin located in the lumen of the NPC and comprises a carboxyterminal domain as well as a luminal domain with several N-linked high mannose-type oligosaccharide groups (Wozniak et al. 1989; Greber et al. 1990). The similarity between the Atgp210 and human gp210 lies in the C-terminal amino acid sequence (Rose et al. 2004).

gp210 is known to play a role in NPC assembly (Wozniak et al. 1989; Greber et al. 1990), NPC biogenesis (Gerace et al. 1982; Bodoor et al. 1999), and in incorporation of nucleoporin subcomplexes to the NE and to the NPC (Eriksson et al. 2004). Furthermore, RNAi experiments in *C. elegans* and HeLa cells revealed that gp210 is essential for viability and its loss coincides with a high frequency of disorganized NPCs and defects in chromatin condensation (Cohen et al. 2003). However, in other studies, gp210 was found to be dispensable for NPC anchoring to the NE and for NPC stability maintenance (Galy et al. 2003; Eriksson et al. 2004).

1.6.2 Nup98 and Nup96

The first identified *Arabidopsis* protein containing a large number of FG-repeats

motif is AtNup98, which aligned with FG-repeats of mammalian Nup98 (Rose et al. 2004). Whereas mammalian Nup98 is transcribed from one gene (Powers et al. 1995; Radu et al. 1995), two *NUP98* genes have been identified in *Arabidopsis* (*At1g10390* and *At1g59660)* (Zhang and Li 2005), similar to yeast where three homologues of Nup98 are known, i.e. Nup100p, Nup116p, Nup145-Np (Wente and Blobel 1993; Fabre et al. 1994; Bailer et al. 1998). Nup98 and its yeast homologue Nup145p-Np are generated by proteolytic cleavage from a precursor protein, which yields in mammalian nucleoporins Nup98 and Nup96 as well as in the yeast nucleoporin Nup145-Np and Nup145-Cp (Dockendorff et al. 1997; Emtage et al. 1997; Teixeira et al. 1997).

Initially Nup98 was thought to exclusively play a role in nuclear export, but more recent data provided evidence that Nup98 functions in nuclear import as well (Blevins et al. 2003). Immuno-EM revealed that Nup98 localizes to both sides of the NPC, where it interacts with Nup88 on the cytoplasmic side and Nup96 as well as Tpr on the nuclear side (Radu et al. 1995). Besides this, Nup98 is known to interact with a number of distinct nuclear transport factors as RaeI/Gle2, TAP and CRM1 (Neville et al. 1997; Pritchard et al. 1999; Strasser et al. 2000; Strawn et al. 2001).

In humans, Nup98 is frequently detected in rare chromosomal translocations associated with distinct forms acute and chronic myelogenous leukemia (AML and CML), T cell acute lymphoblastic leukemia (T-ALL), as well as myelodysplastic syndrome (MDS) (Lam and Aplan 2001). Up to 19 different Nup98 fusion partners have been identified up to now, such as various homeobox genes (*HOXA9*, *HOXA11*, *HOXA13*, *HOXC11*, *HOXC13*, *HOXD11* and *HOXD13*), the helicase DDX10, and the topoisomerase TOP1 (Romana et al. 2006). These fusions of *NUP98* and *HOX* genes typically compromise the N-terminal GLFG-repeats of Nup98 due to breakpoints in exon 8 and 16 in the *NUP98* gene, which leads to transcriptional transactivation of genes involved in *HOX* gene-regulated hematopoiesis (Slape and Aplan 2004).

As mentioned above, Nup98 is autocatalytically cleaved from a Nup98/Nup96 precursor protein, which results in the two nucleoporins Nup98 and Nup96 (Enninga et al. 2003). Nup96, like Nup98, localizes to both sides of the NPC, and is a component of Nup107-160 complex (Enninga et al. 2002), which has a crucial role in NPC assembly (Harel et al. 2003; Walther et al. 2003) and mRNA export (Vasu et al. 2001). A homologue of Nup96 has been recently been identified in *A. thaliana* but, in contrast to vertebrates and yeast it is not expressed from a common precursor with Nup98 and the AtNup98 and AtNup96 genes locate to different chromosomal regions (Mans et al. 2004; Zhang and Li 2005). AtNup96 (also named MOS3) is required for basal defense and constitutive resistance responses to pathogens mediated by the resistance gene (R-gene) (Li et al. 2001; Zhang et al. 2003). Interestingly, human Nup96 can be induced by interferons (Enninga et al. 2003), and more

recently it has been shown that Nup96 play a role innate and adaptive immunity (Faria et al. 2006). As nucleoporins are not only involved in mediating nucleocytoplasmic transport, but also in a number of other cellular processes, such as regulation of gene expression, chromatin organization, chromosome positioning, apoptosis and the secretory pathway (reviewed in (Fahrenkrog and Aebi 2003; Fahrenkrog et al. 2004)) it will be interesting to see if AtNup96 function in pathogen response is related to a putative role in nucleocytoplasmic transport or exclusively due to dysfunction of signaling events.

1.6.3 Tpr

In a protein-protein BLAST search, Rose et al. identified a putative *Arabidopsis* homologue of mammalian Tpr (Rose et al. 2004), a 267 kDa coiled-coil protooncogenic protein localized to the nucleoplasmic side of the NPC and some intranuclear foci (Frosst et al. 2002; Krull et al. 2004), similar to the two putative Tpr homologues in budding yeast, Mlp1 and Mlp2 (Strambio-de-Castillia et al. 1999). Within the nuclear basket of mammalian NPCs, Tpr seems to act as scaffold for other nuclear basket proteins, such as Nup153 and it is known to have roles in protein and RNA export (Bangs et al. 1998; Frosst et al. 2002; Shibata et al. 2002), as well as probably in the recycling of the nuclear transport factors Importin-α and Importin-β (Bangs et al. 1998). Its role in plants remains to be elucidated.

1.6.4 Nup155

In their BLAST search, Rose et al. identified a fifth *Arabidopsis* nucleoporin, the homologue of human Nup155 (Rose et al. 2004), which harbors no FG-repeat domains and was first identified in rat cells. Immuno-EM revealed that Nup155 resides on both the nuclear and cytoplasmic face of the NPC (Radu et al. 1993). Human Nup155 and its yeast homologue yNup170/yNup157 play a role in mRNA export due to their interaction with the putative mRNA export factor Gle1(Rayala et al. 2004). However, the exact targeting mechanism of hGle1 to the NPC has remained unclear (Kendirgi et al. 2005). RNAi studies as well as in vitro nuclear assembly assays have shown that Nup155 is required for postmitotic NE and NPC formation in *C. elegans* embryos and *Xenopus* egg extracts (Franz et al. 2005). However, how Nup155 exactly contributes to NPC structure has remained elusive (see also (Kendirgi et al. 2005)).

1.6.5 Nup133

Another plant nucleoporin that has been identified and found to be involved in plant-microbe interaction is Nup133 from *Lotus japonicus* (Kanamori et al. 2006). These findings indicate an essential function for nucleoporins and probably nucleocytoplasmic transport in plant response to microbes. *Lotus* Nup133 shows 54% identity to the predicted *Arabidopsis* protein At2g05120 and 47% identity to a predicted rice protein (AAN52748), but only 20% identity to yeast and human Nup133 (Kanamori et al. 2006). Consistently, *Lotus* Nup133 cannot complement Nup133 function in yeast strains deleted for Nup133 [85]. Despite this lack of conservation between species on sequence level, secondary structure prediction revealed an N-terminal β-propeller structure and a C-terminal helical domain, exactly as shown for the human and yeast Nup133 proteins (Berke et al. 2004; Schwartz 2005). *Lotus* Nup133 is expressed in all plant organs and mutations in *NUP133* caused defects in root modulators, but, however, no general developmental defects (Kanamori et al. 2006). In contrast, *Lotus* lines expressing Nup133 mutants have a lower number of seeds in mature pods as compared to wild type lines.

Nup133, as Nup96, is a constituent of the Nup107-160 complex in vertebrates and the Nup84p complex in yeast, respectively (Siniossoglou et al. 1996; Allen et al. 2002; Lutzmann et al. 2002). Therefore, the role of plant Nup133 and Nup96 in plant-pathogen interaction gives rise to the question if other members of the Nup107-160 complex have similar functions in plants as well. Also, it will be interesting to see if besides Nup96 other members of the Nup107-160 complex play a role in human immune response.

1.6.6 Glycoprotein gp40

O-Linked *N*-acetylglucosamine (*O*-Glc*N*Ac) glycosylation is a posttranslational modification of proteins by a single N-acetylglucosamine residue on serine and threonine groups. A subset of vertebrate, but not yeast, nucleoporins show Glc*N*Ac-modification and they specifically bind the lectin wheat germ agglutinin (WGA), which causes an inhibition of nucleocytoplasmic transport (Davis and Blobel 1987; Holt et al. 1987; Snow et al. 1987; Finlay et al. 1991; Guan et al. 1995). Sugar modifications are also found on plant proteins, although it occurs in a different manner compared to the addition of single *O*-linked Glc*N*Ac found in vertebrate nucleoporins (Hicks and Raikhel 1995). The addition of the *O*-Glc*N*Ac seems to take place in the cytoplasm, in vertebrates as well as in plants (Kreppel et al. 1997). The best characterized vertebrate *O*-Glc*N*Ac nucleoporin is Nup62, whose glycosylation has been investigated extensively (Starr and Hanover 1990; Carmo-Fonseca et al. 1991; Cordes et al. 1991; Cordes and Krohne 1993). However, the exact function of the *O*-

Glc*N*Ac modifications still remains elusive (Hanover et al. 1987; Hart 1997). *O*-Glc*N*Ac modifications play no role for either nucleocytoplasmic transport or NPC assembly (Miller and Hanover 1994), but may protect proteins from proteolysis (Hart et al. 1989; Haltiwanger et al. 1992).

In search for glycoproteins in plant NEs, a 40 kDa glycoprotein called gp40 has been isolated from tobacco nuclear extracts (Heese-Peck and Raikhel 1998). gp40 localizes to the plant NPC and shows homology to bacterial aldose-1-epimerase, which functions in carbohydrate metabolism. The function of plant gp40 at the NPC and for plant metabolism remains to be elucidated.

1.6.7 Other plant nucleoporins

Functional analysis of plant nucleoporins is still at the very beginning and besides nucleoporinsNup98, Nup96, Nup133 and gp40, no other nucleoporin has been characterized in plants thus far. A recent systemic BLAST and phylogenetic study, however, has revealed that out of 60 NPC or NPC-associated proteins, 45 are present in green plants. Interestingly, no homologues of the integral membrane proteins gp210 and POM121 have been identified in this study (Bapteste et al. 2005). Moreover, no homologues of Nup214 and Nup358, which are located to the cytoplasmic periphery of the NPC, as well as of Nup153, a component of the nuclear basket, appear to be present in plants. Nup214, Nup358 and Nup153 are the major FG-repeat containing nucleoporins in vertebrates, indicating differences in the regulation of nucleocytoplasmic transport in plants as compared to vertebrates.

1.7 Nucleocytoplasmic transport

The main function of the NPC is mediating the bidirectional trafficking of proteins and RNAs between the cytoplasm and nucleus of interphase eukaryotic cells (Fried and Kutay 2003; Pemberton and Paschal 2005). Small molecules, such as ions as wells as proteins that have a molecular mass of less than 40 kDa can traverse the NPC simply by diffusion, whereas the nuclear import of larger proteins is energy- and signal-dependent. Proteins destined for the nucleus with a molecular mass larger than ~40 kDa typically harbor nuclear localization signals (NLSs) within their amino acid sequence, a stretch of basic amino acids first identified in the simian virus (SV40) large T-antigen (Makkerh et al. 1996). NLS sequences are recognized by a class of nuclear import receptors, known as importins or karyopherins (Kutay et al. 1997; Fried and Kutay 2003; Rollenhagen et al. 2003). Most importins are able

to bind to their cargo directly, but some use adapter molecules, just as in case of the so-called classical nuclear import pathway (Fig. 1.4). The classical NLS, as found in the SV40 large T-antigen, is recognized by the adapter protein importin-α, which, in turn, interacts with the actual receptor importin-β. Such an importin-cargo complex is able to interact and traverses the NPC via interaction of importin-β with FG-repeat nucleoporins. Once the complex reaches the nuclear face of the NPC, binding of the small GTPase RanGTP to importin-β induces a conformational change within the receptor and causes the dissociation of the cargo from the receptor and the dissociation of the receptor from the NPC, which, in complex with RanGTP, next is recycled back to the cytoplasm (Fig. 1.4). Importin-α is exported out of the nucleus by its own export receptor, known as CAS, which is a importin-β-like protein (Fried and Kutay 2003; Pemberton and Paschal 2005).

Similarly, a cargo for nuclear export requires a nuclear export signal (NES), which is recognized by an exportin (Gorlich and Kutay 1999). The binding of the exportin to its cargo can only occur in the presence of RanGTP. Such as heterotrimeric export complex is able to interact with the NPC via the receptor and after NPC translocation it becomes dissociated upon RanGTP hydrolysis by the GTPase activating protein RanGAP at the cytoplasmic face of the NPC (Fig. 1.4). The exportin shuttles back into the nucleus, whereas RanGDP gets re-imported into the nucleus by its own import receptor, known as NTF2 (nuclear transport factor 2) (Bayliss et al. 1999). Once in the nucleus, RanGDP is reloaded with GTP by the guanine nucleotide exchange factor RanGEF, called RCC1, a chromatin-associated nuclear protein.

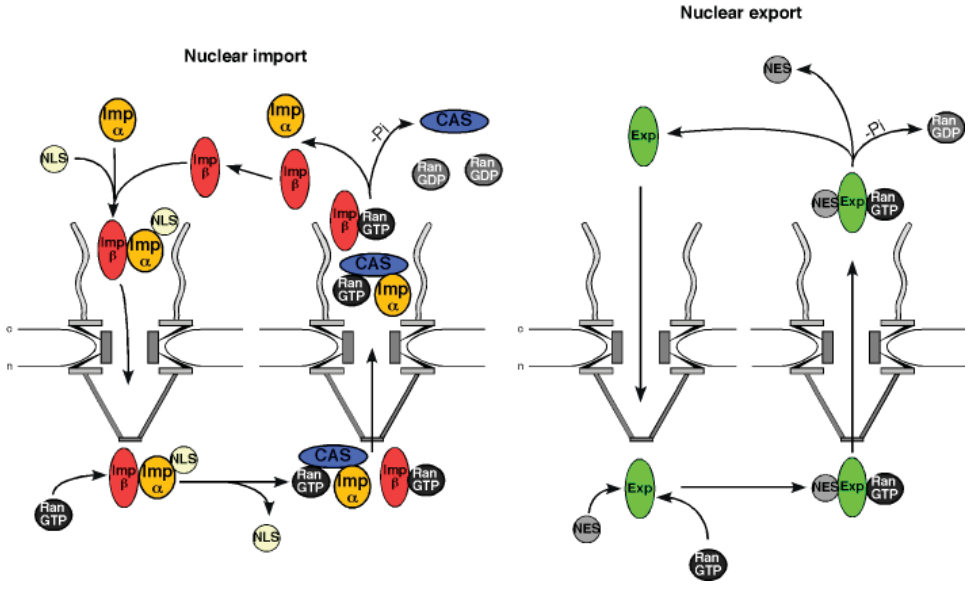

Figure 1.4: Nucleocytoplasmic transport pathways. Importin-α/β dimers bind to cargo molecules harboring a nuclear localization signal (NLS) in the cytoplasm and mediate the interaction with the nuclear pore complex (NPC). In the nucleus, after NPC translocation, RanGTP binds to the importin-β, which induces a conformational change in importin-β, and leads to the dissociation of the cargo-receptor complex and the release from the NPC. The importin-β, -RanGTP complex and a

trimeric importin-α-CAS-RanGTP complex then recycle back into the cytoplasm, where RanGTP is displaced upon GTP hydrolysis mediated by a concerted action of RanGAP, RanBP1 and RanBP2 at the cytoplasmic filaments. CAS represents the exclusive export receptor for importin-α. RanGDP is imported back into the nucleus by its own import receptor, called NTF2 (not shown). Exportins bind to cargo harboring a nuclear export signal (NES), which requires the presence of RanGTP. An export complex becomes dissociated upon GTP hydrolysis at the cytoplasmic face of the NPC and the exportin shuttles back to the nucleus.

1.7.1 Nucleocytoplasmic transport in plants

In contrast to the NPC itself, nucleocytoplasmic transport in plants is much better understood. Vertebrate and yeast NLS as well as NES sequences have been found to be functional in plants (Ward and Lazarowitz 1999; Merkle 2001) and endogenous NLS and NES sequences have been found in a number of plants proteins (Meier 2005). Moreover, plant homologues to virtually all known vertebrate and yeast transport factors have been identified in plants, indicating the evolutionary conservation of nucleocytoplasmic transport. However, plant nuclear import shows some unusual features as compared to yeast and vertebrates (Smith and Raikhel 1999). A unique feature of plant nuclear import, for example, is its occurrence at 4°C (Hicks et al. 1996; Merkle et al. 1996) and that it is not blocked by wheat germ agglutinin, a lectin that, in vertebrates, specifically binds to Glc*N*Ac residues on glycosylated nucleoporins (see above).

At least eight homologues of importin-α have been identified in the *Arabidopsis* genome with high similarity to human importin-α (Meier 2005). In vitro binding assays using recombinant plant importin-α revealed that the different isoforms are recognizing different types of NLSs (Jiang et al. 2001). At-importin-α proteins show a similar domain organization as known from yeast and vertebrates, i.e. an amino-terminal importin-binding (IBB) domain (Gorlich et al. 1996; Weis et al. 1996), a central armadillo (arm)-repeat domain (Conti et al. 1998), and a carboxyl-terminal domain that contains a critical acidic patch implicated in the interaction with its nuclear export receptor CAS (Herold et al. 1998). At-importin-α shows NE association similar to importin-β in mammalian cells (Hicks and Raikhel 1995) and can mediate nuclear import in the absence of importin-β in vitro (Hubner et al. 1999). Moreover, plant importin-α seems to interact with cytoskeleton proteins through its armadillo repeats, and the association of At-importin-α with microtubules and actin microfilaments occurs in an NLS-dependent manner in vitro (Smith and Raikhel 1998). Interestingly, At-importin-α3,which is encoded by the gene MOS6 gene, appears to play a role in plant disease response (Palma et al. 2005), similar to Nup96/MOS3 (see above).

Seventeen genes encoding importin-β-like proteins have been found in the

Arabidopsis genome, yet most of these predicted proteins are not characterized (Bollman et al. 2003). Rice importin-β, however, associates with importin-α and RanGTP (Jiang et al. 1998). A homologue to human transportin 1, also known as importin-β2 has been identified in *Arabidopsis*, which, similar to vertebrates and yeast, promotes the nuclear import of hnRNP proteins (Ziemienowicz et al. 2003). Two orthologues for CRM1/XPO1, the export receptor for cargoes harboring a leucine-rich NES, and CAS, the nuclear export receptor for importin-α, have been also identified in *Arabidopsis* (Haasen et al. 1999). HASTY, the homologue of vertebrate exportin-5 and yeast Msn5p, respectively, is another importin-β-like protein in *Arabidopsis* and it has been shown to have an essential function in plants growth and development (Bollman et al. 2003). PAUSED was identified as the *Arabidopsis* orthologue of exportin-t/Los1p, the export receptors for tRNA in vertebrates and yeast, and evidences suggests that PAUSED is involved in tRNA export as well (Hunter et al. 2003). All identified plants importin-β-like proteins interact with RanGTP (Meier 2005) and, together, these findings suggest that most nuclear transport pathways are conserved in plants.

Components of the Ran cycle have been identified in plants as well. Ran homologues have been found in distinct plant species (Meier 2005) and in *Arabidopsis*, Ran appears to be encoded by a small gene family as three gene have been identified (Haizel et al. 1997). At-RanGAP can complement yeast mutants defective in the yeast RanGAP homologue Rna1p (Pay et al. 2002), and interestingly its anchoring to the NE is mediated by an unique tryptophan-proline-proline (WPP) domain, which is not present in yeast or vertebrate RanGAP (Rose and Meier 2001). This WPP domain, which is predicted to contain three α helices and one β strand, is necessary and sufficient to target At-RanGAP to the NE (Patel et al. 2004). These findings, together with the apparent absence of Nup358/RanBP2 in the *Arabidopsis* genome, suggest that although nuclear transport pathways appear to be predominantly conserved during evolution, plants have evolved a different mechanism of RanGTP hydrolysis. This might be true for GTP loading as well, since a homologue to RCC1, the RanGEF, has not been identified in plants thus far.

Acknowledgements

This work was supported by a research grant from the Swiss National Science Foundation (to B.F.), the M. E. Müller Foundation, and the Kanton Basel Stadt.

References

Adachi, Y., G. N. Pavlakis, et al. (1994). "Identification of in vivo phosphorylation sites of SET, a nuclear phosphoprotein encoded by the translocation breakpoint in acute undifferentiated leukemia." FEBS Lett **340**(3): 231-5.

Agudo, D., F. Gomez-Esquer, et al. (2004). "Nup88 mRNA overexpression is associated with high aggressiveness of breast cancer." Int J Cancer **109**(5): 717-20.

Akey, C. W. and M. Radermacher (1993). "Architecture of the *Xenopus* nuclear pore complex revealed by three-dimensional cryo-electron microscopy." J Cell Biol **122**(1): 1-19.

Allen, N. P., S. S. Patel, et al. (2002). "Deciphering networks of protein interactions at the nuclear pore complex." Mol Cell Proteomics **1**(12): 930-46.

Antonin, W., C. Franz, et al. (2005). "The integral membrane nucleoporin pom121 functionally links nuclear pore complex assembly and nuclear envelope formation." Mol Cell **17**(1): 83-92.

Askjaer, P., A. Bachi, et al. (1999). "RanGTP-regulated interactions of CRM1 with nucleoporins and a shuttling DEAD-box helicase." Mol Cell Biol **19**(9): 6276-85.

Bachi, A., I. C. Braun, et al. (2000). "The C-terminal domain of TAP interacts with the nuclear pore complex and promotes export of specific CTE-bearing RNA substrates." Rna **6**(1): 136-58.

Bailer, S. M., S. Siniossoglou, et al. (1998). "Nup116p and nup100p are interchangeable through a conserved motif which constitutes a docking site for the mRNA transport factor gle2p." Embo J **17**(4): 1107-19.

Ball, J. R. and K. S. Ullman (2005). "Versatility at the nuclear pore complex: lessons learned from the nucleoporin Nup153." Chromosoma **114**(5): 319-30.

Bangs, P., B. Burke, et al. (1998). "Functional analysis of Tpr: identification of nuclear pore complex association and nuclear localization domains and a role in mRNA export." J Cell Biol **143**(7): 1801-12.

Bapteste, E., R. L. Charlebois, et al. (2005). "The two tempos of nuclear pore complex evolution: highly adapting proteins in an ancient frozen structure." Genome Biol **6**(10): R85.

Bastos, R., A. Lin, et al. (1996). "Targeting and function in mRNA export of nuclear pore complex protein Nup153." J Cell Biol **134**(5): 1141-56.

Bastos, R., L. Ribas de Pouplana, et al. (1997). "Nup84, a novel nucleoporin that is associated with CAN/Nup214 on the cytoplasmic face of the nuclear pore complex." J Cell Biol **137**(5): 989-1000.

Bayliss, R., K. Ribbeck, et al. (1999). "Interaction between NTF2 and xFxFG-containing nucleoporins is required to mediate nuclear import of RanGDP." J Mol Biol **293**(3): 579-93.

Beck, M., F. Forster, et al. (2004). "Nuclear pore complex structure and dynamics revealed by cryoelectron tomography." Science **306**(5700): 1387-90.

Belgareh, N., G. Rabut, et al. (2001). "An evolutionarily conserved NPC subcomplex, which redistributes in part to kinetochores in mammalian cells." J Cell Biol **154**(6): 1147-60.

Ben-Efraim, I. and L. Gerace (2001). "Gradient of increasing affinity of importin beta for nucleoporins along the pathway of nuclear import." J Cell Biol **152**(2): 411-7.

Berke, I. C., T. Boehmer, et al. (2004). "Structural and functional analysis of Nup133 domains reveals modular building blocks of the nuclear pore complex." J Cell Biol **167**(4): 591-7.

Bernad, R., H. van der Velde, et al. (2004). "Nup358/RanBP2 attaches to the nuclear pore complex via association with Nup88 and Nup214/CAN and plays a supporting role in CRM1-mediated nuclear protein export." Mol Cell Biol **24**(6): 2373-84.

Blevins, M. B., A. M. Smith, et al. (2003). "Complex formation among the RNA export proteins Nup98, Rae1/Gle2, and TAP." J Biol Chem **278**(23): 20979-88.

Bodoor, K., S. Shaikh, et al. (1999). "Sequential recruitment of NPC proteins to the nuclear periphery at the end of mitosis." J Cell Sci **112 (Pt 13)**: 2253-64.

Boer, J., J. Bonten-Surtel, et al. (1998). "Overexpression of the nucleoporin CAN/NUP214 induces growth arrest, nucleocytoplasmic transport defects, and apoptosis." Mol Cell Biol **18**(3): 1236-47.

Bogerd, H. P., A. Echarri, et al. (1998). "Inhibition of human immunodeficiency virus Rev

and human T-cell leukemia virus Rex function, but not Mason-Pfizer monkey virus constitutive transport element activity, by a mutant human nucleoporin targeted to Crm1." J Virol **72**(11): 8627-35.

Bollman, K. M., M. J. Aukerman, et al. (2003). "HASTY, the *Arabidopsis* ortholog of exportin 5/MSN5, regulates phase change and morphogenesis." Development **130**(8): 1493-504.

Brunet, A., F. Kanai, et al. (2002). "14-3-3 transits to the nucleus and participates in dynamic nucleocytoplasmic transport." J Cell Biol **156**(5): 817-28.

Bustamante, J. O., E. R. Michelette, et al. (2000). "Calcium, ATP and nuclear pore channel gating." Pflugers Arch **439**(4): 433-44.

Canela, N., A. Rodriguez-Vilarrupla, et al. (2003). "The SET protein regulates G2/M transition by modulating cyclin B-cyclin-dependent kinase 1 activity." J Biol Chem **278**(2): 1158-64.

Carman, J. A. and S. G. Nadler (2004). "Direct association of tristetraprolin with the nucleoporin CAN/Nup214." Biochem Biophys Res Commun **315**(2): 445-9.

Carmo-Fonseca, M., H. Kern, et al. (1991). "Human nucleoporin p62 and the essential yeast nuclear pore protein NSP1 show sequence homology and a similar domain organization." Eur J Cell Biol **55**(1): 17-30.

Chi, N. C., E. J. Adam, et al. (1996). "RanBP1 stabilizes the interaction of Ran with p97 nuclear protein import." J Cell Biol **135**(3): 559-69.

Cohen, M., N. Feinstein, et al. (2003). "Nuclear pore protein gp210 is essential for viability in HeLa cells and Caenorhabditis elegans." Mol Biol Cell **14**(10): 4230-7.

Compagnone, N. A., P. Zhang, et al. (2000). "Novel role for the nuclear phosphoprotein SET in transcriptional activation of P450c17 and initiation of neurosteroidogenesis." Mol Endocrinol **14**(6): 875-88.

Conti, E., M. Uy, et al. (1998). "Crystallographic analysis of the recognition of a nuclear localization signal by the nuclear import factor karyopherin alpha." Cell **94**(2): 193-204.

Cordes, V., I. Waizenegger, et al. (1991). "Nuclear pore complex glycoprotein p62 of *Xenopus*

laevis and mouse: cDNA cloning and identification of its glycosylated region." Eur J Cell Biol **55**(1): 31-47.

Cordes, V. C. and G. Krohne (1993). "Sequential O-glycosylation of nuclear pore complex protein gp62 in vitro." Eur J Cell Biol **60**(1): 185-95.

Cronshaw, J. M., A. N. Krutchinsky, et al. (2002). "Proteomic analysis of the mammalian nuclear pore complex." J Cell Biol **158**(5): 915-27.

Dabauvalle, M. C., K. Loos, et al. (1990). "Identification of a soluble precursor complex essential for nuclear pore assembly in vitro." Chromosoma **100**(1): 56-66.

Danker, T. and H. Oberleithner (2000). "Nuclear pore function viewed with atomic force microscopy." Pflugers Arch **439**(6): 671-81.

Davis, L. I. and G. Blobel (1987). "Nuclear pore complex contains a family of glycoproteins that includes p62: glycosylation through a previously unidentified cellular pathway." Proc Natl Acad Sci U S A **84**(21): 7552-6.

Del Priore, V., C. Heath, et al. (1997). "A structure/function analysis of Rat7p/Nup159p, an essential nucleoporin of Saccharomyces cerevisiae." J Cell Sci **110 (Pt 23)**: 2987-99.

Denning, D. P., S. S. Patel, et al. (2003). "Disorder in the nuclear pore complex: the FG repeat regions of nucleoporins are natively unfolded." Proc Natl Acad Sci U S A **100**(5): 2450-5.

Denning, D. P., V. Uversky, et al. (2002). "The Saccharomyces cerevisiae nucleoporin Nup2p is a natively unfolded protein." J Biol Chem **277**(36): 33447-55.

Devos, D., S. Dokudovskaya, et al. (2006). "Simple fold composition and modular architecture of the nuclear pore complex." Proc Natl Acad Sci U S A **103**(7): 2172-7.

Dimaano, C., J. R. Ball, et al. (2001). "RNA association defines a functionally conserved domain in the nuclear pore protein Nup153." J Biol Chem **276**(48): 45349-57.

Dockendorff, T. C., C. V. Heath, et al. (1997). "C-terminal truncations of the yeast nucleoporin Nup145p produce a rapid temperature-conditional mRNA export defect and alterations to nuclear structure." Mol Cell Biol **17**(2): 906-20.

Emtage, J. L., M. Bucci, et al. (1997). "Defining the essential functional regions of the nucleoporin Nup145p." J Cell Sci **110 (Pt 7)**: 911-25.

Enarson, P., M. Enarson, et al. (1998). "Amino-terminal sequences that direct nucleoporin nup153 to the inner surface of the nuclear envelope." Chromosoma **107**(4): 228-36.

Enninga, J., A. Levay, et al. (2003). "Sec13 shuttles between the nucleus and the cytoplasm and stably interacts with Nup96 at the nuclear pore complex." Mol Cell Biol **23**(20): 7271-84.

Enninga, J., D. E. Levy, et al. (2002). "Role of nucleoporin induction in releasing an mRNA nuclear export block." Science **295**(5559): 1523-5.

Eriksson, C., C. Rustum, et al. (2004). "Dynamic properties of nuclear pore complex proteins in gp210 deficient cells." FEBS Lett **572**(1-3): 261-5.

Estanyol, J. M., M. Jaumot, et al. (1999). "The protein SET regulates the inhibitory effect of p21(Cip1) on cyclin E-cyclin-dependent kinase 2 activity." J Biol Chem **274**(46): 33161-5.

Fabre, E., W. C. Boelens, et al. (1994). "Nup145p is required for nuclear export of mRNA and binds homopolymeric RNA in vitro via a novel conserved motif." Cell **78**(2): 275-89.

Fahrenkrog, B. and U. Aebi (2003). "The nuclear pore complex: nucleocytoplasmic transport and beyond." Nat Rev Mol Cell Biol **4**(10): 757-66.

Fahrenkrog, B., J. Koser, et al. (2004). "The nuclear pore complex: a jack of all trades?" Trends Biochem Sci **29**(4): 175-82.

Fahrenkrog, B., B. Maco, et al. (2002). "Domain-specific antibodies reveal multiple-site topology of Nup153 within the nuclear pore complex." J Struct Biol **140**(1-3): 254-67.

Fan, Z., P. J. Beresford, et al. (2003). "Tumor suppressor NM23-H1 is a granzyme A-activated DNase during CTL-mediated apoptosis, and the nucleosome assembly protein SET is its inhibitor." Cell **112**(5): 659-72.

Faria, A. M., A. Levay, et al. (2006). "The nucleoporin nup96 is required for proper expression of interferon-regulated proteins and functions." Immunity **24**(3): 295-304.

Farjot, G., M. Buisson, et al. (2000). "Epstein-Barr virus EB2 protein exports unspliced RNA via a Crm-1-independent pathway." J Virol **74**(13): 6068-76.

Finlay, D. R. and D. J. Forbes (1990). "Reconstitution of biochemically altered nuclear pores: transport can be eliminated and restored." Cell **60**(1): 17-29.

Finlay, D. R., E. Meier, et al. (1991). "A complex of nuclear pore proteins required for pore function." J Cell Biol **114**(1): 169-83.

Fornerod, M., J. Boer, et al. (1995). "Relocation of the carboxyterminal part of CAN from the nuclear envelope to the nucleus as a result of leukemia-specific chromosome rearrangements." Oncogene **10**(9): 1739-48.

Fornerod, M., J. Boer, et al. (1996). "Interaction of cellular proteins with the leukemia specific fusion proteins DEK-CAN and SET-CAN and their normal counterpart, the nucleoporin CAN." Oncogene **13**(8): 1801-8.

Fornerod, M., S. van Baal, et al. (1997). "Chromosomal localization of genes encoding CAN/Nup214-interacting proteins--human CRM1 localizes to 2p16, whereas Nup88 localizes to 17p13 and is physically linked to SF2p32." Genomics **42**(3): 538-40.

Fornerod, M., J. van Deursen, et al. (1997). "The human homologue of yeast CRM1 is in a dynamic subcomplex with CAN/Nup214 and a novel nuclear pore component Nup88." Embo J **16**(4): 807-16.

Franke, W. W. (1970). "On the universality of nuclear pore complex structure." Z Zellforsch Mikrosk Anat **105**(3): 405-29.

Franz, C., P. Askjaer, et al. (2005). "Nup155 regulates nuclear envelope and nuclear pore complex formation in nematodes and vertebrates." Embo J **24**(20): 3519-31.

Fried, H. and U. Kutay (2003). "Nucleocytoplasmic transport: taking an inventory." Cell Mol Life Sci **60**(8): 1659-88.

Frosst, P., T. Guan, et al. (2002). "Tpr is localized within the nuclear basket of the pore complex and has a role in nuclear protein export." J Cell Biol **156**(4): 617-30.

Galy, V., I. W. Mattaj, et al. (2003). "Caenorhabditis elegans nucleoporins Nup93 and Nup205 determine the limit of nuclear pore complex size exclusion in vivo." Mol Biol Cell **14**(12): 5104-15.

Gerace, L., Y. Ottaviano, et al. (1982). "Identification of a major polypeptide of the nuclear pore complex." J Cell Biol **95**(3): 826-37.

Goldberg, M. W. and T. D. Allen (1993). "The nuclear pore complex: three-dimensional surface structure revealed by field emission, in-lens scanning electron microscopy, with underlying structure uncovered by proteolysis." J Cell Sci **106 (Pt 1)**: 261-74.

Gorlich, D., P. Henklein, et al. (1996). "A 41 amino acid motif in importin-alpha confers binding to importin-beta and hence transit into the nucleus." Embo J **15**(8): 1810-7.

Gorlich, D. and U. Kutay (1999). "Transport between the cell nucleus and the cytoplasm." Annu Rev Cell Dev Biol **15**: 607-60.

Gould, V. E., N. Martinez, et al. (2000). "A novel, nuclear pore-associated, widely distributed molecule overexpressed in oncogenesis and development." Am J Pathol **157**(5): 1605-13.

Graux, C., J. Cools, et al. (2004). "Fusion of NUP214 to ABL1 on amplified episomes in T-cell acute lymphoblastic leukemia." Nat Genet **36**(10): 1084-9.

Greber, U. F., A. Senior, et al. (1990). "A major glycoprotein of the nuclear pore complex is a membrane-spanning polypeptide with a large lumenal domain and a small cytoplasmic tail." Embo J **9**(5): 1495-502.

Greber, U. F. and M. Way (2006). "A superhighway to virus infection." Cell **124**(4): 741-54.

Guan, T., S. Muller, et al. (1995). "Structural analysis of the p62 complex, an assembly of O-linked glycoproteins that localizes near the central gated channel of the nuclear pore complex." Mol Biol Cell **6**(11): 1591-603.

Haasen, D., C. Kohler, et al. (1999). "Nuclear export of proteins in plants: AtXPO1 is the export receptor for leucine-rich nuclear export signals in *Arabidopsis thaliana*." Plant J **20**(6): 695-705.

Haizel, T., T. Merkle, et al. (1997). "Characterization of proteins that interact with the GTP-bound form of the regulatory GTPase Ran in *Arabidopsis*." Plant J **11**(1): 93-103.

Haltiwanger, R. S., W. G. Kelly, et al. (1992). "Glycosylation of nuclear and cytoplasmic proteins is ubiquitous and dynamic." Biochem Soc Trans **20**(2): 264-9.

Hanover, J. A., C. K. Cohen, et al. (1987). "O-linked N-acetylglucosamine is attached to proteins of the nuclear pore. Evidence for cytoplasmic and nucleoplasmic glycoproteins." J Biol Chem **262**(20): 9887-94.

Harel, A., A. V. Orjalo, et al. (2003). "Removal of a single pore subcomplex results in vertebrate nuclei devoid of nuclear pores." Mol Cell **11**(4): 853-64.

Hart, G. W. (1997). "Dynamic O-linked glycosylation of nuclear and cytoskeletal proteins." Annu Rev Biochem **66**: 315-35.

Hart, G. W., R. S. Haltiwanger, et al. (1989). "Glycosylation in the nucleus and cytoplasm." Annu Rev Biochem **58**: 841-74.

Heese-Peck, A., R. N. Cole, et al. (1995). "Plant nuclear pore complex proteins are modified by novel oligosaccharides with terminal N-acetylglucosamine." Plant Cell **7**(9): 1459-71.

Heese-Peck, A. and N. V. Raikhel (1998). "A glycoprotein modified with terminal N-acetylglucosamine and localized at the nuclear rim shows sequence similarity to aldose-1-epimerases." Plant Cell **10**(4): 599-612.

Herold, A., R. Truant, et al. (1998). "Determination of the functional domain organization of the importin alpha nuclear import factor." J Cell Biol **143**(2): 309-18.

Hicks, G. R. and N. V. Raikhel (1995). "Protein import into the nucleus: an integrated view." Annu Rev Cell Dev Biol **11**: 155-88.

Hicks, G. R., H. M. Smith, et al. (1996). "Nuclear import in permeabilized protoplasts from higher plants has unique features." Plant Cell **8**(8): 1337-52.

Hinshaw, J. E., B. O. Carragher, et al. (1992). "Architecture and design of the nuclear pore complex." Cell **69**(7): 1133-41.

Holt, G. D., C. M. Snow, et al. (1987). "Nuclear pore complex glycoproteins contain cytoplasmically disposed O-linked N-acetylglucosamine." J Cell Biol **104**(5): 1157-64.

Hu, T., T. Guan, et al. (1996). "Molecular and functional characterization of the p62 complex, an assembly of nuclear pore complex glycoproteins." J Cell Biol **134**(3): 589-601.

Hubner, S., H. M. Smith, et al. (1999). "Plant importin alpha binds nuclear localization sequences with high affinity and can mediate nuclear import independent of importin beta." J Biol Chem **274**(32): 22610-7.

Hunter, C. A., M. J. Aukerman, et al. (2003). "PAUSED encodes the *Arabidopsis* exportin-t ortholog." Plant Physiol **132**(4): 2135-43.

Hussey, D. J. and A. Dobrovic (2002). "Recurrent coiled-coil motifs in NUP98 fusion partners provide a clue to leukemogenesis." Blood **99**(3): 1097-8.

Hutten, S. and R. H. Kehlenbach (2006). "Nup214 is required for CRM1-dependent nuclear protein export in vivo." Mol Cell Biol **26**(18): 6772-85.

Jiang, C. J., N. Imamoto, et al. (1998). "In vitro characterization of rice importin beta1: molecular interaction with nuclear transport factors and mediation of nuclear protein import." FEBS Lett **437**(1-2): 127-30.

Jiang, C. J., K. Shoji, et al. (2001). "Molecular cloning of a novel importin alpha homologue from rice, by which constitutive photomorphogenic 1 (COP1) nuclear localization signal (NLS)-protein is preferentially nuclear imported." J Biol Chem **276**(12): 9322-9.

Joseph, J., S. T. Liu, et al. (2004). "The RanGAP1-RanBP2 complex is essential for microtubule-kinetochore interactions in vivo." Curr Biol **14**(7): 611-7.

Joseph, J., S. H. Tan, et al. (2002). "SUMO-1 targets RanGAP1 to kinetochores and mitotic spindles." J Cell Biol **156**(4): 595-602.

Joseph, T. W. and U. M. Moll (2003). "Analysis of nuclear and cytoplasmic degradation of p53 in cells after stress." Methods Mol Biol **234**: 211-7.

Kanamori, N., L. H. Madsen, et al. (2006). "A nucleoporin is required for induction of Ca2+ spiking in legume nodule development and essential for rhizobial and fungal symbiosis." Proc Natl Acad Sci U S A **103**(2): 359-64.

Kandilci, A., E. Mientjes, et al. (2004). "Effects of SET and SET-CAN on the differentiation of the human promonocytic cell line U937." Leukemia **18**(2): 337-40.

Kappes, F., K. Burger, et al. (2001). "Subcellular localization of the human proto-oncogene protein DEK." J Biol Chem **276**(28): 26317-23.

Kappes, F., C. Damoc, et al. (2004). "Phosphorylation by protein kinase CK2 changes the DNA binding properties of the human chromatin protein DEK." Mol Cell Biol **24**(13): 6011-20.

Katahira, J., K. Strasser, et al. (1999). "The Mex67p-mediated nuclear mRNA export pathway is conserved from yeast to human." Embo J **18**(9): 2593-609.

Kehlenbach, R. H., A. Dickmanns, et al. (1999). "A role for RanBP1 in the release of CRM1 from the nuclear pore complex in a terminal step of nuclear export." J Cell Biol **145**(4): 645-57.

Kendirgi, F., D. J. Rexer, et al. (2005). "Interaction between the shuttling mRNA export factor Gle1 and the nucleoporin hCG1: a conserved mechanism in the export of Hsp70 mRNA." Mol Biol Cell **16**(9): 4304-15.

Kita, K., S. Omata, et al. (1993). "Purification and characterization of a nuclear pore glycoprotein complex containing p62." J Biochem (Tokyo) **113**(3): 377-82.

Kreppel, L. K., M. A. Blomberg, et al. (1997). "Dynamic glycosylation of nuclear and cytosolic proteins. Cloning and characterization of a unique O-GlcNAc transferase with multiple tetratricopeptide repeats." J Biol Chem **272**(14): 9308-15.

Krull, S., J. Thyberg, et al. (2004). "Nucleoporins as components of the nuclear pore complex core structure and Tpr as the architectural element of the nuclear basket." Mol Biol Cell **15**(9): 4261-77.

Kutay, U., F. R. Bischoff, et al. (1997). "Export of importin alpha from the nucleus is mediated by a specific nuclear transport factor." Cell **90**(6): 1061-71.

Lam, D. H. and P. D. Aplan (2001). "NUP98 gene fusions in hematologic malignancies." Leukemia **15**(11): 1689-95.

Levesque, L., Y. C. Bor, et al. (2006). "Mutations in Tap Uncouple RNA Export Activity from Translocation through the Nuclear Pore Complex." Mol Biol Cell **17**(2): 931-43.

Li, M., A. Makkinje, et al. (1996). "The myeloid leukemia-associated protein SET is a potent inhibitor of protein phosphatase 2A." J Biol Chem **271**(19): 11059-62.

Li, X., J. D. Clarke, et al. (2001). "Activation of an EDS1-mediated R-gene pathway in

the snc1 mutant leads to constitutive, NPR1-independent pathogen resistance." Mol Plant Microbe Interact **14**(10): 1131-9.

Lim, R. Y. and U. Aebi (2005). "In silico access to the nuclear pore complex." Structure **13**(12): 1741-3.

Lim, R. Y. a. F., B. (2006). "The nuclear pore complex up close." Current Opinion in Cell Biology **18**: in press.

Liu, J., A. J. Prunuske, et al. (2003). "The COPI complex functions in nuclear envelope breakdown and is recruited by the nucleoporin Nup153." Dev Cell **5**(3): 487-98.

Lutzmann, M., R. Kunze, et al. (2002). "Modular self-assembly of a Y-shaped multiprotein complex from seven nucleoporins." Embo J **21**(3): 387-97.

Macaulay, C., E. Meier, et al. (1995). "Differential mitotic phosphorylation of proteins of the nuclear pore complex." J Biol Chem **270**(1): 254-62.

Makkerh, J. P., C. Dingwall, et al. (1996). "Comparative mutagenesis of nuclear localization signals reveals the importance of neutral and acidic amino acids." Curr Biol **6**(8): 1025-7.

Mans, B. J., V. Anantharaman, et al. (2004). "Comparative genomics, evolution and origins of the nuclear envelope and nuclear pore complex." Cell Cycle **3**(12): 1612-37.

Marg, A., Y. Shan, et al. (2004). "Nucleocytoplasmic shuttling by nucleoporins Nup153 and Nup214 and CRM1-dependent nuclear export control the subcellular distribution of latent Stat1." J Cell Biol **165**(6): 823-33.

Martinez, N., A. Alonso, et al. (1999). "The nuclear pore complex protein Nup88 is overexpressed in tumor cells." Cancer Res **59**(21): 5408-11.

Matsubayashi, Y., M. Fukuda, et al. (2001). "Evidence for existence of a nuclear pore complex-mediated, cytosol-independent pathway of nuclear translocation of ERK MAP kinase in permeabilized cells." J Biol Chem **276**(45): 41755-60.

Matsuoka, Y., M. Takagi, et al. (1999). "Identification and characterization of nuclear pore subcomplexes in mitotic extract of human somatic cells." Biochem Biophys Res Commun **254**(2): 417-23.

Matunis, M. J., J. Wu, et al. (1998). "SUMO-1 modification and its role in targeting the Ran GTPase-activating protein, RanGAP1, to the nuclear pore complex." J Cell Biol **140**(3): 499-509.

Maul, G. G. (1971). "On the octagonality of the nuclear pore complex." J Cell Biol **51**(21): 558-63.

Meier, I. (2005). "Nucleocytoplasmic trafficking in plant cells." Int Rev Cytol **244**: 95-135.

Melchior, F. (2000). "SUMO--nonclassical ubiquitin." Annu Rev Cell Dev Biol **16**: 591-626.

Merkle, T. (2001). "Nuclear import and export of proteins in plants: a tool for the regulation of signalling." Planta **213**(4): 499-517.

Merkle, T., D. Leclerc, et al. (1996). "A plant in vitro system for the nuclear import of proteins." Plant J **10**(6): 1177-86.

Miller, M. W., M. R. Caracciolo, et al. (1999). "Phosphorylation and glycosylation of nucleoporins." Arch Biochem Biophys **367**(1): 51-60.

Miller, M. W. and J. A. Hanover (1994). "Functional nuclear pores reconstituted with beta 1-4 galactose-modified O-linked N-acetylglucosamine glycoproteins." J Biol Chem **269**(12): 9289-97.

Miyaji-Yamaguchi, M., M. Okuwaki, et al. (1999). "Coiled-coil structure-mediated dimerization of template activating factor-I is critical for its chromatin remodeling activity." J Mol Biol **290**(2): 547-57.

Morita, A., N. Suzuki, et al. (2000). "p41 as a possible marker for cell death is generated by caspase cleavage of p42/SETbeta in irradiated MOLT-4 cells." Biochem Biophys Res Commun **278**(3): 627-32.

Nakielny, S., S. Shaikh, et al. (1999). "Nup153 is an M9-containing mobile nucleoporin with a novel Ran-binding domain." Embo J **18**(7): 1982-95.

Neville, M., F. Stutz, et al. (1997). "The importin-beta family member Crm1p bridges the interaction between Rev and the nuclear pore complex during nuclear export." Curr Biol **7**(10): 767-75.

Palma, K., Y. Zhang, et al. (2005). "An importin alpha homolog, MOS6, plays an important role in plant innate immunity." Curr Biol **15**(12): 1129-35.

Pante, N. and M. Kann (2002). "Nuclear pore complex is able to transport macromolecules with diameters of about 39 nm." Mol Biol Cell **13**(2): 425-34.

Patel, S., A. Rose, et al. (2004). "*Arabidopsis* WPP-domain proteins are developmentally associated with the nuclear envelope and promote cell division." Plant Cell **16**(12): 3260-73.

Paulillo, S. M., E. M. Phillips, et al. (2005). "Nucleoporin domain topology is linked to the transport status of the nuclear pore complex." J Mol Biol **351**(4): 784-98.

Pay, A., K. Resch, et al. (2002). "Plant RanGAPs are localized at the nuclear envelope in interphase and associated with microtubules in mitotic cells." Plant J **30**(6): 699-709.

Pemberton, L. F. and B. M. Paschal (2005). "Mechanisms of receptor-mediated nuclear import and nuclear export." Traffic **6**(3): 187-98.

Pichler, A., A. Gast, et al. (2002). "The nucleoporin RanBP2 has SUMO1 E3 ligase activity." Cell **108**(1): 109-20.

Pichler, A., P. Knipscheer, et al. (2004). "The RanBP2 SUMO E3 ligase is neither HECT- nor RING-type." Nat Struct Mol Biol **11**(10): 984-91.

Powers, M. A., C. Macaulay, et al. (1995). "Reconstituted nuclei depleted of a vertebrate GLFG nuclear pore protein, p97, import but are defective in nuclear growth and replication." J Cell Biol **128**(5): 721-36.

Pritchard, C. E., M. Fornerod, et al. (1999). "RAE1 is a shuttling mRNA export factor that binds to a GLEBS-like NUP98 motif at the nuclear pore complex through multiple domains." J Cell Biol **145**(2): 237-54.

Prunuske, A. J., J. Liu, et al. (2006). "Nuclear Envelope Breakdown Is Coordinated by Both Nup358/RanBP2 and Nup153, Two Nucleoporins with Zinc Finger Modules." Mol Biol Cell **17**(2): 760-9.

Rabut, G., V. Doye, et al. (2004). "Mapping the dynamic organization of the nuclear pore complex inside single living cells." Nat Cell Biol **6**(11): 1114-21.

Radu, A., G. Blobel, et al. (1993). "Nup155 is a novel nuclear pore complex protein that contains neither repetitive sequence motifs nor reacts with WGA." J Cell Biol **121**(1): 1-9.

Radu, A., M. S. Moore, et al. (1995). "The peptide repeat domain of nucleoporin Nup98 functions as a docking site in transport across the nuclear pore complex." Cell **81**(2): 215-22.

Rayala, H. J., F. Kendirgi, et al. (2004). "The mRNA export factor human Gle1 interacts with the nuclear pore complex protein Nup155." Mol Cell Proteomics **3**(2): 145-55.

Reverter, D. and C. D. Lima (2005). "Insights into E3 ligase activity revealed by a SUMO-RanGAP1-Ubc9-Nup358 complex." Nature **435**(7042): 687-92.

Roberts, K. and D. H. Northcote (1970). "Structure of the nuclear pore in higher plants." Nature **228**(5269): 385-6.

Rollenhagen, C., P. Muhlhausser, et al. (2003). "Importin beta-depending nuclear import pathways: role of the adapter proteins in the docking and releasing steps." Mol Biol Cell **14**(5): 2104-15.

Romana, S. P., I. Radford-Weiss, et al. (2006). "NUP98 rearrangements in hematopoietic malignancies: a study of the Groupe Francophone de Cytogenetique Hematologique." Leukemia.

Rose, A. and I. Meier (2001). "A domain unique to plant RanGAP is responsible for its targeting to the plant nuclear rim." Proc Natl Acad Sci U S A **98**(26): 15377-82.

Rose, A., S. Patel, et al. (2004). "Plant nuclear envelope proteins." Symp Soc Exp Biol(56): 69-88.

Rose, A., S. Patel, et al. (2004). "The plant nuclear envelope." Planta **218**(3): 327-36.

Roth, P., N. Xylourgidis, et al. (2003). "The Drosophila nucleoporin DNup88 localizes DNup214 and CRM1 on the nuclear envelope and attenuates NES-mediated nuclear export." J Cell Biol **163**(4): 701-6.

Rout, M. P., J. D. Aitchison, et al. (2000). "The yeast nuclear pore complex: composition, architecture, and transport mechanism." J Cell Biol **148**(4): 635-51.

Saito, S., M. Miyaji-Yamaguchi, et al. (2004). "Aberrant intracellular localization of SET-CAN fusion protein, associated with a leukemia, disorganizes nuclear export." Int J Cancer **111**(4): 501-7.

Saitoh, H., C. A. Cooke, et al. (1996). "Direct and indirect association of the small GTPase ran with nuclear pore proteins and soluble transport factors: studies in *Xenopus laevis* egg extracts." Mol Biol Cell **7**(9): 1319-34.

Saitoh, H., D. B. Sparrow, et al. (1998). "Ubc9p and the conjugation of SUMO-1 to RanGAP1 and RanBP2." Curr Biol **8**(2): 121-4.

Salina, D., P. Enarson, et al. (2003). "Nup358 integrates nuclear envelope breakdown with kinetochore assembly." J Cell Biol **162**(6): 991-1001.

Schmitt, C., C. von Kobbe, et al. (1999). "Dbp5, a DEAD-box protein required for mRNA export, is recruited to the cytoplasmic fibrils of nuclear pore complex via a conserved interaction with CAN/Nup159p." Embo J **18**(15): 4332-47.

Schwartz, T. U. (2005). "Modularity within the architecture of the nuclear pore complex." Curr Opin Struct Biol **15**(2): 221-6.

Severs, N. J. and E. G. Jordan (1975). "An interpretive freeze-fracture study of plant cell nuclear pore complexes." J Ultrastruct Res **52**(1): 85-99.

Shah, S., S. Tugendreich, et al. (1998). "Major binding sites for the nuclear import receptor are the internal nucleoporin Nup153 and the adjacent nuclear filament protein Tpr." J Cell Biol **141**(1): 31-49.

Shibata, S., Y. Matsuoka, et al. (2002). "Nucleocytoplasmic transport of proteins and poly(A)+ RNA in reconstituted Tpr-less nuclei in living mammalian cells." Genes Cells **7**(4): 421-34.

Singh, B. B., H. H. Patel, et al. (1999). "The zinc finger cluster domain of RanBP2 is a specific docking site for the nuclear export factor, exportin-1." J Biol Chem **274**(52): 37370-8.

Siniossoglou, S., C. Wimmer, et al. (1996). "A novel complex of nucleoporins, which includes Sec13p and a Sec13p homolog, is essential for normal nuclear pores." Cell **84**(2): 265-75.

Slape, C. and P. D. Aplan (2004). "The role of NUP98 gene fusions in hematologic malignancy." Leuk Lymphoma **45**(7): 1341-50.

Smith, H. M. and N. V. Raikhel (1998). "Nuclear localization signal receptor importin alpha associates with the cytoskeleton." Plant Cell **10**(11): 1791-9.

Smith, H. M. and N. V. Raikhel (1999). "Protein targeting to the nuclear pore. What can we learn from plants?" Plant Physiol **119**(4): 1157-64.

Snow, C. M., A. Senior, et al. (1987). "Monoclonal antibodies identify a group of nuclear pore complex glycoproteins." J Cell Biol **104**(5): 1143-56.

Starr, C. M. and J. A. Hanover (1990). "Glycosylation of nuclear pore protein p62. Reticulocyte lysate catalyzes O-linked N-acetylglucosamine addition in vitro." J Biol Chem **265**(12): 6868-73.

Stoffler, D., B. Fahrenkrog, et al. (1999). "The nuclear pore complex: from molecular architecture to functional dynamics." Curr Opin Cell Biol **11**(3): 391-401.

Stoffler, D., B. Feja, et al. (2003). "Cryo-electron tomography provides novel insights into nuclear pore architecture: implications for nucleocytoplasmic transport." J Mol Biol **328**(1): 119-30.

Strambio-de-Castillia, C., G. Blobel, et al. (1999). "Proteins connecting the nuclear pore complex with the nuclear interior." J Cell Biol **144**(5): 839-55.

Strasser, K., J. Bassler, et al. (2000). "Binding of the Mex67p/Mtr2p heterodimer to FXFG, GLFG, and FG repeat nucleoporins is essential for nuclear mRNA export." J Cell Biol **150**(4): 695-706.

Strawn, L. A., T. Shen, et al. (2004). "Minimal nuclear pore complexes define FG repeat domains essential for transport." Nat Cell Biol **6**(3): 197-206.

Strawn, L. A., T. Shen, et al. (2001). "The GLFG regions of Nup116p and Nup100p serve as binding sites for both Kap95p and Mex67p at the nuclear pore complex." J Biol Chem **276**(9): 6445-52.

Strunze, S., L. C. Trotman, et al. (2005). "Nuclear targeting of adenovirus type 2 requires CRM1-mediated nuclear export." Mol Biol Cell **16**(6): 2999-3009.

Stutz, F., E. Izaurralde, et al. (1996). "A role for nucleoporin FG repeat domains in export of human immunodeficiency virus type 1 Rev protein and RNA from the nucleus." Mol Cell Biol **16**(12): 7144-50.

Sukegawa, J. and G. Blobel (1993). "A nuclear pore complex protein that contains zinc finger motifs, binds DNA, and faces the nucleoplasm." Cell **72**(1): 29-38.

Takano, H. and J. F. Gusella (2002). "The predominantly HEAT-like motif structure of huntingtin and its association and coincident nuclear entry with dorsal, an NF-kB/Rel/dorsal family transcription factor." BMC Neurosci **3**: 15.

Teixeira, M. T., S. Siniossoglou, et al. (1997). "Two functionally distinct domains generated by in vivo cleavage of Nup145p: a novel biogenesis pathway for nucleoporins." Embo J **16**(16): 5086-97.

Trotman, L. C., N. Mosberger, et al. (2001). "Import of adenovirus DNA involves the nuclear pore complex receptor CAN/Nup214 and histone H1." Nat Cell Biol **3**(12): 1092-100.

Uv, A. E., P. Roth, et al. (2000). "members only encodes a Drosophila nucleoporin required for rel protein import and immune response activation." Genes Dev **14**(15): 1945-57.

Vasu, S., S. Shah, et al. (2001). "Novel vertebrate nucleoporins Nup133 and Nup160 play a role in mRNA export." J Cell Biol **155**(3): 339-54.

von Lindern, M., M. Fornerod, et al. (1992). "The translocation (6;9), associated with a specific subtype of acute myeloid leukemia, results in the fusion of two genes, dek and can, and the expression of a chimeric, leukemia-specific dek-can mRNA." Mol Cell Biol **12**(4): 1687-97.

von Lindern, M., S. van Baal, et al. (1992). "Can, a putative oncogene associated with myeloid leukemogenesis, may be activated by fusion of its 3' half to different genes: characterization of the set gene." Mol Cell Biol **12**(8): 3346-55.

Walther, T. C., A. Alves, et al. (2003). "The conserved Nup107-160 complex is critical for nuclear pore complex assembly." Cell **113**(2): 195-206.

Walther, T. C., H. S. Pickersgill, et al. (2002). "The cytoplasmic filaments of the nuclear pore complex are dispensable for selective nuclear protein import." J Cell Biol **158**(1):

63-77.

Ward, B. M. and S. G. Lazarowitz (1999). "Nuclear export in plants. Use of geminivirus movement proteins for a cell-based export assay." Plant Cell **11**(7): 1267-76.

Weirich, C. S., J. P. Erzberger, et al. (2004). "The N-terminal domain of Nup159 forms a beta-propeller that functions in mRNA export by tethering the helicase Dbp5 to the nuclear pore." Mol Cell **16**(5): 749-60.

Weis, K., U. Ryder, et al. (1996). "The conserved amino-terminal domain of hSRP1 alpha is essential for nuclear protein import." Embo J **15**(8): 1818-25.

Wente, S. R. and G. Blobel (1993). "A temperature-sensitive NUP116 null mutant forms a nuclear envelope seal over the yeast nuclear pore complex thereby blocking nucleocytoplasmic traffic." J Cell Biol **123**(2): 275-84.

Whittaker, G. R., M. Kann, et al. (2000). "Viral entry into the nucleus." Annu Rev Cell Dev Biol **16**: 627-51.

Wozniak, R. W., E. Bartnik, et al. (1989). "Primary structure analysis of an integral membrane glycoprotein of the nuclear pore." J Cell Biol **108**(6): 2083-92.

Wu, J., M. J. Matunis, et al. (1995). "Nup358, a cytoplasmically exposed nucleoporin with peptide repeats, Ran-GTP binding sites, zinc fingers, a cyclophilin A homologous domain, and a leucine-rich region." J Biol Chem **270**(23): 14209-13.

Xu, L., C. Alarcon, et al. (2003). "Distinct domain utilization by Smad3 and Smad4 for nucleoporin interaction and nuclear import." J Biol Chem **278**(43): 42569-77.

Xu, L., Y. Kang, et al. (2002). "Smad2 nucleocytoplasmic shuttling by nucleoporins CAN/Nup214 and Nup153 feeds TGFbeta signaling complexes in the cytoplasm and nucleus." Mol Cell **10**(2): 271-82.

Xylourgidis, N., P. Roth, et al. (2006). "The nucleoporin Nup214 sequesters CRM1 at the nuclear rim and modulates NF{kappa}B activation in Drosophila." J Cell Sci: jcs.03201.

Yang, Q., M. P. Rout, et al. (1998). "Three-dimensional architecture of the isolated yeast nuclear pore complex: functional and evolutionary implications." Mol Cell **1**(2): 223-34.

Yokoyama, N., N. Hayashi, et al. (1995). "A giant nucleopore protein that binds Ran/TC4." Nature **376**(6536): 184-8.

Zeitler, B. and K. Weis (2004). "The FG-repeat asymmetry of the nuclear pore complex is dispensable for bulk nucleocytoplasmic transport in vivo." J Cell Biol **167**(4): 583-90.

Zhang, H., H. Saitoh, et al. (2002). "Enzymes of the SUMO modification pathway localize to filaments of the nuclear pore complex." Mol Cell Biol **22**(18): 6498-508.

Zhang, Y., S. Goritschnig, et al. (2003). "A gain-of-function mutation in a plant disease resistance gene leads to constitutive activation of downstream signal transduction pathways in suppressor of npr1-1, constitutive 1." Plant Cell **15**(11): 2636-46.

Zhang, Y. and X. Li (2005). "A putative nucleoporin 96 Is required for both basal defense and constitutive resistance responses mediated by suppressor of npr1-1,constitutive 1." Plant Cell **17**(4): 1306-16.

Ziemienowicz, A., D. Haasen, et al. (2003). "*Arabidopsis* transportin1 is the nuclear import receptor for the circadian clock-regulated RNA-binding protein AtGRP7." Plant Mol Biol **53**(1-2): 201-12.

Zolotukhin, A. S. and B. K. Felber (1999). "Nucleoporins nup98 and nup214 participate in nuclear export of human immunodeficiency virus type 1 Rev." J Virol **73**(1): 120-7.

Chapter 2

Nucleoporin Domain Topology is Linked to the Transport Status of the Nuclear Pore Complex

Nucleoporin domain topology is linked to the transport status of the nuclear pore complex

Sara M. Paulillo[1], Erica M. Phillips[2], Joachim Köser[1], Ursula Sauder[1], Katharine S. Ullman[3], Maureen A. Powers[2], and Birthe Fahrenkrog[1,*]

[1]M.E. Müller Institute for Structural Biology, Biozentrum, University of Basel, Klingelbergstr. 70, 4056 Basel, Switzerland, [2]Department of Cell Biology,

Emory University School of Medicine, 615 Michael Street, Atlanta, GA 30322, USA, [3]Department of Oncological Sciences, Huntsman Cancer Institute, University of Utah, Salt Lake City, Utah, USA

*corresponding author: birthe.fahrenkrog@unibas.ch

Summary

Nuclear pore complexes (NPCs) facilitate macromolecular exchange between the nucleus and cytoplasm of eukaryotic cells. The vertebrate NPC is composed of ~30 different proteins (nucleoporins), of which around one third contain phenylalanine-glycine (FG)-repeat domains that are thought to mediate the main interaction between the NPC and soluble transport receptors. We have recently shown that the FG-repeat domain of Nup153 is flexible within the NPC, although this nucleoporin is anchored to the nuclear side of the NPC. By using domain-specific antibodies, we have now mapped the domain topology of Nup214 in *Xenopus* oocytes and in human somatic cells by immuno-EM. We have found that whereas Nup214 is anchored to the cytoplasmic side of the NPC via its N-terminal and central domain, its FG-repeat domain appears flexible, residing on both sides of the NPC. Moreover, the spatial distribution of the FG-repeat domains of both Nup153 and Nup214 shifts in a transport-dependent manner, suggesting that the location of FG-repeat domains within the NPC correlates with cargo/receptor interactions and that they concomitantly move with cargo through the central pore of the NPC.

Keywords: Nuclear pore complex; nuclear transport; FG-repeats; Nup214; Nup153

2.1 Introduction

Nuclear pore complexes (NPCs) facilitate the exchange of proteins and RNPs between the nucleus and cytoplasm of eukaryotic cells (Fried and Kutay 2003; Mosammaparast and Pemberton 2004). The vertebrate ~125 MDa NPC (Reichelt et al. 1990) is composed of ~30 different proteins (Cronshaw et al. 2002) collectively termed nucleoporins (Nups). Extensive electron microscopy (EM) studies mainly in *Xenopus* oocytes have led to a draft of the 3-D NPC architecture (Hinshaw et al. 1992; Akey and Radermacher 1993; Stoffler et al. 2003; Beck et al. 2004). Accordingly, the NPC is composed of an eightfold symmetric central framework that is continuous with a cytoplasmic and a nuclear ring moiety. Eight cytoplasmic filaments decorate the cytoplasmic ring, whereas the nuclear ring is topped by the nuclear basket. Enclosed by the central framework is the central pore, ~90 nm long and 40-50 nm in diameter in its narrowest part (Pante and Kann 2002; Stoffler et al. 2003), which allows diffusion of small ions and molecules and facilitated, signal-dependent nuclear transport in and out of the nucleus (see (Fahrenkrog and Aebi 2003; Suntharalingam and Wente 2003; Fahrenkrog et al. 2004)).

For typical facilitated nuclear transport, receptors of the karyopherin family recognize nuclear import signals (NLSs) or nuclear export signals (NESs) on their cargo (Fried and Kutay 2003; Mosammaparast and Pemberton 2004). The transport receptor, in turn, is able to mediate the interaction of the cargo-receptor complex with the NPC. It is thought that the main, albeit not the exclusive (Strawn et al. 2004), interaction between the transport receptors and the NPC is mediated by a subset of nucleoporins that harbor FG (phenylalanine-glycine)-repeat domains. Based on X-ray crystallography and biophysical analysis, FG-repeat domains exhibit little secondary structure (Bayliss et al. 2000; Bayliss et al. 2000; Fribourg et al. 2001; Bayliss et al. 2002; Denning et al. 2002; Grant et al. 2002; Denning et al. 2003).

Immuno-EM studies of the vertebrate nucleoporin Nup153 demonstrated a high degree of mobility and structural flexibility of its FG-repeat domain (Fahrenkrog et al. 2002). Nup153 is a constituent of the nuclear basket of the NPC (Pante et al. 1994) and immuno-EM analysis indicates that its N-terminal domain is anchored to the nuclear ring (Walther et al. 2001; Fahrenkrog et al. 2002), whereas its central zinc-finger domain resides at the distal ring (Fahrenkrog et al. 2002). The ~700 amino acid C-terminal domain of Nup153 harbors ~40 FG-repeats, and seems to be flexible within the NPC, since it can be detected at the nuclear basket and even at the cytoplasmic periphery of the central pore (Fahrenkrog et al. 2002). Nup153 is known to be critical for both nuclear import and nuclear export (Bastos et al. 1996; Shah et al. 1998; Nakielny et al. 1999; Ullman et al. 1999; Walther et al. 2001).

The vertebrate nucleoporin Nup214, also called CAN, is an FG-repeat nucleoporin

previously mapped to the cytoplasmic face of the NPC (Kraemer et al. 1994; Pante et al. 1994; Walther et al. 2001). Like Nup153, Nup214 participates in both nuclear import and export (van Deursen et al. 1996). Nup214 depletion, however, does not lead to a complete block of nuclear import (van Deursen et al. 1996; Walther et al. 2002). Based on its amino acid sequence, Nup214 can be subdivided into three distinct domains: a N-terminal domain, a central domain with a region of predicted coiled-coil at its N-terminus, and a C-terminal FG-repeat domain that spans ~800 amino acids (Fornerod et al. 1997) and mediates interactions with various transport factors (Fornerod et al. 1997; Katahira et al. 1999; Kuersten et al. 2002; Rollenhagen et al. 2003).

Based on the structural flexibility and mobility of the FG-repeat domain of Nup153, we asked whether this might be a general attribute of FG-repeat domains, in particular those of peripheral nucleoporins such as Nup214. We therefore aimed to map the domain topology of Nup214 within the 3-D architecture of the NPC. To achieve this, we raised three antibodies against the distinct domains of human Nup214 and determined the precise location of these domains in intact *Xenopus* nuclei as well as in somatic human cells by immuno-EM. Our data clearly show that the three domains of Nup214 are located at distinct sites within the NPC and that the FG-repeat domain of Nup214 is flexible within the NPC. Moreover, our data demonstrate that the localization of the FG-repeat domains of both Nup153 and Nup214 is responsive to transport activity at the nuclear pore.

2.2 Results

2.2.1 Production and characterization of domain-specific antibodies to Nup214

In order to gain a better understanding of the topology and domain accessibility of Nup214 within the NPC, a number of domain-specific antibodies were generated (see Materials and Methods and Fig. 2.1A). To characterize the specificity of these antibodies, their reactivity was tested in an immunoblot (Fig. 2.1B). Each antibody selectively recognized Nup214 in HeLa cell extracts, *Xenopus* egg extracts and among isolated *Xenopus* WGA-binding proteins (Fig. 2.1B, lane 1-3 each panel). The Nup214-A antibody recognizes an additional protein of ~50 kDa in *Xenopus* egg extracts (Fig. 2.1B, arrow head), but not in HeLa cell extracts. This ~50 kDa protein is unlikely to be NPC-associated, however, as it is not detected in an NPC-rich annulate lamellae (AL) fraction (see 214A, Fig. 2.1B). All antibodies recognize to some extent a protein of ~40 kDa (Fig. 2.1B, asterisk). This band is still present in AL prepared in the presence of BAPTA to prevent NPC assembly (most noticeable in the 214D blot, Fig. 2.1B), suggesting that this band is a cross-reacting membrane protein. Together, these tests indicate that, while some cross-reactivity cannot be ruled out, reactivity at the NPC itself should clearly reflect the presence and domain exposure of Nup214.

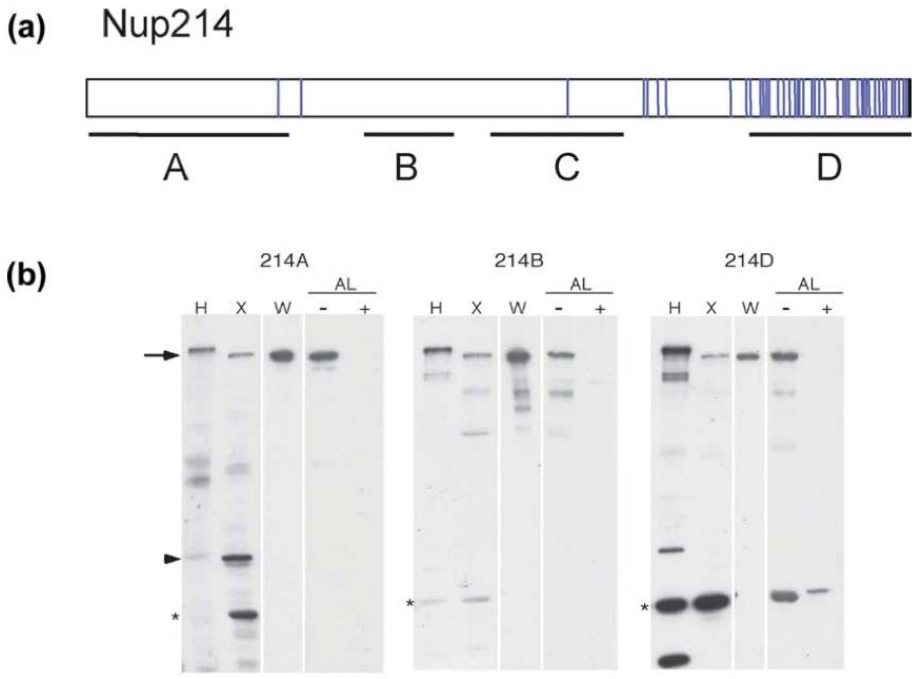

Figure 2.1: Domain-specific Nup214 antibodies. (**A**) Schematic representation of Nup214. Blue lines indicate the positions of individual FG-repeats. Recombinant domains used as immunogens are indicated (see Materials and Methods). (**B**) Nup214 antibodies were used to probe immunoblots. HeLa cell extract (H), *Xenopus* egg extracts (X), *Xenopus* WGA-binding proteins (W) and *Xenopus* annulate lamellae (AL) assembled in the presence or absence of the inhibitor BAPTA (+/-) were separated by SDS-PAGE and processed for immunoblotting (see Material and Methods).

2.2.2 The N-terminal domain of Nup214 localizes to the cytoplasmic side of the NPC

To localize the distinct domains of Nup214 within the NPC, we used domain-specific antibodies for immuno-EM. Although the antibodies were raised against human Nup214, *Xenopus* oocyte nuclei were used due to the better structural resolution and higher density of NPCs in comparison to somatic cells. Intact nuclei were isolated and incubated with anti-Nup214-A antibody, a secondary anti-rabbit IgG antibody conjugated to 10-nm colloidal gold, and then analyzed by thin section immuno-EM. We found the N-terminal domain of Nup214 to reside close to the nuclear membrane at a mean distance from the central plane of the NE of 31 nm (± 6 nm; Table 2.1), corresponding to an epitope at the cytoplasmic ring of the NPC. The anti-Nup214-A antibody showed some degree of cross reactivity in *Xenopus* nuclei with an epitope at the nuclear basket (data not shown). Based on Western blot analysis (Fig. 2.1B) we suppose this to be the protein of ~50 kDa, which is recognized by the antibody in *Xenopus* but not in human.

To confirm the exclusive cytoplasmic location of the N-terminal domain of Nup214 we determined its location in HL-60 cells, human promyelocytic leukocytes. As shown in Fig. 2.2A, in these human somatic cells the anti-Nup214-A recognized an epitope exclusively on the cytoplasmic side of the NE. Quantification of the gold particle distribution (Fig. 2.2B and Table 2.1) revealed a mean distance of 20 nm (± 13 nm) from the central plane of the NE and a corresponding average radial distance of 15 nm (± 13 nm), representing an epitope near or at the cytoplasmic ring of the NPC.

Antibody	*Xenopus laevis*	HL-60 cells
Anti-Nup214-A	+31 nm±6 nm	+20 nm±13 nm
Anti-Nup214-B	+21 nm±12 nm	+9 nm±10 nm
Anti-Nup214-D	+11 nm±10 nm	+14 nm±12 nm
Anti-Nup214-D	–29nm±12 nm	–30 nm±12 nm
Anti-Nup214-D	–86 nm±13 nm	–75 nm±18 nm

Numbers represent the distance from the central plane of the NPC. +, cytoplasmic; −, nuclear.

Table 2.1: Comparison of the location of different Nup214 domains in *Xenopus nuclei* versus HL-60 cells.

2.2.3 Location of the central domain of Nup214

We next examined the location of the central domain of Nup214 within the NPC. Intact *Xenopus* oocyte nuclei were isolated and incubated with anti-Nup214-B (see Fig. 2.1), a secondary anti-rabbit IgG antibody conjugated to 10-nm colloidal gold and analyzed by thin section immuno-EM.

As shown in Fig. 2.2C, the anti-Nup214-B antibody exclusively labelled the cytoplasmic face of the NPC. Quantification of the gold particle distribution (Fig. 2.2D and Table 2.1) revealed an average distance of 21 nm (± 12 nm) from the central plane of the NE. A corresponding mean radial distance of 17 nm (± 15 nm) indicated that this location resides near or at the cytoplasmic ring of the NPC near the entry to the central pore. These results were confirmed in HL-60 cells (see Table 2.1).

2.2.4 The C-terminal domain of Nup214 is flexible

Next, we wanted to resolve the location of the C-terminal FG-repeat domain of Nup214. As before, isolated intact *Xenopus* nuclei were incubated with the repeat domain antibody (anti-Nup214-D) and a secondary anti-rabbit IgG antibody conjugated to 10-nm colloidal gold. The epitope recognized by the antibody was analyzed by thin section immuno-EM.

As shown in Fig. 2.2E, the anti-Nup214-D recognized epitopes on both the cytoplasmic and the nuclear face of the NPC. Quantification of the labelling pattern (Fig. 2.2F and Table 2.1) relative to the central plane of the NPC revealed that 87% of the particles were detected at a mean distance of 11 nm (± 10 nm). With corresponding mean radial distances of 12 nm (± 11 nm), this labelling pattern is consistent with a location near or at the cytoplasmic ring. 13% of the gold particles were found on the nuclear side of the NPC, of which 2% were detected at a mean distance of -29 nm (± 12 nm) and 11% at -86 nm (± 12 nm), reflecting epitopes within the nuclear basket of the NPC. Again, these results were confirmed in HL-60 cells and a similar distribution was observed (see Table 2.1). Moreover, similar results were obtained in *Xenopus* nuclei with a distinct anti-peptide antibody raised against the FG-repeat domain of human Nup214 (R. Kehlenbach and B. Fahrenkrog, unpublished results). Taken together, the multiple locations of the C-terminal, FG-repeat domain of Nup214 indicate a flexible topology of this domain.

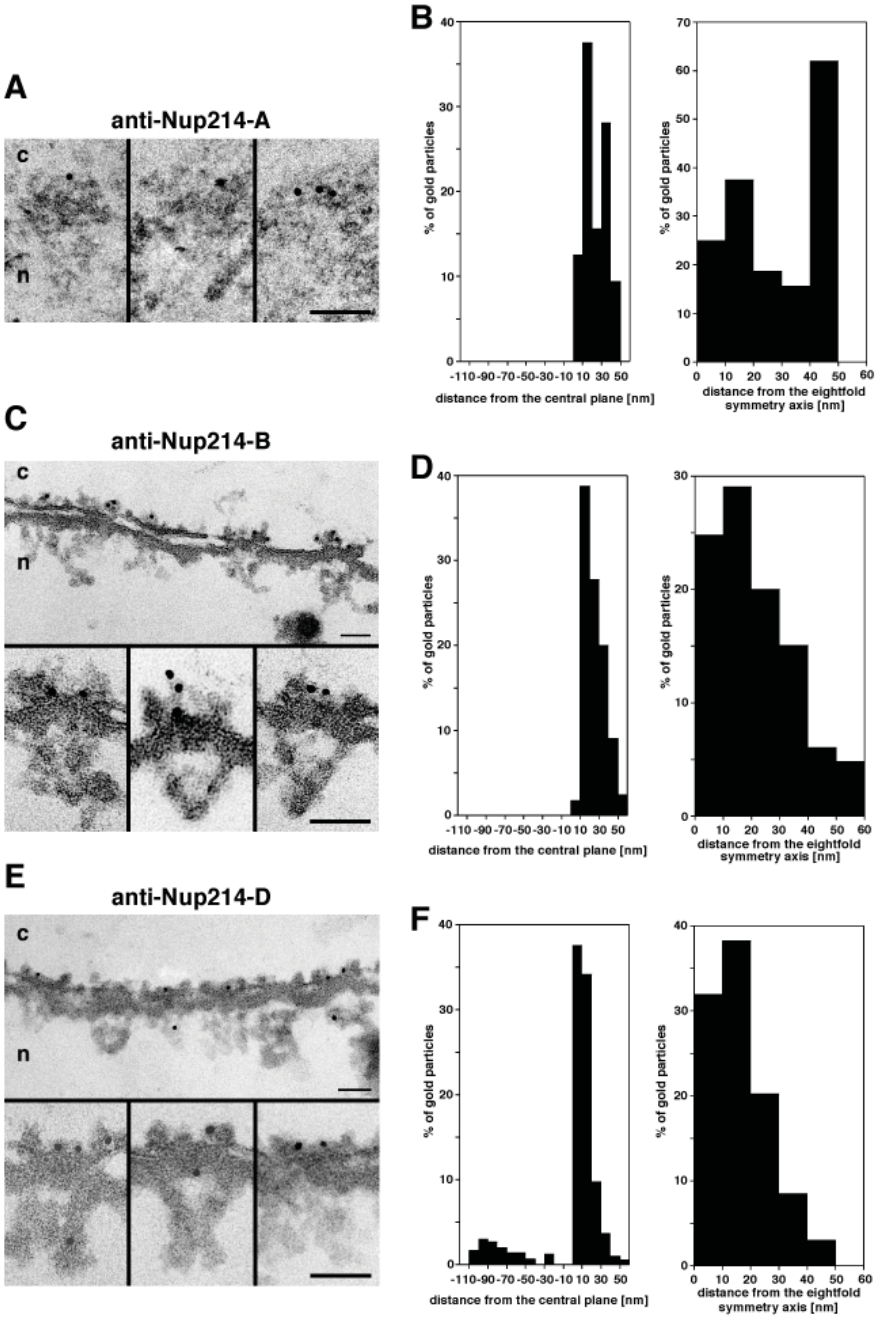

Figure 2.2: Domain-topology of Nup214 within the NPC. (**A**) HL-60 cells were pre-embedding labelled with anti-Nup214-A antibody and a secondary anti-rabbit IgG antibody conjugated to 10-nm gold and prepared for thin section EM. Shown are selected examples of gold-labelled NPCs in cross-section. c, cytoplasm; n, nucleus (**B**) Quantitative analysis of the gold particle distribution associated with the NPC. 36 gold particles were scored. (**C**) Intact isolated *Xenopus* nuclei were incubated with anti-Nup214-B antibody and (**E**) anti-Nup214-D antibody and a secondary anti-rabbit IgG antibody conjugated to 10-nm colloidal gold. Shown are a stretch along the NE in cross-sections (top) and a gallery of selected examples of gold-labelled NPCs (bottom). c, cytoplasm; n, nucleus. (**D**) Quantification of the gold particles associated with the NPC after labelling with the anti-Nup214-B antibody and (**F**) with the anti-Nup214-D antibody. One hundred sixty-six and two hundred fifty-nine, respectively, gold particles were scored. Scale bars, 100 nm.

2.2.5 Recombinant expression of epitope-tagged hNup214 into *Xenopus* NPCs

Previously we have shown that tagged hNup153 incorporates into the NPC after microinjection of a plasmid encoding epitope-tagged hNup153 into the nuclei of *Xenopus* oocytes (Fahrenkrog et al. 2002). We therefore aimed to confirm the location of the N-terminus and the multiple locations of the C-terminus of Nup214 by similarly employing epitope tagged versions of Nup214. To achieve this, we generated a plasmid encoding hNup214 with either a N-terminal GFP-tag (GFP-Nup214) or a C-terminal myc-tag (Nup214-myc). By transient transfection of different cultured cell lines we first verified that the fusion proteins were expressed and incorporated into the NPC (Fig. 2.S1). Next, we microinjected the plasmids into the nuclei of *Xenopus* oocytes. To determine the location of the incorporated proteins we used either a polyclonal anti-GFP antibody or a monoclonal anti-myc antibody, both directly conjugated to 8-nm colloidal gold.

As shown in Fig. 2.3A, the N-terminal GFP-tag localizes predominantly to the cytoplasmic face of the NPC (mean distance from the central plane of the NPC 25 nm ± 9 nm with radial distances of 12 nm ± 10 nm). However, about 23% of the gold particles associated with the nuclear side of the NPC (Fig. 2.3B). This nuclear signal may be due in part to some mislocalization previously shown to be caused by overexpression (Boer et al. 1997)

As shown in Fig. 2.3C, the C-terminal myc-tag localizes to both faces of the NPC. Quantification of the labelling distribution revealed that 63% of the gold particles were associated with the cytoplasmic side of the NPC (mean distance from the central plane of the NPC 31 nm ± 11 nm with a corresponding radial distance of 19 nm ± 13 nm). 37% of the gold particles labelled the nuclear face of the NPC. Of these, 13 % of the gold particles

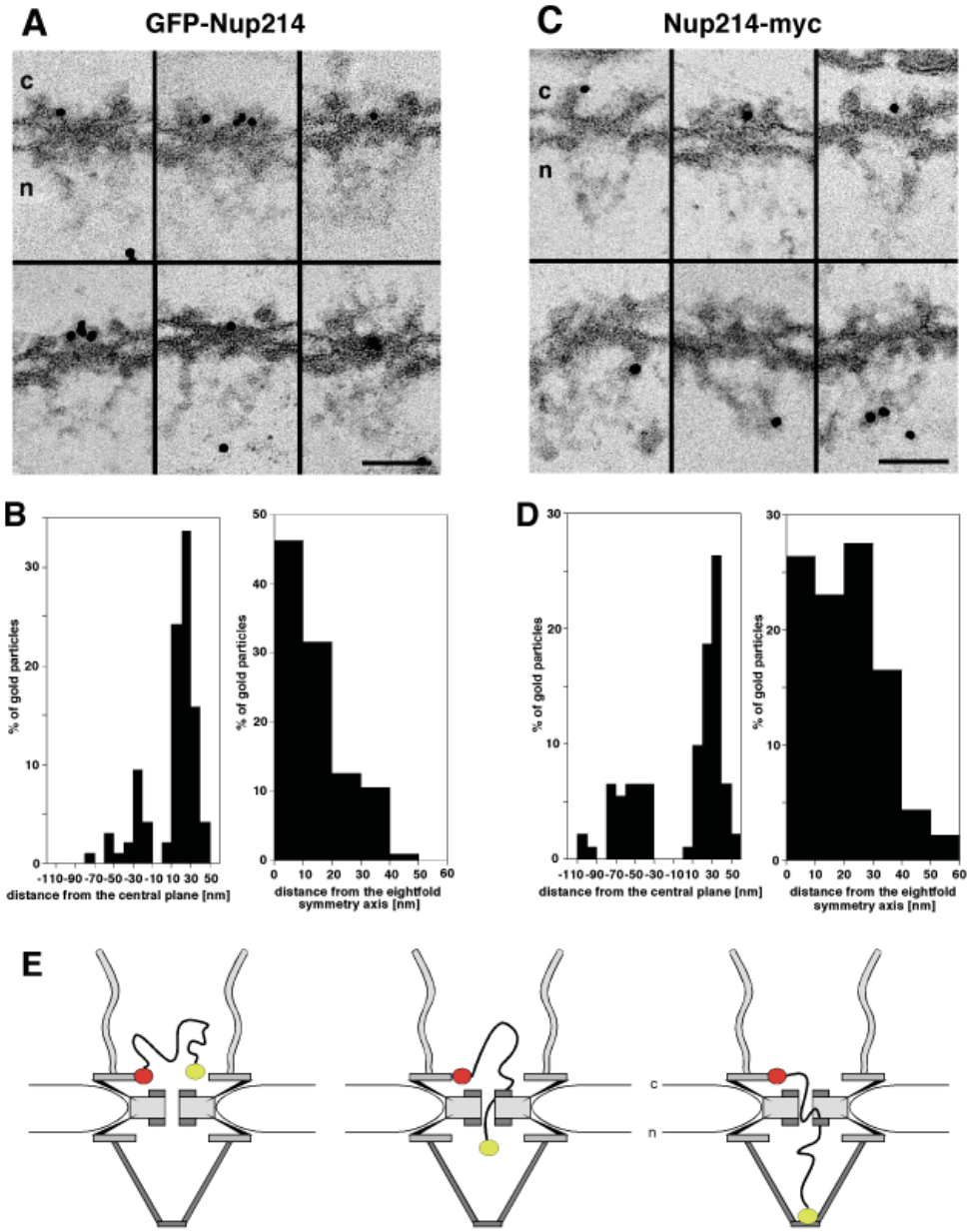

Figure 2.3: Incorporation of tagged hNup214 into *Xenopus* NPCs. (**A**) Immunolocalization of N-terminally GFP-tagged Nup214 (GFP-Nup214) expressed in *Xenopus* oocytes with a polyclonal anti-GFP antibody directly conjugated to 8-nm colloidal gold. Selected examples of labelled NPCs in cross-sections are shown. c, cytoplasm; n, nucleus. (**B**) Quantification of the gold particle distribution associated with the NPC after labelling with an anti-GFP antibody. Ninety-seven gold particles were scored. (**C**) Immunolocalization of C-terminally myc-tagged Nup214 (Nup214-myc) expressed in *Xenopus* oocytes with a monoclonal anti-myc antibody directly conjugated to 8-nm colloidal gold. Selected examples of gold-labelled NPCs are shown. c, cytoplasm; n, nucleus. (**D**) Quantitative analysis of the distribution of gold particles associated with the NPC after labelling with an anti-myc antibody. Ninety-two gold particles were scored. (**E**) Schematic representation of the domain-topology of Nup214 in the 3-D architecture of the NPC. Nup214 is anchored to the cytoplasmic ring of the NPC by its N-terminal and central domain (red), whereas the C-terminal FG-repeat domain (yellow) is flexible and can be mapped at the cytoplasmic face of the NPC (left), the nuclear periphery of the central pore (middle), and even at the distal ring of the nuclear basket (right). c, cytoplasm; n, nucleus. Scale bars, 100 nm.

were found at a mean distance of-40 nm ± 7 nm, and 24 % at a mean distance of -76 nm ± 14 nm from the central plane representing locations within the nuclear basket of the NPC. Taking into account that some gold particles might be associated with the nuclear face of the NPC due to overexpression (~23%; see above), we estimate that ~14% of the gold particles should reflect specific location of this region to the nuclear side of the NPC. This extent of C-terminal myc-tag detection is similar to the labelling seen with the domain-specific antibody against the FG-repeat domain of Nup214 (anti-Nup214-D; see above and Fig. 2.2E and F).

Taken together, our immuno-EM data using domain-specific antibodies and incorporation of epitope-tagged hNup214 into *Xenopus* oocyte NPCs suggest that the N-terminal and central region of Nup214 are anchored near or at the cytoplasmic ring of the NPC, whereas the C-terminal FG-repeat domain is flexible and present on both the cytoplasmic and nuclear periphery of the NPC (Fig. 2.3E).

2.2.6 Attenuation of nuclear transport constrains FG-repeat domains to their anchoring site

The pronounced heterogeneous distribution of FG-repeat domains could be due to mobility that is linked to nuclear transport activity, especially in cargo translocation through the central pore of the NPC. This hypothesis predicts that the location of the FG-repeat domains within the NPC would be influenced by the transport activity of the NPC. We therefore analyzed whether the location of the FG-repeat domains of the nucleoporins Nup153 and Nup214 is dependent on the transport state of the cell.

Nuclear transport is readily attenuated at 4°C (Pante and Aebi 1996). To study the influence of attenuated nuclear transport on the location of the FG-repeat domains of Nup153 and Nup214, nuclei were isolated from *Xenopus* oocytes and incubated at 4°C for 1h. After fixation in 4% formaldehyde, the nuclei were labelled with anti-Nup153-C2 antibody (Fahrenkrog et al. 2002) or anti-Nup214-D antibody to determine the location of the FG-repeat domains of these nucleoporins under these conditions.

At steady-state, the FG-repeat domain of Nup153 localizes to the nuclear basket as well as to some extent (~12%) to the cytoplasmic periphery of the central pore (Fahrenkrog et al. 2002). In contrast, when nuclear transport is arrested, the anti-Nup153-C2 antibody exclusively decorates the nuclear face of the NPC (Fig. 2.4A). 76% of the gold particles were found in the area of the distal ring of the NPC (mean distance from the central plane of the NPC -77 nm ± 12 nm) and 24% of the gold particles were closer to the nuclear ring (mean distance of -36 nm ± 9 nm from the central plane) (Fig. 2.4B). Under the same conditions,

the expression level of Nup153 does not change within the nuclei and the location of the N-terminal and the central Zn-finger domain of Nup153 are not altered in comparison to steady-state conditions (Fig. 2.S2A).

The FG-repeat domain of Nup214 localizes to the cytoplasmic periphery of the

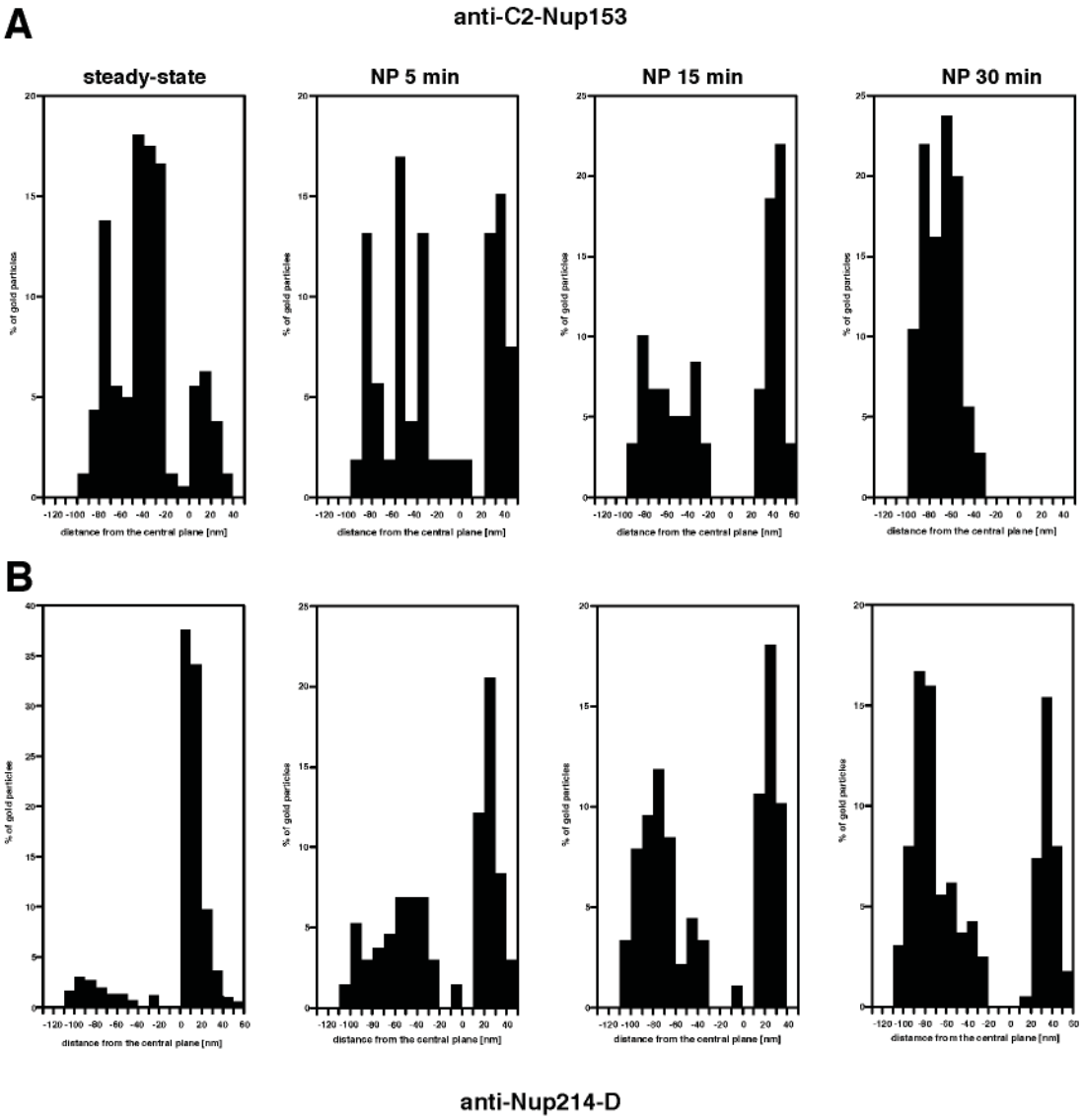

Figure 2.4: Attenuated nuclear transport constrains the FG-repeat domains of Nup153 and Nup214 to their anchoring site in the NPC. (**A**) Isolated *Xenopus* nuclei were incubated at 4°C prior labelling with an antibody against the FG-repeat domain of Nup153 (anti-C2-Nup153) directly conjugated to 8-nm colloidal gold. c, cytoplasm; n, nucleus. (**B**) Quantitative analysis of the gold particles associated with the NPC after labelling with the anti-C2-Nup153 antibody at 4°C. Eighty-eight gold particles were scored. (**C**) Immunolabelling of isolated *Xenopus* nuclei after incubation at 4°C with the anti-Nup214-D antibody and a secondary anti-rabbit IgG antibody conjugated to 10-nm colloidal gold. c, cytoplasm; n, nucleus. (**D**) Quantification of the gold particle distribution associated with the NPC after labelling with the anti-Nup214-D antibody at 4°C. One hundred thirty-four gold particles were scored. Scale bars, 100 nm.

central pore and, additionally, to the nuclear side of the NPC at steady-state (Figs. 2.2 and 2.3). At 4°C, when nuclear transport is attenuated, the FG-repeat domain of Nup214 localizes exclusively to the cytoplasmic periphery of the central pore at a mean distance of 25 nm ± 11 nm (Fig. 2.4D). Attenuation of nuclear transport at 4°C has no effect on the expression level of Nup214 in the oocyte nuclei or significantly influenced the location of the central domain of Nup214 (Fig. 2.S2B).

Similar results for Nup153 were obtained when nuclear transport was attenuated by either WGA or a dominant-negative mutant of importin-β, importin-β 45-462, known to inhibit distinct nuclear transport pathways (Kutay et al. 1997) (Fig. 2.S3A). In case of Nup214, however, the distribution of the FG-repeat domain after attenuating nuclear transport by either WGA or importin-β 45-462 was similar to steady-state conditions (Fig. 2.S3B). Therefore, attenuating nuclear transport at 4°C constrains the distribution of the FG-repeat domains of Nup153 as well as Nup214 to the site at which the corresponding nucleoporin is anchored within the NPC, whereas WGA and importin-β 45-462 have different influence on the distribution of the FG-repeat domains of Nup153 as compared to Nup214.

2.2.7 Nuclear import cargo influences the localization of FG-repeat domains

Next we attempted to interfere with steady-state nuclear transport by challenging the system with an excess of import cargo and then analyzing how this influences the location of the FG-repeat domains of Nup153 and Nup214 within the NPC. As import cargo we used nucleoplasmin, a nuclear protein that readily becomes imported in *Xenopus* oocytes (Dingwall et al. 1982; Adam et al. 1992). To study the effect of import cargo on the location of the FG-repeat domains of Nup153 and Nup214, we isolated nuclei from *Xenopus* oocytes and incubated them in an import competent mixture containing excess nucleoplasmin. The nuclei were incubated for various length of time in this import mixture and then labelled with anti-Nup153-C2 or anti-Nup214-D antibody to determine the location of these FG-repeat domains.

As shown in Fig. 2.5A (and Fig. 2.S4A), after 5 min of incubation, the FG-repeat domain of Nup153 localizes to both sides of the NPC, as observed previously (Fahrenkrog et al. 2002). In comparison to steady-state conditions, however, the number of NPCs that are labelled on their cytoplasmic side has significantly increased to 39% in the presence of excessive nucleoplasmin versus 12% at steady-state (Fahrenkrog et al. 2002). The percentage of cytoplasmic labelling further increases to 50% after 15 min of incubation (Fig. 2.5A). Finally, after 30 min incubation the FG-repeat domain of Nup153 localizes exclusively to the nuclear face of the NPC (Fig. 2.5A) with approximately 90% of the gold being located at the distal ring of the NPC. Import mixture alone without addition of nucleoplasmin has no influence on the location of the FG-repeat domain of Nup153 (Fig. 2.S5A). The location

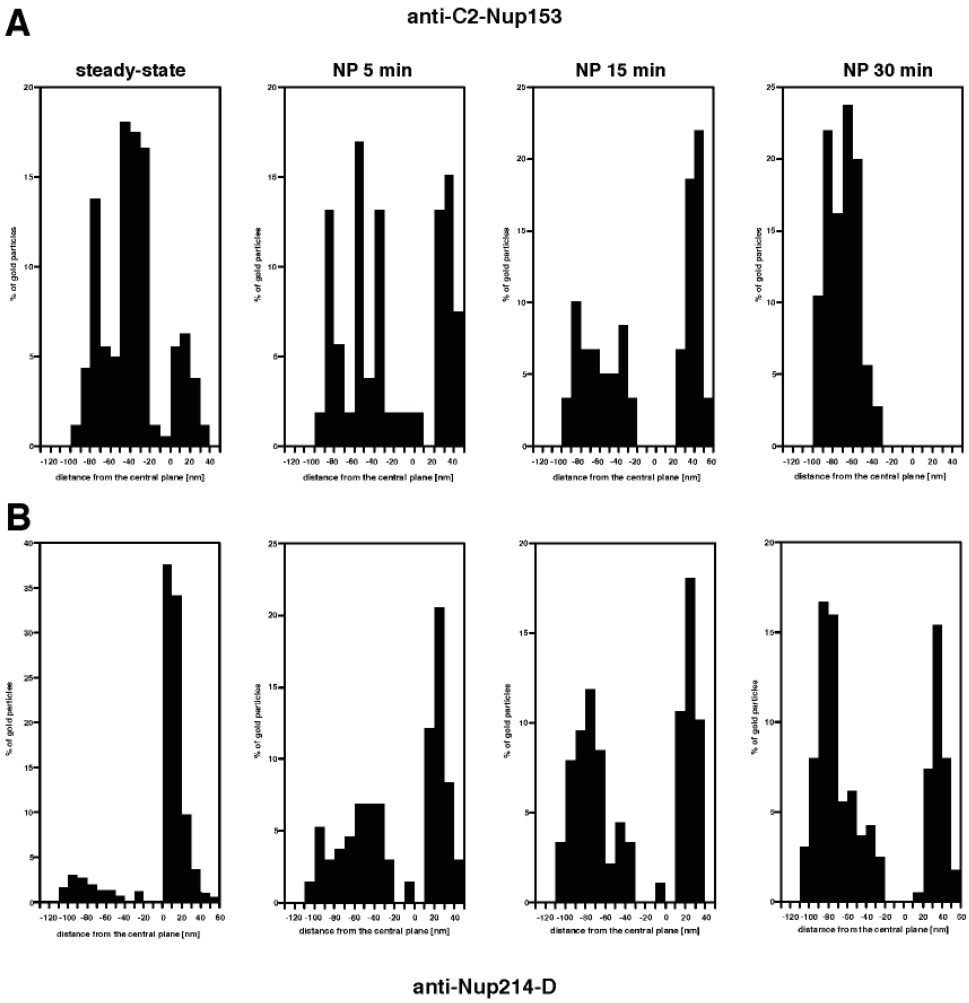

Figure 2.5: The location of the FG-repeat domains of Nup153 and Nup214 in the presence of excess import cargo. Quantitative analysis of the gold particles associated with the NPC after labelling with (**A**) the anti-C2-Nup153 antibody and (**B**) the anti-Nup214-D antibody, respectively, in the presence of excess nucleoplasmin. Import of nucleoplasmin into isolated intact *Xenopus* oocytes nuclei was allowed for the indicated time-points before the nuclei were shortly prefixed in formaldehyde and pre-embedding labelled with the corresponding antibody. The following number of gold particles were scored for the individual experiments: fifty-five (anti-C2-Nup153, 5 min), sixty (anti-C2-Nup153, 15 min), one hundred and six (anti-C2-Nup153, 30 min), one hundred thirty-two (anti-Nup214-D, 5 min), one hundred seventy-eight (anti-Nup214-D, 15 min), and one hundred sixty-three (anti-Nup214-D, 30 min).

of the N-terminal and the central Zn-finger domain of Nup153 remained unchanged in the presence of import mixture containing excess nucleoplasmin (Fig. 2.S5B and C).

Under the same incubation conditions, the FG-repeat domain of Nup214 also shows a higher proportion of nucleoplasmic location in comparison to steady-state conditions (Fig. 2.5B). Whereas at steady-state conditions about 13% of the NPCs were labelled on the nuclear side (see above), after incubation for 5 min. in excess nucleoplasmin this fraction increased to 43%, and further to about 60% after 15 min and 30 min (Fig. 2.5B; see also

Fig. 2.S4B). As the number of gold particles associated with the nuclear face of the NPC increased, the cytoplasmic value decreased correspondingly from ~57% after 5 min to ~33% after 30 min incubation with nucleoplasmin.

Taken together, our data suggest that the localizations of the FG-repeat domains of Nup153 and Nup214 shift, corresponding to a wave of transport moving through the NPC and possibily reflecting steps which promote a certain arrangement of the FG-repeat domain in the bulk of transport events at each particular time point.

2.2.8 The influence of RNA export on the localization of FG-repeat domains

Next we wanted to examine how excess export cargo would influence the location of the FG-repeat domains of Nup153 and Nup214. We therefore isolated poly (A+) RNA from HeLa cells and microinjected this RNA into the nuclei of *Xenopus* oocytes. Nuclei were isolated following various incubation times and labelled with either the anti-Nup153-C2 antibody or the anti-Nup214-D antibody. Since RNA export is slower than protein import (Pante et al. 1997), longer incubation times were performed.

As illustrated in Fig. 2.6A (and Fig. 2.S6A), the FG-repeat domain of Nup153 localizes predominantly to the nuclear face of the NPC 30 min after microinjection of poly (A+) RNA into the nuclei of *Xenopus* oocytes. Compared to steady-state conditions (Fahrenkrog et al. 2002) (Fig. 2.6A, first panel), however, the number of the gold particles associated with the cytoplasmic side of the NPC increased to ~26% (Fig. 2.6A, second panel). The cytoplasmic location of the FG-repeat domain of Nup153 further increased by 60 min of incubation with excess poly (A+) RNA (Fig. 2.6A, third panel), when 37% of the gold particles were detected on this side of the NPC. By 90 min, the cytoplasmic proportion of the FG-repeat domain of Nup153 reached its maximum to ~63% (Fig. 2.6A, fourth panel).

Microinjection of poly (A+) RNA into the nucleus of *Xenopus* oocytes results in a predominant nuclear localization of the FG-repeats of Nup214 after 30 min of incubation

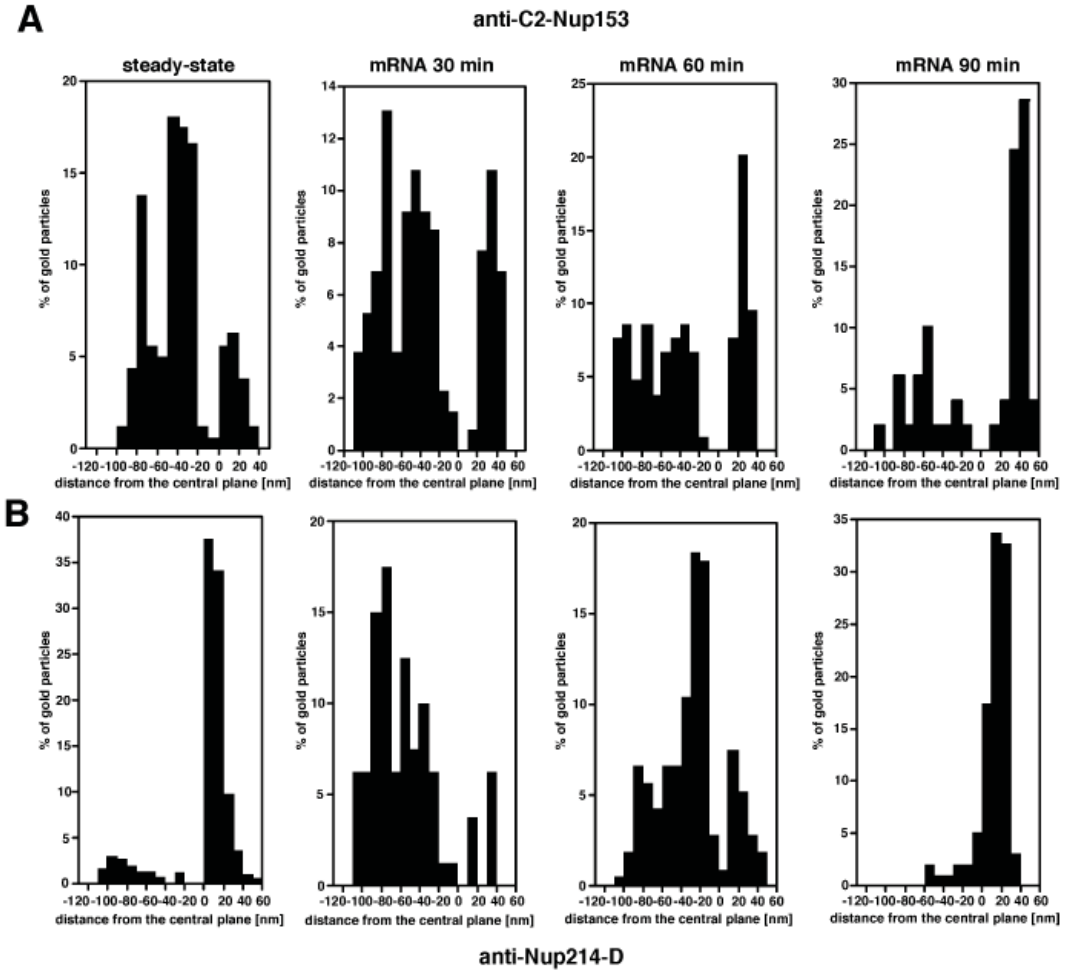

Figure 2.6: The influence of export cargo on the location of the FG-repeat domains of Nup153 and Nup214. Quantification of the gold particle distribution associated with the NPC after microinjection of poly (A+) RNA into the nuclei of *Xenopus* oocytes and pre-embedding labelling with the (**A**) anti-C2-Nup153 and the (**B**) anti-Nup214-D antibody. The following numbers of gold particles were scored for the individual experiments: one hundred thirty (anti-C2-Nup153, 30 min), one hundred four (anti-C2-Nup153, 60 min), forty-nine (anti-C2-Nup153, 90 min), eighty (anti-Nup214-D, 30 min), two hundred twelve (anti-Nup214-D, 60 min), and eighty (anti-Nup214-D, 90 min).

(Fig. 2.6B; see also Fig. 2.S6B). 89 % of the gold particles were on the nuclear side of the NPC and predominantly at or near the distal ring of the NPC, whereas only ~11 % of the gold particles were found to be associated with the cytoplasmic face of the NPC. 60 min after microinjection of RNA into *Xenopus* nuclei (Fig. 2.6B, third panel) ~80 % of the gold particles were associated with the nuclear side of the NPC (67% of these in the area of the central pore) and ~20 % associated with the cytoplasmic face. After 90 min (Fig. 2.6B, fourth panel), ~92% of the gold particles were detected on the cytoplasmic face of the NPC and only ~8% on its nuclear side, similar to steady-state conditions. Largely analogous results were obtained after microinjection of total RNA isolated from HeLa cells into the nuclei of *Xenopus* oocytes, except for the 90 min time point in case of Nup153 (Figs. S7 and S8). This

might reflect a difference in Nup153 conformation in the presence of excess mRNA versus, for example, ribosomal RNA, which is present in the total RNA preparation.

In conclusion, the location of Nup153 and Nup214 FG-repeat domains shifts concomitant with a transport wave of export cargo through the NPC.

2.2.9 Localization of FG-repeat domains in nuclei that lack RNA export cargo

Next, we assessed whether depletion of cargo would also bias the location of the FG-repeat domains of Nup153 and Nup214 within the NPC. To do so, we injected actinomycin D into the nuclei of *Xenopus* oocytes to inhibit endogenous RNA polymerases. After 3h incubation of actinomycin D treatment, the location of the FG-repeat domains of Nup153 and Nup214 in manually isolated *Xenopus* nuclei was determined by immuno-EM.

As shown in Fig. 2.7A (see also Fig. 2.S9A), depletion of RNA polymerase I and II

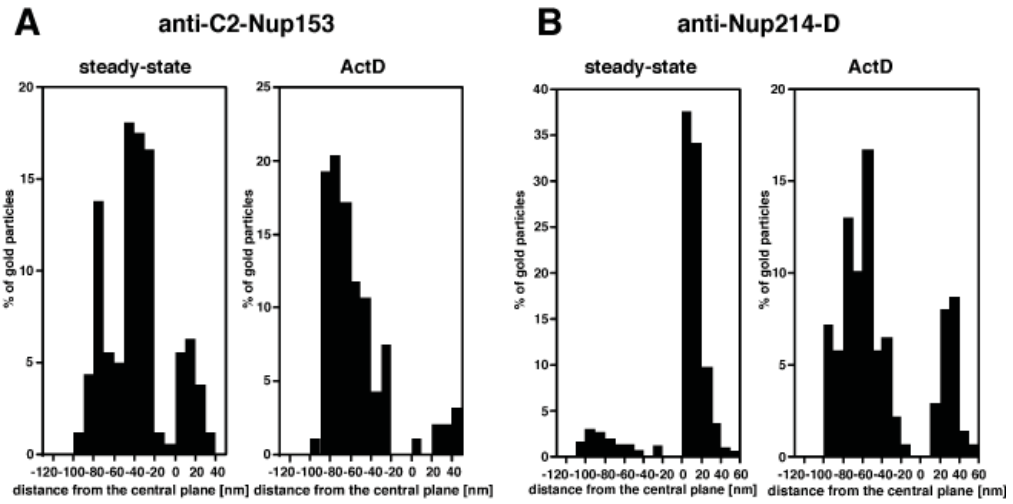

Figure 2.7: Actinomycin D and its influence on the location of the FG-repeat domains of Nup153 and Nup214. Actinomycin D was microinjected into the nuclei of *Xenopus* oocytes 3 hours prior nuclei isolation and pre-embedding labelling with the anti-C2-Nup153 and the anti-Nup214-D antibody, respectively. Quantification of the gold particle distribution associated with the NPC after labelling with the (**A**) anti-C2-Nup153 antibody and (**B**) the anti-Nup214-D antibody, respectively. Ninety-five gold particles were scored for the anti-C2-Nup153 antibody and one hundred forty for the anti-Nup214-D antibody.

transcripts has only a slight effect on the location of the FG-repeat domain of Nup153. 8 % of the gold particles were detected on the cytoplasmic face of the NPC. On the nuclear side, 22 % of the gold particles were found at or near the nuclear ring of the NPC and 70 % at or near the distal ring. In comparison to steady-state conditions, this represents a movement of the FG-repeats towards the distal ring on the nuclear side of the NPC (70 % versus 34 % at steady state), whereas the cytoplasmic value is rather unaffected (8 % versus 12 % at steady-state (Fahrenkrog et al. 2002)).

In contrast, the location of the FG-repeat domain of Nup214 is more strongly influenced by the treatment of *Xenopus* nuclei with actinomycin D. Compared to steady-state, actinomycin D treatment leads to increased nuclear localization Nup214 FG-repeat domain (Fig. 2.7B and Fig. 2.S9B). In the absence of transcription, 76% of the gold particles were associated with the nuclear side of the NPC, whereas only 25 % of the gold particles were found on the cytoplasmic face of the NPC.

Taken together, preventing new transcription in *Xenopus* nuclei appears to cause an arrest of the FG-repeat domains of Nup153 and Nup214 near or at the distal ring of the NPC.

2.3 Discussion

Along with the identification of presumably all vertebrate nucleoporins (Cronshaw et al. 2002), many of these nucleoporins have been mapped within the NPC by different immuno-EM techniques (Belgareh et al. 2001; Walther et al. 2001; Fahrenkrog et al. 2002; Frosst et al. 2002; Walther et al. 2002; Enninga et al. 2003; Griffis et al. 2003). Nucleoporins are large proteins with, at least in case of the FG-repeat nucleoporins, flexibility in secondary structure that implies a complex topology within the NPC. Individual antibodies against a particular nucleoporin therefore do not yield a holistic view of the organization of this nucleoporin within the 3-D architecture of the NPC. In contrast, use of domain-specific antibodies against nucleoporins, such as Nup153 (Fahrenkrog et al. 2002) and Tpr (Frosst et al. 2002; Krull et al. 2004) has helped to resolve discrepancies regarding their localization and organization within the vertebrate NPC. Moreover, in the case of the FG-repeat nucleoporin Nup153, this approach revealed that while its N-terminal domain and central zinc-finger domain are stationary within the NPC, the C-terminal FG-repeat domain exhibits a wider distribution. With the present study we have now resolved the domain organization and topology of another large FG-repeat nucleoporin, Nup214, within the NPC. Moreover, by immuno-EM we show for the first time that the location of the FG-repeat domains of Nup153 and Nup214 is influenced by the transport state of the cell.

2.3.1 Multiple-site topology of Nup214 within the NPC

To determine the spatial organization of a given nucleoporin within the 3-D NPC architecture, domain-specific antibodies are required (Fahrenkrog et al., 2002; Frosst et al., 2002). By this approach, we show here that the N-terminal domain of Nup214 resides near or at the cytoplasmic ring of the NPC close to the entry to the central pore (see Fig. 2.2A, 2.3A and 2.3E), consistent with a previous finding (Walther et al. 2002) in which a polyclonal antibody against an N-terminal fragment of *Xenopus* Nup214 was used. We further found that the central domain of Nup214 is also stationary and localizes near or at the cytoplasmic ring of the NPC, too (see Figs. 2.2C and 2.3E). This is in agreement with the location reported by Kraemer et al. using a polyclonal antibody specific for the central region of human Nup214 (Kraemer et al. 1994).

With the present study we have for the first time mapped the FG-repeat domain of Nup214 within the NPC. Interestingly, this domain is not confined to a specific subdomain of the NPC. Instead, by using domain-specific antibodies and by expressing C-terminal myc-tagged Nup214 in *Xenopus* oocytes, we could show that this domain is flexible in its arrangement, appearing at both the cytoplasmic and nuclear face of the NPC (see Figs. 2.2E, 2.3C, and 2.3E).

Taken together, our immuno-EM studies on the domain topology of Nup214 suggest that it is anchored to the cytoplasmic face of the NPC by its N-terminal and/or central domain, whereas the FG-repeat domain of Nup214 is flexible within the NPC and might exist in a rather unstructured, more or less extended conformation.

2.3.2 Natively unfolded, extended character of FG-repeat domains

The C-terminal domain of Nup214 spans about 800 amino acids (residues 1225 to 2091 of the human protein). Biophysical measurements have suggested that the FG-repeat domains of yeast nucleoporins are natively unfolded, i.e. they have little secondary structure (Denning et al. 2002; Denning et al. 2003). This leads to the possibility that the FG-repeat domains of vertebrate nucleoporins, too, have little secondary structure, and might have a more or less extended conformation. If extended, the FG-repeat domain of Nup214 could span a distance of up to ~275 nm (Strelkov et al. 2002). This length would easily allow the repeat domain to span the distance from the cytoplasmic periphery of the NPC to the distal ring of the nuclear basket. Indeed, secondary structure prediction reveals that the FG-repeat domain of Nup214 to be predominantly unstructured (S.M. Paulillo, O. Mayans and B. Fahrenkrog, unpublished data). Moreover, ~67% of the amino acids of the FG-repeat

domain of human Nup214/CAN have disorder-promoting character (data not shown; (Dunker et al. 2001; Uversky 2002)). These disorder-promoting residues are scattered across the FG-repeat domain, further supporting the notion that the FG-repeat domain has an extended conformation. Based on immuno-EM data an extended conformation has also been suggested for the FG-repeat domain of Nup153, which spans about 700 amino acids (Fahrenkrog et al. 2002). Again, about 62% of the amino acids of the FG-repeat domain of *Xenopus* Nup153 have disorder-promoting character (data not shown). Furthermore, atomic force microscopy measurements indeed revealed that the FG-repeat domain of Nup153 has an extended conformation (R. Lim, J. Koeser, and U. Aebi; personal communication).

Natively unfolded, extended proteins usually encompass multiple binding domains and are thus capable of simultaneous interactions with multiple binding partners (Dunker et al. 2001; Uversky 2002). Both Nup153 and Nup214 are able to interact with a number of different nuclear transport receptors (Boer et al. 1997; Fornerod et al. 1997; Shah et al. 1998; Katahira et al. 1999). The flexible nature of their FG-repeat domains would allow Nup153 and Nup214 to act as scaffolds for the assembly of transport complexes. The export complex that mediates the recycling of Kap60p, the yeast importin-α, is formed directly at the yeast FG-nucleoporin Nup2p (Matsuura et al. 2003). Furthermore, it has been shown that the U1 snRNP import complex is formed while associated with Nup214 (Rollenhagen et al. 2003).

2.3.3 Flexible FG-repeat domains: implications for nuclear transport

Our localization studies have revealed the FG-repeat domain of Nup214 to be flexible within the NPC. Similarly, we have documented the FG-repeat domain of Nup153 to also be flexible within the NPC (Fahrenkrog et al., 2002). Here, we have now shown that the location of the FG-repeat domains of Nup153 and Nup214 is correlated to the transport state of the cell, suggesting that they may associate with cargo-receptor complexes and accompany them through the central pore.

Arresting nuclear transport constrains the spatial distribution of flexible FG-repeat domains of both nucleoporins to their respective anchoring sites within the NPC, i.e. the distal ring of the NPC in case of Nup153 and near the cytoplasmic ring in case of Nup214 (see Fig. 2.4). A surge of nuclear import promotes cytoplasmic exposure of the FG-repeat domain of Nup153 followed by a distribution predominantly on the nuclear face of the NPC (see Fig. 2.5). The spatial distribution of the FG-repeat domain of Nup214 appears responsive to import cargo as well. In the presence of excess import cargo, Nup214's FG-repeat domain transiently accumulates at the nuclear NPC periphery. Similarly, the FG-repeat domain of Nup153 predominates on the nuclear side under these conditions. These results indicate

that the spatial distribution of the FG-repeat domains within the NPC correlates with cargo/receptor interactions.

Microinjecting excess poly (A+) RNA into the nucleus leads first to a higher frequency of the FG-repeat domains of Nup214 on the nuclear face of the NPC (see Fig. 2.6). Next, the nuclear portion of the FG-repeat domains of Nup153 and Nup214 decreases as the cytoplasmic portion increases. At late time points, when the burst of poly (A+) RNA export is presumably complete, the FG-repeat distribution within the NPC returns to steady-state conditions. In the case of RNA export the spatial location of the FG-repeat domains of Nup153 and Nup214 is biased toward the point of cargo contact, and seems to shift concomitantly with the cargo through the central pore of the NPC.

Surprisingly, recent studies in yeast have shown that FG-repeat domains of asymmetric nucleoporins are not essential for receptor-mediated nuclear transport and that the importin-β pathway is rather unaffected by depleting the maximal number of FG-repeats (Strawn et al. 2004; Zeitler and Weis 2004). Asymmetric nucleoporins, such as Nup153, may play a role in receptor-independent nuclear transport, as shown for the nuclear import of the transcription factor PU.1 (Zhong et al. 2005).

Taken together, our findings suggest that FG-repeat domains have a more active role in cargo translocation through the NPC than simply acting as a scaffold for the formation of cargo-receptor complexes or providing docking sites for cargo-receptor complexes at the NPC. Indeed, our results indicate that FG repeat domains accompany and guide cargo through the NPC's central pore to its final destination. In this context, transport substrates might be passed from an asymmetric FG-repeat nucleoporin residing on the cytoplasmic face of the NPC, such as Nup214, to a symmetric FG-repeat nucleoporin, for example p62, to an asymmetric FG-repeat nucleoporin residing on the nuclear side of the NPC, such as Nup153, or vice versa. It is also conceivable that transport substrates are directly passed from one extended asymmetric FG-repeat nucleoporin to the next, thereby optimizing cargo translocation through the central pore of the NPC. It will be interesting to analyze if the FG-repeat domains of symmetric nucleoporins, which are, as in case of p62, are relatively short as compared to the FG-repeat domains of Nup214 and Nup153, have an extended conformation as well. Such as scenario, in fact, might explain why the deletion of individual or a minimal number of FG-repeat domains have only a slight effect on nuclear transport kinetics.

2.4 Material and Methods

All experimental procedures were performed at room temperature (rt) unless otherwise stated.

2.4.1 Antibody production and purification

Full length human Nup214 in pBluescript was a gift from Dr. Gerard Grosveld (St. Jude Children's Research Hospital). Four non-overlapping fragments were created by PCR for expression and antibody production. 214A corresponds to the N-terminal domain (amino acids 1-469), 214B corresponds to the coiled-coil section of the central domain (amino acids 702-931), 214 C corresponds to the non-coiled-coil section of the central domain (amino acids 1026-1364), and 214D corresponds to the FG repeat domain (amino acids 1684-2091). Following PCR, each DNA fragment was inserted into the pTrcHis-TOPO vector (Invitrogen, Carlsbad, CA) for expression of N-terminal hexahistidine-tagged protein. Recombinant fusion proteins were expressed in BL21(DE3) cells and purified on His-Bind resin (Novagen/EMD Biosciences, Madison, WI). Expression of the 214C fragment was insufficient for antibody production. The 214B and 214D proteins were solubilized and purified in the presence of 6M urea. Purified protein was used to inoculate rabbits (Spring Valley Laboratories; Sykesville, MD) and the rabbit sera were affinity purified using the corresponding recombinant protein bound to a CNBr-activated Sepharose 4 Fast Flow support (Amersham Pharmacia Biosciences, Buckinghamshire, England).

For immunoblots, proteins were separated by 8% acrylamide SDS-PAGE and transferred to PVDF membrane. The membrane was blocked with either 2% BSA (anti-214A) or 5% nonfat milk (anti-214B and anti-214D) in PBS with 0.2% Tween-20. Affinity purified antibodies were used at 1/1000 dilution in immunoblots. Antibody signals were detected by chemiluminescence with ECL substrate (Amersham Pharmacia Biosciences).

2.4.2 Immuno-EM of isolated nuclei from *Xenopus* oocytes

Mature (stage 6) oocytes were surgically removed from female *Xenopus laevis*, and their nuclei were isolated as described (Pante et al. 1994). Colloidal gold particles, ~8-nm in diameter, were prepared by reduction of tetrachloroauric acid with sodium citrate in the presence of tannic acid and antibodies were conjugated to colloidal gold particles as described (Baschong and Wrigley 1990). Isolated nuclei were labelled as described

previously (Fahrenkrog et al. 2002) with the following modifications. Nuclei were incubated in a solution of anti-Nup214 antibodies diluted 1:1000 in PBS for 2 h and washed twice in PBS. After washing, nuclei were incubated for 2h in an anti-rabbit IgG antibody conjugated to 10-nm colloidal gold (BBI International, Cardiff, UK). Labelled nuclei were fixed and processed for EM as described (Fahrenkrog et al. 2002).

2.4.3 Immuno-EM of human cultured cells

HL-60 cells were cultivated in Dulbecco Modified Eagle Medium (DMEM; Vitromex, Geilenkirchen, Germany) containing 10% fetal calf serum plus penicillin and streptomycin (Gibco BRL, Grand Island, NY). Cells were washed twice in PBS and fixed for 15 min in freshly prepared PBS containing 4% paraformaldehyde. After washing twice in PBS, cells were permeabilized with PBS containing 0.1% Triton X-100 for 2 min, and washed again twice in PBS.

For immunolabelling, cells were resuspended in the corresponding anti-Nup214 antibody diluted 1: 100 in PBS and incubated for 2h. Next cells were washed twice in PBS containing 0.1% BSA, and resuspended in secondary anti-rabbit-IgG antibody conjugated to 10-nm colloidal gold (see above) diluted 1:2 in PBS containing 0.1% BSA and incubated for 2h. After two washes in PBS containing 0.1% BSA, the cells were fixed in 2% glutaraldehyde for 1h, washed twice in PBS and post-fixed in 1% OsO_4 for 1h. Fixed samples were dehydrated, embedded in Epon 812 resin (Fluka, Buchs, Switzerland), and processed for EM as described (Fahrenkrog et al. 2002).

2.4.4 Microinjection and immuno-EM of tagged human Nup214 in *Xenopus* nuclei

Full-length human Nup214 was subcloned from pET21b (a kind gift of Dr. Doris Kraemer, University of Würzburg) into EcoRI and NotI cut pcDNA3.1/myc-His (Invitrogen Corporation, Carlsbad, CA) to produce C-terminally tagged hNup214-myc. To produce N-terminally tagged GFP-Nup214, full-length human Nup214 was subcloned from pET21b into EcoRI and SacII cut pEGFP-C1 (Clontech, Palo Alto, CA). For microinjection into nuclei, freshly isolated oocytes from *Xenopus laevis* were prepared and processed for microinjection as described (Fahrenkrog et al. 2002). The localization of the fusion proteins within the NPC were determined by using a polyclonal anti-GFP and a monoclonal anti-myc antibody, respectively, directly conjugated to 8-nm colloidal gold.

2.4.5 Immunolocalization of FG-repeat domains at 4°C

Freshly isolated nuclei from *Xenopus* oocytes were collected in low salt buffer (LSB) containing 1 mM KCl, 0.5 mM $MgCl_2$, 10 mM HEPES, pH 7.5, and equilibrated to 4°C for 1 h. Next the nuclei were fixed for 15 min in LSB containing 4% formaldehyde. The nuclei were washed twice in LSB for 5 min each, and incubated in anti-C2-Nup153 antibody directly conjugated to 8-nm gold (Fahrenkrog et al. 2002) for 2h to determine the localization of the FG-repeat domains of Nup153. For localization of the FG-repeat domain of Nup214, nuclei were incubated in anti-Nup214-D antibody and secondary anti-rabbit-IgG antibody conjugated to 10-nm colloidal gold as described above. After labelling the nuclei were prepared for EM as described (Fahrenkrog et al. 2002).

2.4.6 Nuclear import of nucleoplasmin

Xenopus nucleoplasmin was expressed from a pQE70 vector and purified (Qiagen GmbH, Hilden, Germany) as described by (Gorlich et al. 1994). Nuclei were isolated manually from *Xenopus* oocytes, collected in LSB and incubated in an import mixture (50% HeLa cytosol, 20mM HEPES, pH 7.3, 110 mM potassium acetate, 5 mM sodium acetate, 1 mM EGTA, 2 mM DTT, 1 mM ATP, 5 mM creatine phosphate, 20 U/ml creatine phosphokinase, and 1 µg/ml each aprotinin, leupeptin, and pepstatin (Adam et al. 1992) containing 100 ng recombinantly expressed nucleoplasmin as indicated. Next the nuclei were fixed in 4% formaldehyde and labelled with anti-C2-Nup153 and anti-Nup214-D antibody as described above.

2.4.7 Export of poly (A+) RNA and inhibition of transcription

Total RNA was purified from HeLa cells using the RNAeasy kit (Qiagen GmbH, Hilden, Germany) following the instructions of the manufacturer. From this total RNA, poly (A+) RNA was purified using the GenElute mRNA miniprep kit (Sigma, St. Louis, MO) following the instructions of the manufacturer. Oocytes were microinjected into their nuclei with 10-20 nl purified poly (A+) RNA (0.1 µg/µl) and incubated for different time points as indicated. Nuclei were isolated, collected in LSB, fixed in 4% formaldehyde and labelled with anti-C2-Nup153 and anti-Nup214-D antibody, respectively, as described above. Actinomycin D (Sigma, St. Louis, MO) was dissolved in ethanol to 5 mg/ml. 10-20 nl of a 5

µg/ml diluted solution were microinjected into nuclei of *Xenopus* oocytes and incubated for 3h. Next the nuclei were isolated, fixed and labelled with anti-C2-Nup153 and anti-Nup214-D antibody, respectively, as described.

Acknowledgements

The authors wish to thank Doris Kraemer (University of Würzburg, Germany) and Gerard Grosveld (St. Jude Children's Research Hospital) for providing us with clones of human Nup214, Dirk Görlich (University of Heidelberg, Germany) for the plasmid to express nucleoplasmin, and Ulrike Kutay (ETH Zürich, Switzerland) for the importin-β 45-462 fragment. Ueli Aebi is greatly acknowledged for critically reading of the manuscript and Laurent Kreplak for helpful discussions. This work was supported by research grants from the Swiss National Science Foundation (to B.F.) and the National Institutes of Health (grants GM59975 to M.A.P and GM61275 to K.S.U), by the Kanton Basel Stadt, and the M.E. Müller Foundation.

References

Adam, S. A., R. Sterne-Marr, et al. (1992). "Nuclear protein import using digitonin-permeabilized cells." Methods Enzymol **219**: 97-110.

Akey, C. W. and M. Radermacher (1993). "Architecture of the *Xenopus* nuclear pore complex revealed by three-dimensional cryo-electron microscopy." J Cell Biol **122**(1): 1-19.

Baschong, W. and N. G. Wrigley (1990). "Small colloidal gold conjugated to Fab fragments or to immunoglobulin G as high-resolution labels for electron microscopy: a technical overview." J Electron Microsc Tech **14**(4): 313-23.

Bastos, R., A. Lin, et al. (1996). "Targeting and function in mRNA export of nuclear pore complex protein Nup153." J Cell Biol **134**(5): 1141-56.

Bayliss, R., H. M. Kent, et al. (2000). "Crystallization and initial X-ray diffraction characterization of complexes of FxFG nucleoporin repeats with nuclear transport factors." J Struct Biol **131**(3): 240-7.

Bayliss, R., S. W. Leung, et al. (2002). "Structural basis for the interaction between NTF2 and nucleoporin FxFG repeats." Embo J **21**(12): 2843-53.

Bayliss, R., T. Littlewood, et al. (2000). "Structural basis for the interaction between FxFG nucleoporin repeats and importin-beta in nuclear trafficking." Cell **102**(1): 99-108.

Beck, M., F. Forster, et al. (2004). "Nuclear pore complex structure and dynamics revealed by cryoelectron tomography." Science **306**(5700): 1387-90.

Belgareh, N., G. Rabut, et al. (2001). "An evolutionarily conserved NPC subcomplex, which redistributes in part to kinetochores in mammalian cells." J Cell Biol **154**(6): 1147-60.

Boer, J. M., J. M. van Deursen, et al. (1997). "The nucleoporin CAN/Nup214 binds to both the cytoplasmic and the nucleoplasmic sides of the nuclear pore complex in overexpressing cells." Exp Cell Res **232**(1): 182-5.

Cronshaw, J. M., A. N. Krutchinsky, et al. (2002). "Proteomic analysis of the mammalian nuclear pore complex." J Cell Biol **158**(5): 915-27.

Denning, D. P., S. S. Patel, et al. (2003). "Disorder in the nuclear pore complex: the FG

repeat regions of nucleoporins are natively unfolded." Proc Natl Acad Sci U S A **100**(5): 2450-5.

Denning, D. P., V. Uversky, et al. (2002). "The Saccharomyces cerevisiae nucleoporin Nup2p is a natively unfolded protein." J Biol Chem **277**(36): 33447-55.

Dingwall, C., S. V. Sharnick, et al. (1982). "A polypeptide domain that specifies migration of nucleoplasmin into the nucleus." Cell **30**(2): 449-58.

Dunker, A. K., J. D. Lawson, et al. (2001). "Intrinsically disordered protein." J Mol Graph Model **19**(1): 26-59.

Enninga, J., A. Levay, et al. (2003). "Sec13 shuttles between the nucleus and the cytoplasm and stably interacts with Nup96 at the nuclear pore complex." Mol Cell Biol **23**(20): 7271-84.

Fahrenkrog, B. and U. Aebi (2003). "The nuclear pore complex: nucleocytoplasmic transport and beyond." Nat Rev Mol Cell Biol **4**(10): 757-66.

Fahrenkrog, B., J. Koser, et al. (2004). "The nuclear pore complex: a jack of all trades?" Trends Biochem Sci **29**(4): 175-82.

Fahrenkrog, B., B. Maco, et al. (2002). "Domain-specific antibodies reveal multiple-site topology of Nup153 within the nuclear pore complex." J Struct Biol **140**(1-3): 254-67.

Fornerod, M., J. van Deursen, et al. (1997). "The human homologue of yeast CRM1 is in a dynamic subcomplex with CAN/Nup214 and a novel nuclear pore component Nup88." Embo J **16**(4): 807-16.

Fribourg, S., I. C. Braun, et al. (2001). "Structural basis for the recognition of a nucleoporin FG repeat by the NTF2-like domain of the TAP/p15 mRNA nuclear export factor." Mol Cell **8**(3): 645-56.

Fried, H. and U. Kutay (2003). "Nucleocytoplasmic transport: taking an inventory." Cell Mol Life Sci **60**(8): 1659-88.

Frosst, P., T. Guan, et al. (2002). "Tpr is localized within the nuclear basket of the pore complex and has a role in nuclear protein export." J Cell Biol **156**(4): 617-30.

Gorlich, D., S. Prehn, et al. (1994). "Isolation of a protein that is essential for the first step of nuclear protein import." Cell **79**(5): 767-78.

Grant, R. P., E. Hurt, et al. (2002). "Structure of the C-terminal FG-nucleoporin binding domain of Tap/NXF1." Nat Struct Biol **9**(4): 247-51.

Griffis, E. R., S. Xu, et al. (2003). "Nup98 localizes to both nuclear and cytoplasmic sides of the nuclear pore and binds to two distinct nucleoporin subcomplexes." Mol Biol Cell **14**(2): 600-10.

Hinshaw, J. E., B. O. Carragher, et al. (1992). "Architecture and design of the nuclear pore complex." Cell **69**(7): 1133-41.

Katahira, J., K. Strasser, et al. (1999). "The Mex67p-mediated nuclear mRNA export pathway is conserved from yeast to human." Embo J **18**(9): 2593-609.

Kraemer, D., R. W. Wozniak, et al. (1994). "The human CAN protein, a putative oncogene product associated with myeloid leukemogenesis, is a nuclear pore complex protein that faces the cytoplasm." Proc Natl Acad Sci U S A **91**(4): 1519-23.

Krull, S., J. Thyberg, et al. (2004). "Nucleoporins as Components of the Nuclear Pore Complex Core Structure and Tpr as the Architectural Element of the Nuclear Basket." Mol Biol Cell.

Kuersten, S., G. J. Arts, et al. (2002). "Steady-state nuclear localization of exportin-t involves RanGTP binding and two distinct nuclear pore complex interaction domains." Mol Cell Biol **22**(16): 5708-20.

Kutay, U., E. Izaurralde, et al. (1997). "Dominant-negative mutants of importin-beta block multiple pathways of import and export through the nuclear pore complex." Embo J **16**(6): 1153-63.

Matsuura, Y., A. Lange, et al. (2003). "Structural basis for Nup2p function in cargo release and karyopherin recycling in nuclear import." Embo J **22**(20): 5358-69.

Mosammaparast, N. and L. F. Pemberton (2004). "Karyopherins: from nuclear-transport mediators to nuclear-function regulators." Trends Cell Biol **14**(10): 547-56.

Nakielny, S., S. Shaikh, et al. (1999). "Nup153 is an M9-containing mobile nucleoporin with a novel Ran-binding domain." Embo J **18**(7): 1982-95.

Pante, N. and U. Aebi (1996). "Sequential binding of import ligands to distinct nucleopore regions during their nuclear import." Science **273**(5282): 1729-32.

Pante, N., R. Bastos, et al. (1994). "Interactions and three-dimensional localization of a group of nuclear pore complex proteins." J Cell Biol **126**(3): 603-17.

Pante, N., A. Jarmolowski, et al. (1997). "Visualizing nuclear export of different classes of RNA by electron microscopy." Rna **3**(5): 498-513.

Pante, N. and M. Kann (2002). "Nuclear pore complex is able to transport macromolecules with diameters of about 39 nm." Mol Biol Cell **13**(2): 425-34.

Reichelt, R., A. Holzenburg, et al. (1990). "Correlation between structure and mass distribution of the nuclear pore complex and of distinct pore complex components." J Cell Biol **110**(4): 883-94.

Rollenhagen, C., P. Muhlhausser, et al. (2003). "Importin beta-depending nuclear import pathways: role of the adapter proteins in the docking and releasing steps." Mol Biol Cell **14**(5): 2104-15.

Shah, S., S. Tugendreich, et al. (1998). "Major binding sites for the nuclear import receptor are the internal nucleoporin Nup153 and the adjacent nuclear filament protein Tpr." J Cell Biol **141**(1): 31-49.

Stoffler, D., B. Feja, et al. (2003). "Cryo-electron tomography provides novel insights into nuclear pore architecture: implications for nucleocytoplasmic transport." J Mol Biol **328**(1): 119-30.

Strawn, L. A., T. Shen, et al. (2004). "Minimal nuclear pore complexes define FG repeat domains essential for transport." Nat Cell Biol **6**(3): 197-206.

Strelkov, S. V., H. Herrmann, et al. (2002). "Conserved segments 1A and 2B of the intermediate filament dimer: their atomic structures and role in filament assembly." Embo J **21**(6): 1255-66.

Suntharalingam, M. and S. R. Wente (2003). "Peering through the pore: nuclear pore complex structure, assembly, and function." Dev Cell **4**(6): 775-89.

Ullman, K. S., S. Shah, et al. (1999). "The nucleoporin nup153 plays a critical role in multiple types of nuclear export." Mol Biol Cell **10**(3): 649-64.

Uversky, V. N. (2002). “What does it mean to be natively unfolded?” Eur J Biochem **269**(1): 2-12.

van Deursen, J., J. Boer, et al. (1996). “G2 arrest and impaired nucleocytoplasmic transport in mouse embryos lacking the proto-oncogene CAN/Nup214.” Embo J **15**(20): 5574-83.

Walther, T. C., M. Fornerod, et al. (2001). “The nucleoporin Nup153 is required for nuclear pore basket formation, nuclear pore complex anchoring and import of a subset of nuclear proteins.” Embo J **20**(20): 5703-14.

Walther, T. C., H. S. Pickersgill, et al. (2002). “The cytoplasmic filaments of the nuclear pore complex are dispensable for selective nuclear protein import.” J Cell Biol **158**(1): 63-77.

Zeitler, B. and K. Weis (2004). “The FG-repeat asymmetry of the nuclear pore complex is dispensable for bulk nucleocytoplasmic transport in vivo.” J Cell Biol **167**(4): 583-90.

Zhong, H., A. Takeda, et al. (2005). “Carrier-independent nuclear import of the transcription factor PU.1 via RANGTP-stimulated binding to NUP153.” J Biol Chem.

Chapter 3

Changes in Nucleoporin Domain Topology in Response to Chemical Effectors

Changes in nucleoporin domain topology in response to chemical effectors

Sara M. Paulillo[1], Maureen A. Powers[2], Katharine S. Ullman[3], and Birthe Fahrenkrog[1,*]

[1]M.E. Müller Institute for Structural Biology, Biozentrum, University of Basel, Klingelbergstrasse 70, 4056 Basel, Switzerland, [2]Department of Cell Biology,

Emory University School of Medicine, 615 Michael Street, Atlanta, GA 30322, USA, [3]Department of Oncological Sciences, Huntsman Cancer Institute, University of Utah, Salt Lake City, Utah, USA

*corresponding author: birthe.fahrenkrog@unibas.ch

Running title: Nucleoporin domain topology and chemical effectors.

Summary

Nucleoporins represent the molecular building blocks of nuclear pore complexes (NPCs), which mediate facilitated macromolecular trafficking between the cytoplasm and nucleus of eukaryotic cells. Phenylalanine-glycine (FG) repeat motifs are found in about one third of the nucleoporins and they provide major binding or docking sites for soluble transport receptors. We have recently shown that localization of the FG-repeat domains of vertebrate nucleoporins Nup153 and Nup214 within the NPC is influenced by its transport state. To test whether chemical effectors, such as calcium and ATP, influence the localization of the FG-repeat domains of Nup153 and Nup214 within the NPC, we performed immuno-electron microscopy of *Xenopus* oocyte nuclei using domain specific antibodies against Nup153 and Nup214, respectively. Ca^{2+} and ATP are known to induce conformational changes in the NPC architecture, especially at the cytoplasmic face, but also at the nuclear basket of the NPC. We have found calcium concentrations in the micromolar range or 1mM ATP in the surrounding buffer leaves the spatial distribution of the FG-repeat of Nup153 and Nup214 largely unchanged. In contrast, ATP depletion, calcium store depletion by EGTA or thapsigargin, and high divalent cation concentrations (i.e. 2 mM Ca^{2+} and 2 mM Mg^{2+}) constrain the distribution of the FG-repeats of Nup153 and Nup214. Our data suggest that the location of the FG-repeat domains of Nup153 and Nup214 is sensitive to chemical changes within the near-field environment of the NPC.

Keywords: nuclear pore complex; nuclear transport; calcium, Nup153; Nup214; ATP

3.1 Introduction

Nuclear pore complexes (NPCs) are supramolecular assemblies embedded in the double membrane of the nuclear envelope (NE) that mediate diffusion of small molecules and ions as well as facilitated, signal-dependent transport of proteins and RNPs between the nucleus and cytoplasm of eukaryotic cells (Fried and Kutay 2003; Pemberton and Paschal 2005). The ~120 MDa vertebrate NPC (Reichelt et al. 1990) is composed of a set of ~30 different proteins (Cronshaw et al. 2002) known as nucleoporins (Nups). According to electron microscopy studies, mainly in *Xenopus* oocytes, the NPC is composed of a central framework that is continuous with a cytoplasmic and a nuclear ring moiety (Hinshaw et al. 1992; Akey and Radermacher 1993; Yang et al. 1998; Stoffler et al. 2003; Beck et al. 2004). The cytoplasmic ring moiety is decorated by eight, short, kinky filaments, whereas a nuclear basket, an assembly of eight filaments that join into a distal ring, tops the nuclear ring moiety (reviewed in (Fahrenkrog and Aebi 2003; Fahrenkrog et al. 2004)). The central framework exhibits 8-fold rotational symmetry and it encloses the central pore of the NPC, which mediates all trafficking between the nucleus and cytoplasm. The central pore has a length of about 90 nm and it is narrowest in the midplane of the NE with a diameter of about 45-50 nm (Stoffler et al. 2003; Beck et al. 2004). The physical and functional diameters of the central pore coincide as cargo up to 39 nm is able to pass through the NPC (Panté and Kann 2002).

The NE is continuous with the endoplasmic reticulum (ER) and, as such, the NE lumen acts, together with that of the ER, as calcium (Ca^{2+}) store. Depletion of the lumenal Ca^{2+} stores inhibits diffusion of 10 kDa dextrans in both cultured mammalian cells and in *Xenopus* oocytes (Greber and Gerace 1995; Stehno-Bittel et al. 1995). The effect of Ca^{2+} store depletion on facilitated nuclear import is controversial: inhibition has been observed in some studies (Stehno-Bittel et al. 1995) but not in others (Strubing and Clapham 1999). Atomic force microscopy (AFM) studies further showed that depletion of nuclear Ca^{2+} stores or variations in extra-nuclear calcium concentrations led to conformational changes within the NPC. Such changes included the appearance of a central plug on the cytoplasmic and nuclear face of the NPC (Perez-Terzic et al. 1996; Wang and Clapham 1999; Moore-Nichols et al. 2002; Mooren et al. 2004) or alterations in the arrangement of the nuclear basket by ~20-30 nm (Stoffler et al. 1999). ATP can influence NPC conformation as well and in this context AFM studies revealed that addition of ATP causes dramatic conformational changes on the cytoplasmic surface of the NPC (Rakowska et al. 1998). A direct link between changes in NPC conformation and nuclear transport has not been established, although it has been speculated that conformational changes of the NPC could alter the accessibility of FG (phenylalanine-glycine)-repeat sites within the NPC, which, in turn, should affect nuclear transport (Erickson et al. 2004).

Facilitated nuclear transport requires the simultaneous interaction of soluble transport receptors with the NPC and with transport cargo. The interaction of the receptors with the NPC is mediated mainly by a subset of nucleoporins that harbor FG-repeat domains. Repeat domains are composed of hydrophobic FG patches that are spaced by hydrophilic linkers of variable length and sequence. Studies in yeast revealed that FG-repeat domains have little secondary structure, i.e. they are natively unfolded (Denning et al. 2002; Denning et al. 2003). These findings are supported by X-ray crystallography data (Bayliss et al. 2000) as well as by immuno-EM studies (Fahrenkrog et al. 2002; Paulillo et al. 2005). AFM studies further document that the FG-repeat domain of Nup153 resembles an unfolded polypeptide chain with a length of about 200 nm and a width of about 0.4 nm (Lim et al. 2006).

We have recently mapped the domain topology of two vertebrate nucleoporins, Nup153 and Nup214, within the NPC of *Xenopus* oocytes (Fahrenkrog et al. 2002; Paulillo et al. 2005). The non-FG-repeat domains of both nucleoporins have a tightly constrained distribution, whereas, in both cases, the FG-repeat domains are flexibly positioned within the NPC. Moreover, the spatial distribution of the FG-repeat domains of Nup153 and Nup214 changes in a transport-dependent manner, suggesting that the location of FG-repeat domains of Nup153 and Nup214 correlates with cargo/receptor interactions at the NPC. To test whether the flexibility of the FG-repeat domains of Nup153 and Nup214 is altered under conditions that lead to changes in NPC conformation, we isolated nuclei from *Xenopus* oocytes, incubated them in buffer solutions that vary in either Ca^{2+} or ATP concentrations and mapped the domain topology of Nup153 and Nup214 by immunogold-EM using domain-specific antibodies. Our data show that high salt concentrations in buffer solutions, the release of lumenal Ca^{2+} stores by thapsigargin, and ATP-depletion lead to distinct changes in the spatial distribution of the FG-repeat domains of Nup153 and Nup214, whereas moderate increase in external calcium or ATP levels has no significant influence on their location. These findings suggest that the variations in FG-repeat accessibility are due to physical changes in response to alterations in the chemical near-field environment of the NPC.

3.2 Results

3.2.1 The influence of increasing Ca^{2+} concentrations on the location of FG-repeat domains

In resting cells, free calcium concentrations in the cytoplasm and the nucleus appear to be approximately equivalent and in the nanomolar range (Erickson et al. 2004). Addition of micromolar amounts of calcium to the buffer surrounding isolated nuclei leads to an increase in nuclear calcium concentration due to diffusion of Ca^{2+} ions through the NPC (Assandri and Mazzanti 1997). AFM studies in *Xenopus* oocyte nuclei have shown that 100 µM Ca^{2+} addition to Ca^{2+}-free buffer leads to an opening of the distal ring of the nuclear basket by 20-30 nm without affecting the actual height of the nuclear basket (Stoffler et al. 1999). The FG-repeat domain of Nup153 is tethered to the distal ring of the nuclear basket via the zinc-finger domain of Nup153 and can extend from there to the cytoplasmic face of the NPC (Fahrenkrog et al. 2002), whereas the FG-repeat domain of Nup214 can extend as far as the nuclear basket from its anchoring site near or at the cytoplasmic ring moiety of the NPC (Paulillo et al. 2005).

To analyze whether an increase in Ca^{2+} and the related conformational changes of the NPC at the level of the nuclear basket affect the epitope exposure of the flexible FG-repeat domains of Nup153 and Nup214 and the stationary zinc-finger domain of Nup153 (Fig. 3.1(a)), we isolated nuclei from *Xenopus* oocytes, incubated the nuclei in low salt buffer (LSB) containing 100 µM Ca^{2+} for 10 min and then fixed and labelled the nuclei with antibodies against the FG-repeat domains of Nup153 (anti-Nup153-C2) (Fahrenkrog et al. 2002) and Nup214 (anti-Nup214-D) (Paulillo et al. 2005), respectively. At equilibrium state (i.e. in LSB without addition of calcium), the FG-repeat domain of Nup153 locates predominantly to the nuclear side of the NPC (89%), but about 11% of the FG-repeats can be detected at the cytoplasmic face (Fig. 3.1(b); see also (Fahrenkrog et al. 2002; Paulillo et al. 2005)). Incubating the nuclei with 100 µM Ca^{2+} did not change the nuclear-cytoplasmic ratio of the distribution of the FG-repeats of Nup153 (85% nuclear versus 15% cytoplasmic; Fig. 3.1 (c)). However, a slight shift from the distal ring of the nuclear basket towards the nuclear ring moiety could be observed.

In the case of Nup214, at steady-state about 14% of the FG-repeat domains of Nup214 localize to the nuclear face of the NPC, whereas 86% reside on the cytoplasmic face of the NPC (Figs. 3.1(d); see also (Paulillo et al. 2005)). In the presence of 100 µM Ca^{2+} this overall distribution of the Nup214 FG-repeat domains is similar (21% nuclear versus 79% cytoplasmic; Fig. 3.1(e)). Similarly, the presence of 100 µM Ca^{2+} does not substantially change the position of the zinc-finger domain of Nup153 within the NPC (Fig. 3.1(f) and (g)), although some cytoplasmic labelling was observed in the presence of 100 µM Ca^{2+}.

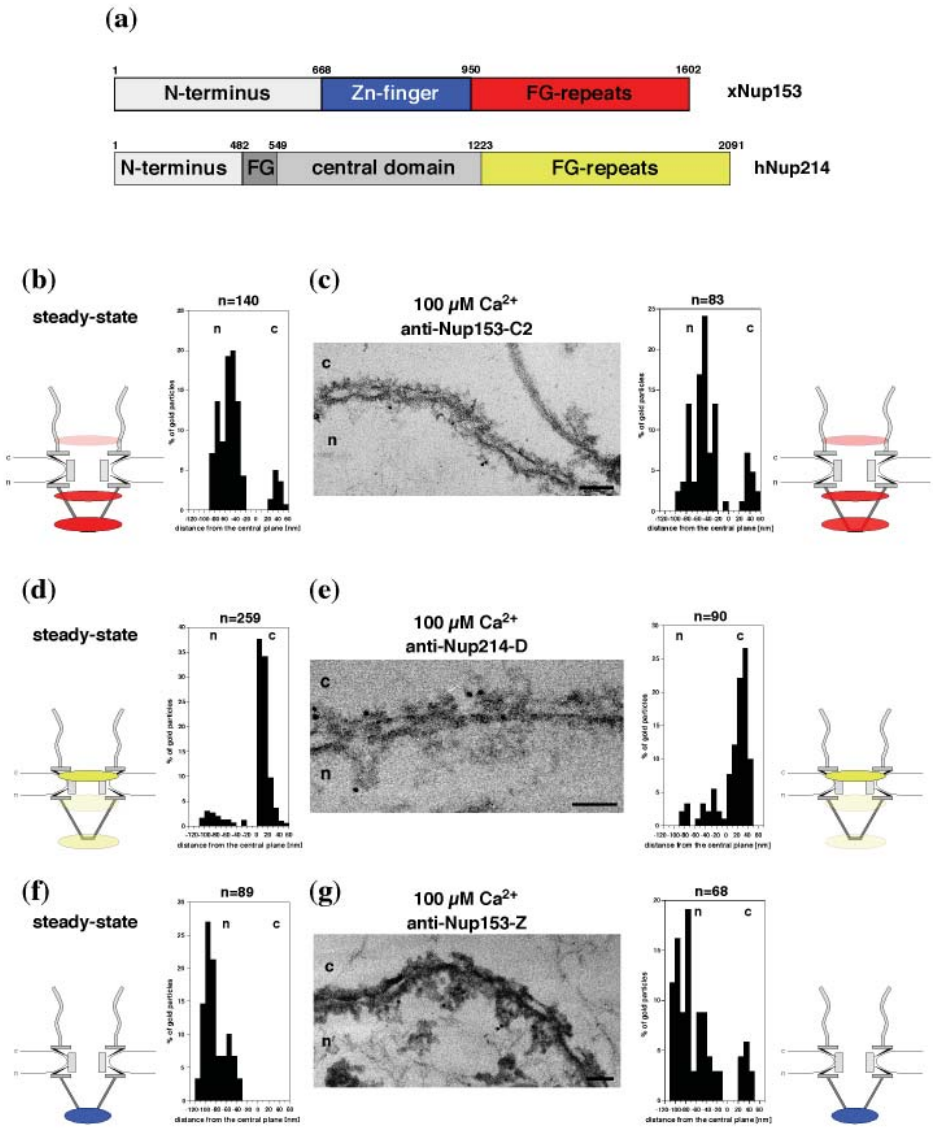

Figure 3.1: Domain organization and localization of Nup153 and Nup214. (**a**) Schematic representation of the domain structure of *Xenopus* Nup153 and human Nup214. Antibodies were raised against Nup153 amino acids 655-926 (anti-Nup153-Z), 1375-1602 (anti-Nup153-C2) and Nup214 amino acids 1684-2091 (anti-Nup214-D). Schematic representation and quantitation of the steady-state localization of the FG-repeat domains of (**b**) Nup153 and (**d**) Nup214 as well as (**f**) the zinc-finger domain of Nup153 in isolated *Xenopus* nuclei. Intact isolated nuclei were collected in low salt buffer (LSB) and immunolabelled with the anti-Nup153-C2 (Fahrenkrog et al. 2002) antibody directly conjugated to 8-nm colloidal gold, anti-Nup214-D antibody (Paulillo et al. 2005) and a secondary anti-rabbit IgG antibody conjugated to 10-nm colloidal gold, and anti-Nup153-Z antibody (Fahrenkrog et al. 2002) directly conjugated to 8-nm colloidal gold and prepared for EM by Epon embedding and thin-sectioning. The center of each location cloud represents the mean distance from the central plane of the NE and the radii are defined by the standard deviation of the vertical distances and the width of the NPC. Full colors, highest probability; subdued color, less probability. The following numbers of gold particles were

scored for the individual experiments: 140 (anti-Nup153-C2, steady-state), 259 (Paulillo et al. 2005) (anti-Nup214-D, steady state), 89 (anti-Nup153-Z, steady-state). Incubating the isolated *Xenopus* nuclei in LSB containing 100 µM prior to immunolabelling with (**c**) the anti-Nup153-C2 antibody, (**e**) the anti-Nup214-D, and (**g**) the anti-Nup153-Z antibody does not significantly affect the localization of the corresponding domains. Shown are stretches along the gold-labelled NE reflecting the (left panels) typical labelling pattern for the individual antibodies. Quantitation of the labelling distribution is shown in the middle panels. Right panels show schematic representation of the epitope distribution revealed by the corresponding domain specific antibodies in form of location clouds. The following numbers of gold particles were scored for the individual experiments: 83 (anti-Nup153-C2, 100 µM Ca^{2+}), 90 (anti-Nup214-D, 100 µM Ca^{2+}), 68 (anti-Nup153-Z, 100 µM Ca^{2+}). c, cytoplasm; n, nuclear. Scale bars, 100 nm.

Thus we conclude that conformational changes at the level of the nuclear basket, such as those reported in response to 100 µM Ca^{2+}, do not necessarily correlate with changes in the spatial distribution of the FG-repeat domains of Nup153 and Nup214.

To mimic conditions of a localized Ca^{2+} flux from the ER, where the Ca^{2+} concentration can transiently reach the millimolar range (Petersen et al. 1998; Gerasimenko and Gerasimenko 2004), we studied the effect of 2 mM Ca^{2+} on the distribution of Nup153 and Nup214 FG-repeat domains within the NPC. As shown in Fig. 3.2(a), the presence of 2 mM Ca^{2+} led to an almost exclusive nuclear localization of the FG-repeat domain of Nup153 (98%), predominantly at the distal ring of the nuclear basket (86%). Under the same conditions, the FG-repeat domains of Nup214 also shift towards the nuclear face of the NPC (50% versus 14% at equilibrium state; Fig. 3.2(b)), whereas the location of the zinc-finger domain of Nup153 remains unchanged (Fig. 3.2(c)). However, these changes in the distribution of the FG-repeat domains are not Ca^{2+}-specific, as 2 mM Mg^{2+} caused a similar shift or even more extensive shift of the FG-repeat domains of Nup153 and Nup214 towards the nuclear face of the NPC (Fig. 3.3 (a) and (b)).

To test if the calcium-induced redistribution of the Nup153 and Nup214 FG-repeat domains is reversed following calcium chelation, isolated nuclei from *Xenopus* oocytes were first incubated in buffer containing 2 mM Ca^{2+} and next in buffer containing 2 mM EGTA (for 10 minutes each) prior to labelling with the domain-specific antibodies. As shown in Fig. 3.4 (a) and (b), calcium-induced changes in the distribution of the Nup153 and Nup214 FG-repeat domains are only partially reversible by application of 2 mM EGTA. To confirm that calcium was adequately quenched by EGTA under these conditions, we next incubated nuclei from *Xenopus* oocytes for 10 minutes in buffer containing 2 mM Ca^{2+} and 2 mM EGTA simultaneously and found that in fact in the presence of 2 mM EGTA the distribution of the FG-repeat domains of Nup153 and Nup214 similar to equilibrium state (Fig. 3.S1 (a) and (b)). Again, no effect on the location of the zinc-finger domain of Nup153 was observed (Fig. 3.S1 (c)).

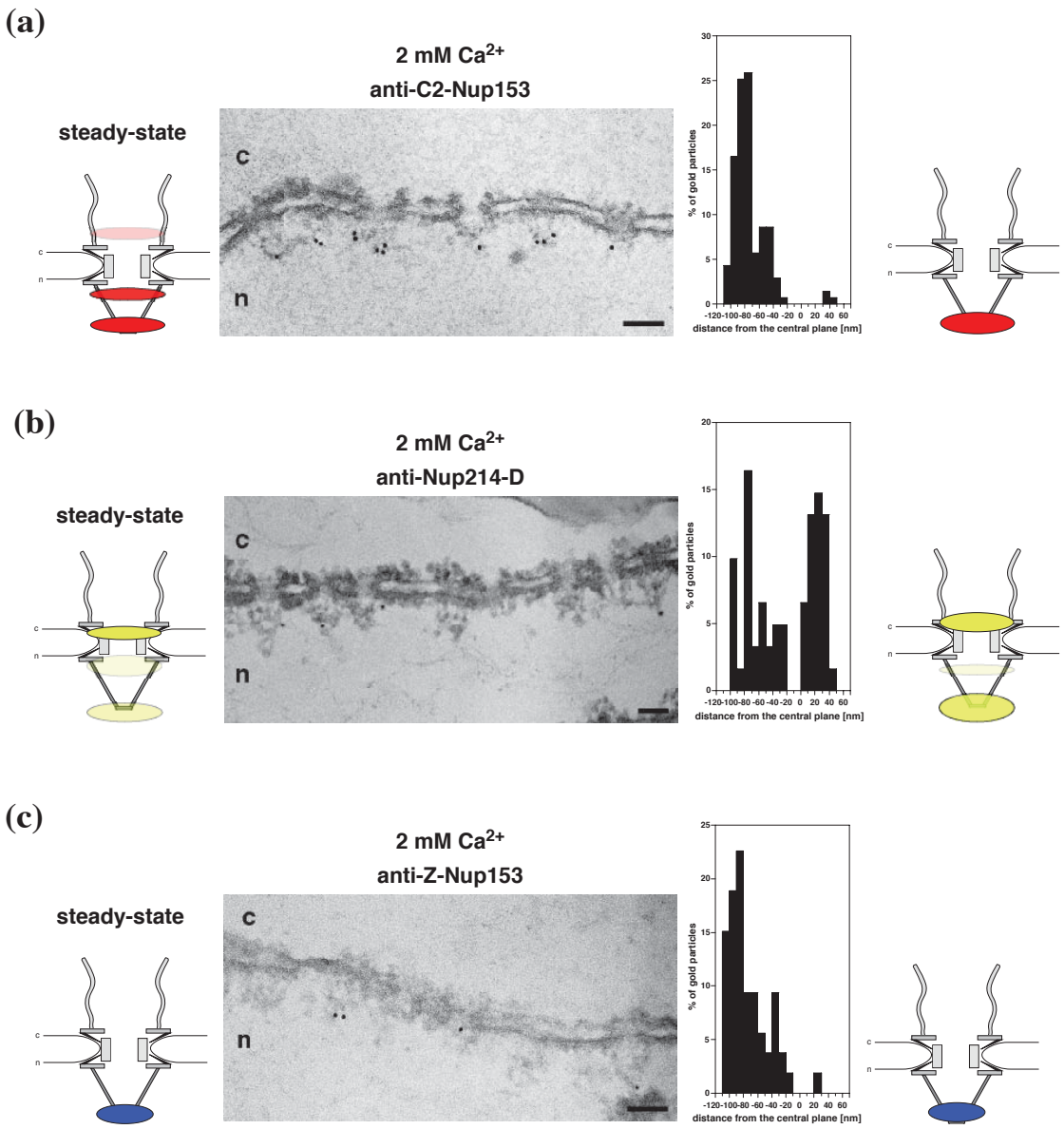

Figure 3.2: Ca^{2+}-dependent domain topology of Nup153 and Nup214. Intact isolated *Xenopus* oocyte nuclei were incubated in buffer containing 2 mM Ca^{2+} prior to labelling with (**a**) an antibody against the FG-repeat domain of Nup153 (anti-Nup153-C2), (**b**) an antibody against the FG-repeat domain of Nup214, and (**c**) the zinc-finger domain of Nup153. Shown are stretches along the NE of *Xenopus* oocyte nuclei with the typical labelling pattern (second panels) as well as the quantitative analysis of the gold particles associated with the NPC (third panels) and a schematic summary of the epitope distribution (fourth panels). The following numbers of gold particles were scored for the individual experiments: 139 (anti-Nup153-C2, 2 mM Ca^{2+}), 150 (anti-Nup214-D, 2 mM Ca^{2+}), 53 (anti-Nup153-Z, 2 mM Ca^{2+}). Steady-state values are as shown in Fig. 3.1 and are included here for reference (first panels). cytoplasm; n, nuclear. Scale bars, 100 nm.

A rise in cytoplasmic calcium above 300 nM was found to decrease both ATP-dependent nuclear transport and passive diffusion (Assandri and Mazzanti 1997) in intact cells, whereas in permeabilized cells no inhibition of nuclear import in response to increased calcium concentrations could be observed (Greber and Gerace 1995). To exclude that the redistribution of the FG-repeat domains of Nup153 and Nup214 was due to inhibition of nuclear transport in the isolated nuclei, we followed nuclear import of nucleoplasmin directly conjugated to 8-nm colloidal gold after incubation of the nuclei with either 100 µM Ca^{2+} or 2 mM Ca^{2+}. We found that under these conditions the import of nucleoplasmin in the isolated *Xenopus* nuclei was not inhibited (Fig. 3.S2 (a)). Similarly, no inhibition of import of GFP-labelled nucleoplasmin in digitonin-permeabilized HeLa cells (Fig. 3.S2 (b)) or export of mRNA from *Xenopus* nuclei (data not shown) were observed.

Taken together, high concentration of divalent cations within the local nuclear environment influences the localization of the FG-repeat domains of nucleoporins Nup153 and Nup214, but this does not interfere significantly with nuclear transport.

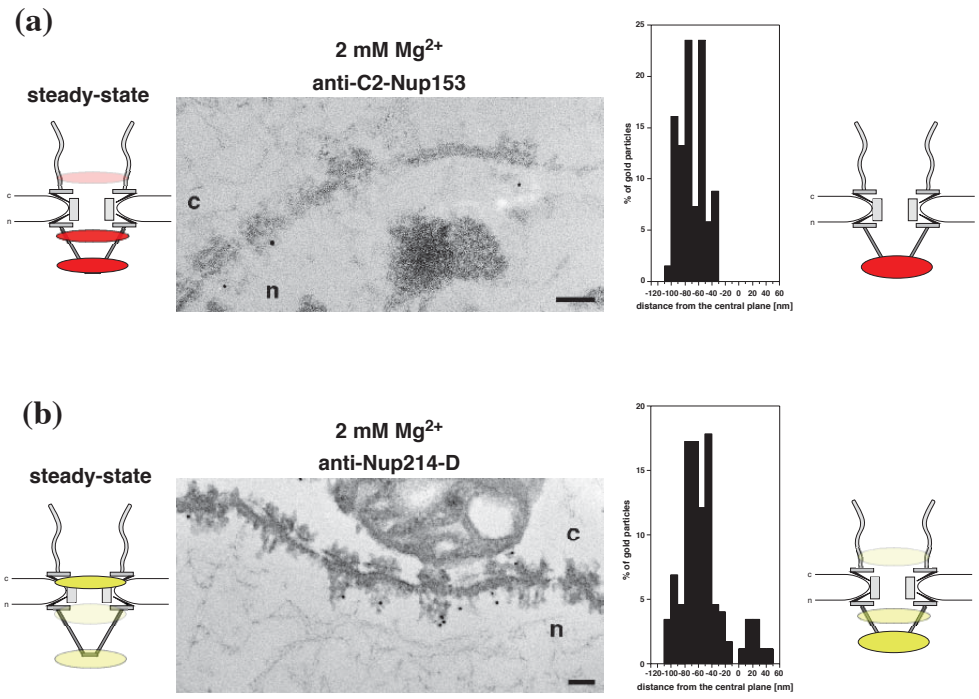

Figure 3.3: Mg^{2+}-dependent domain topology of Nup153 and Nup214. Intact isolated *Xenopus* oocyte nuclei were incubated in buffer containing 2 mM Mg^{2+} prior to labelling with (**a**) an antibody against the FG-repeat domain of Nup153 (anti-Nup153-C2) and (**b**) an antibody against the FG-repeat domain of Nup214. Shown are stretches along the NE with the typical labelling pattern (second panels) as well as the quantitative analysis of the gold particles associated with the NPC (third panels) and a schematic summary of the gold particle distribution within the NPC. The following numbers of gold particles were scored for the individual experiments: 97 (anti-Nup153-C2, 2 mM Mg^{2+}), 174 (anti-Nup214-D). Steady-state values are as shown in Fig. 3.1 and are included here for reference (first panels). cytoplasm; n, nuclear. Scale bars, 100 nm.

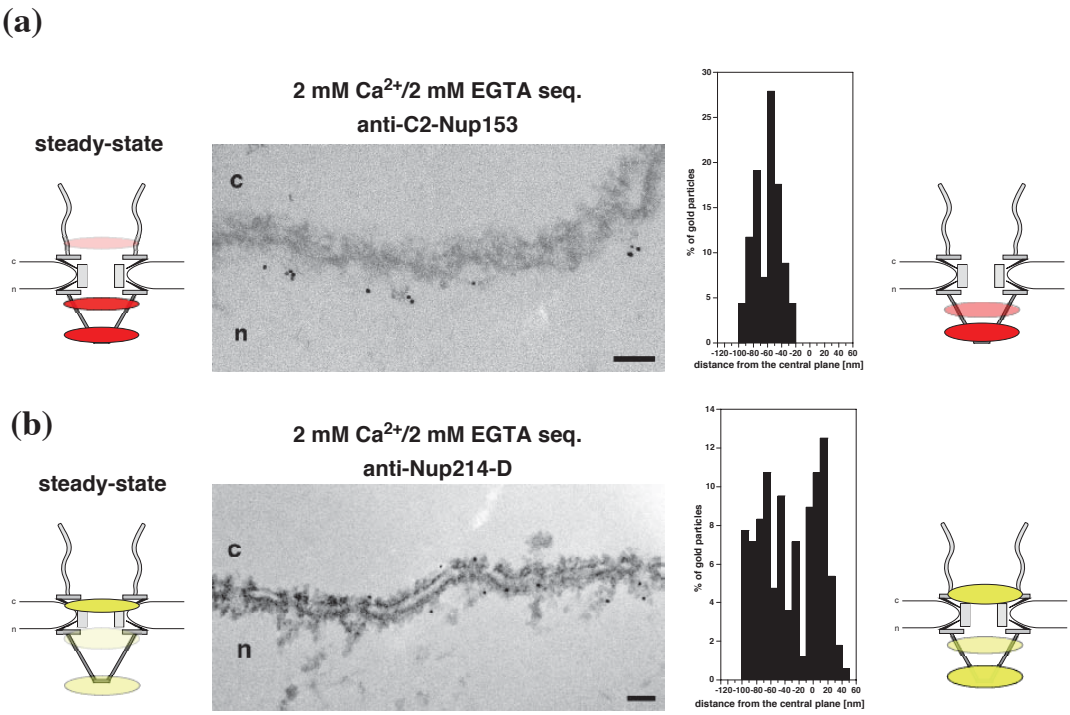

Figure 3.4: EGTA cannot completely reverse the calcium-mediated effect on the domain topology of Nup153 and Nup214. EM micrographs (second panels) show the typical gold particle distribution after isolated intact *Xenopus* nuclei were incubated in buffer containing 2 mM Ca^{2+} for 10 minutes followed by 2 mM EGTA for 10 minutes before nuclei were shortly fixed and pre-embedding labelled with (**a**) the anti-Nup153-C2 antibody, and (**b**) the anti-Nup214-D antibody. Quantitative analysis of gold particles associated with the NPC after labelling with the corresponding antibodies (third panels) and schematic summary of the labelling pattern (fourth panels). The following numbers of gold particles were scored for the individual experiments: 68 (anti-Nup153-C2, 2 mM Ca^{2+}/2 mM EGTA seq.), 168 (anti-Nup214-D, 2 mM Ca^{2+}/2 mM EGTA seq.). Steady-state values are as shown in Fig. 3.1 and are included here for reference (first panels). cytoplasm; n, nuclear. Scale bars, 100 nm.

3.2.2 Depletion of nuclear calcium stores influences FG-repeat domain distribution

Since the calcium levels that influenced domain distribution corresponded to levels obtained by calcium flux, we next aimed to map the distribution of the FG-repeat domains of Nup153 and Nup214 under various conditions known to modify lumenal Ca^{2+} stores. Lumenal calcium stores can be depleted, for example, by the calcium chelator EGTA or by the Ca^{2+}- uptake pump inhibitor, thapsigargin (Strubing and Clapham 1999; Jaggi et al. 2003). To analyze the effect of calcium release from lumenal calcium stores on the localization of the FG-repeat domains of Nup153 and Nup214 and the zinc-finger domain of Nup153, we incubated isolated nuclei from *Xenopus* oocytes in buffer containing 10 mM EGTA for 10 minutes or in buffer containing 1 µM thapsigargin for 30 minutes prior to labelling with the anti-Nup153-C2 antibody, the anti-Nup214-D antibody, and the anti-Nup153-Z antibody,

respectively. Calcium store release by thapsigargin had a strong effect on the position of the FG-repeats of both Nup153 and Nup214. In the case of Nup153, the cytoplasmic fraction decreases to 5%, whereas 86% of the FG-repeats locate to the distal ring of the nuclear basket (Fig. 3.5(a)). In the case of Nup214, the nuclear fraction increased from 14% at steady state to 77% (Fig. 3.5(b)). In contrast, depletion of lumenal calcium stores by 10 mM EGTA leads only to a slight decrease in the presence of the FG-repeats of Nup153 on the cytoplasmic side of the NPC (8% versus 11% at equilibrium state) coinciding with a slight increase in their nuclear location and a shift towards the distal ring of the nuclear basket (Fig. 3.S3 (a)). The FG-repeats of Nup214 showed a more striking enhancement in nuclear location (31.5% versus 14% at steady-state; Fig. 3.S3 (b), but not as strong as after calcium store depletion by thapsigargin (Fig. 3.5(b)). Depletion of lumenal calcium stores either by 10 mM EGTA (Fig. 3.S3 (c)) or by thapsigargin (data not shown) does not affect the location of the zinc-finger domain of Nup153 significantly. Taken together, depletion of Ca^{2+} from nuclear calcium stores by either EGTA or thapsigargin causes the redistribution of the FG-repeat domains of nucleoporins Nup153 and Nup214 within the NPC, although to a different extent.

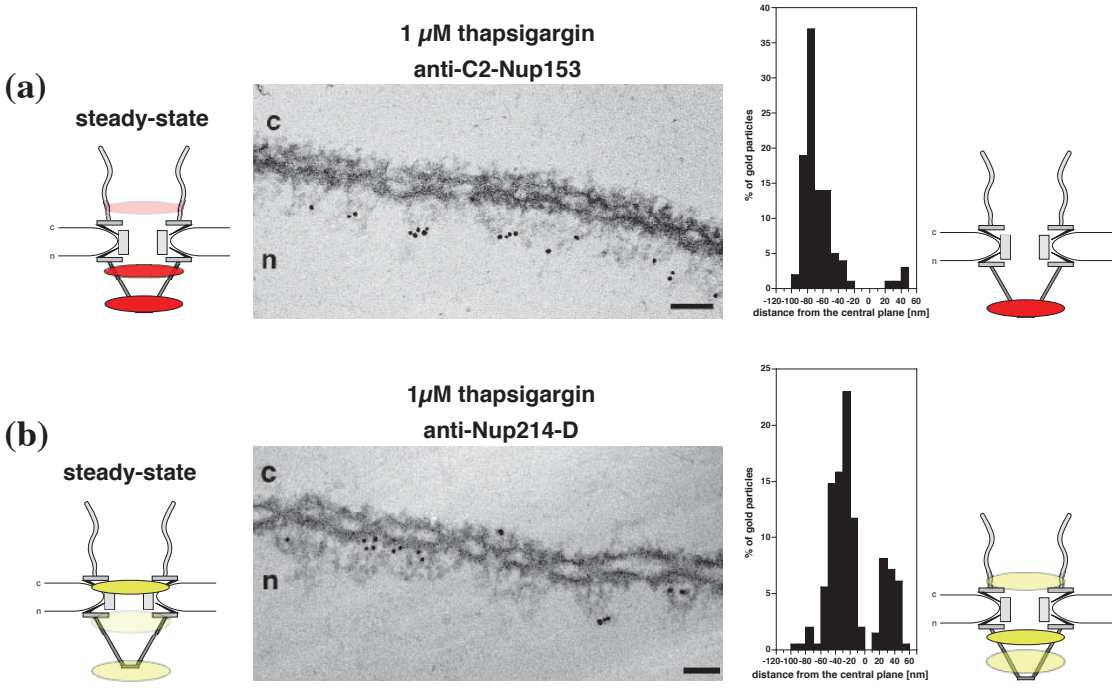

Figure 3.5: Domain topology of Nup153 and Nup214 after depletion of lumenal calcium stores using 1 µM thapsigargin in *Xenopus* oocyte nuclei. Shown are stretches along the NE with the typical labelling pattern (second panels) and quantitative analysis of gold particles associated with the NPC (third panels) as well as schematic representation of the epitope distribution (fourth panels) after labelling with (**a**) the anti-Nup153-C2 antibody and (**b**) the anti-Nup214-D antibody. The following numbers of gold particles were scored for the individual experiments: 100 (anti-Nup153-C2, 1 µM thapsigargin), 150 (anti-Nup214-D, 1 µM thapsigargin). Steady-state values are as shown in Fig. 3.1 and are included here for reference (first panels). cytoplasm; n, nuclear. Scale bars, 100 nm.

3.2.3 Increased ATP concentrations and nucleoporin domain topology

Nuclear transport is energy- and as such ATP-dependent, and high concentrations of ATP are associated with structural changes at the cytoplasmic face of the NPC (Rakowska et al. 1998). To test whether or not increased ATP concentrations affect the domain topology of Nup153 and Nup214, we incubated isolated nuclei from *Xenopus* oocytes in buffer containing 1 mM ATP. The nuclei were incubated for various time points and thereafter labelled with anti-Nup153 or anti-Nup214 antibodies, respectively. We found that additional 1 mM of ATP do not significantly affect the accessibility of the FG-repeat domain of Nup153 at the various time points of incubation, although a slight reduction in the labelling of the cytoplasmic face could be observed (Fig. 3.S5 (a)). Similarly, we did not detect significant alterations in the distribution of the FG-repeat domains of Nup214 or the zinc-finger domain of Nup153 in the presence of high ATP concentrations (Fig. 3.S5 (b) and (c)).

3.2.4 ATP-depletion limits the flexibility of the FG-repeat domains of Nup153 and Nup214

We then asked the converse question of whether ATP-depletion affects the domain topology of Nup153 and Nup214, respectively. To do so, we incubated *Xenopus* oocyte nuclei in buffer containing 2U/ml apyrase for 30 minutes to deplete ATP (Newmeyer et al. 1986; Newmeyer and Forbes 1988) prior to labelling with our domain specific antibodies. After treatment with apyrase, the anti-Nup153-C2 antibody predominantly decorates the distal ring of the nuclear basket (77% of the gold particles), whereas the cytoplasmic labelling decreases (6% versus 11% at steady-state; Fig. 3.6(a)). Similarly, ATP-depletion by apyrase results in an increase of the nuclear localization of the FG-repeat domains of Nup214 (45% versus 14%; Fig. 3.6(b)), whereas the location of the zinc-finger domain of Nup153 remains unaffected by ATP-depletion (data not shown). This data suggest that ATP-depletion affects the distribution of FG-repeat domains, particularly of Nup214.

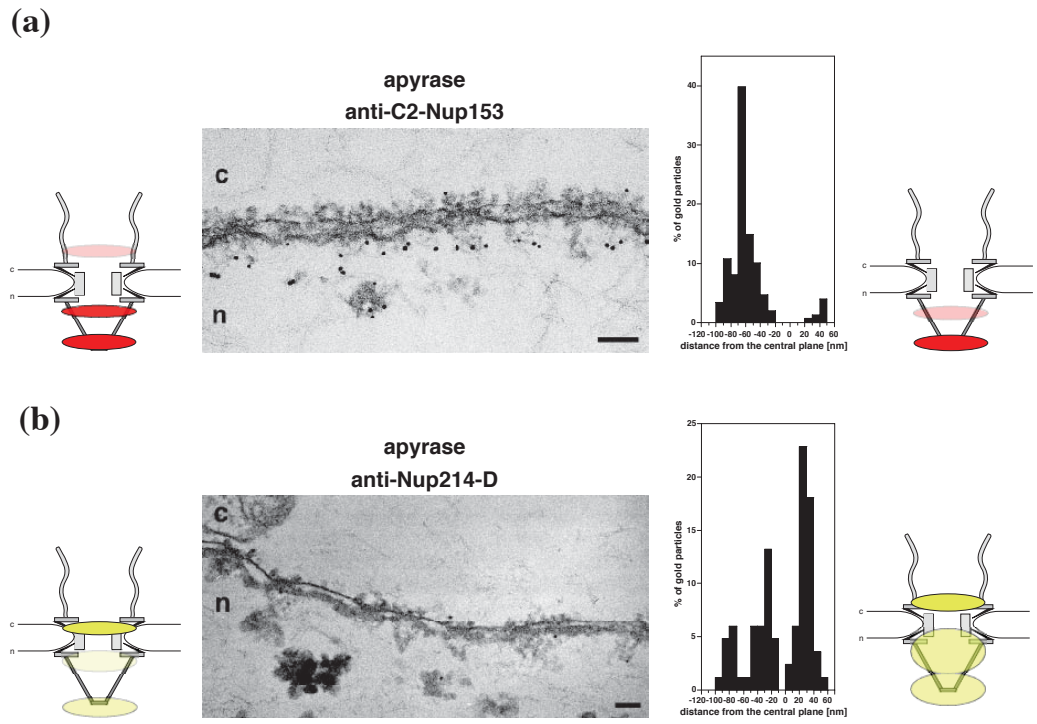

Figure 3.6: ATP-depletion limits the mobility of the FG-repeat domains of Nup153 and Nup214. EM micrographs of stretches along NEs (second panels), quantification of the gold particle distribution associated with the NPC (third panels) and schematic summary of the labelling pattern (fourth panels) after ATP-depletion by apyrase treatment and labelling with (**a**) the anti-Nup153-C2 antibody and (**b**) the anti-Nup214-D antibody are shown. The following numbers of gold particles were scored for the individual experiments: 148 (anti-Nup153-C2, apyrase), 83 (anti-Nup214-D, apyrase). Steady-state values are as shown in Fig. 3.1 and are included here for reference (first panels). cytoplasm; n, nuclear. Scale bars, 100 nm.

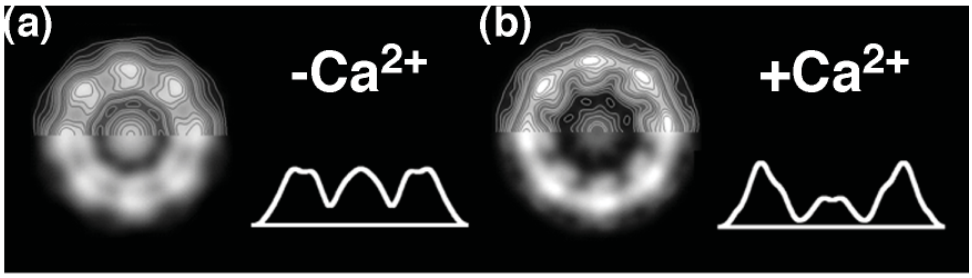

Figure 3.7: Calcium-dependent appearance thick ice-embedded *Xenopus* NPCs. Isolated *Xenopus* nuclei were incubated in (a) calcium-free buffer or (b) buffer containing 100 µM Ca^{2+} and analyzed by cryo-EM. About 900 NPCs were translationally and angularly aligned and averaged, and their average radial mass density profiles computed.

3.3 Discussion

Domain-specific antibodies against the nucleoporins Nup153 and Nup214 have allowed mapping of the domain topology of these two nucleoporins within the NPC and have revealed that both harbor flexible FG-repeat domains (Fahrenkrog et al. 2002; Paulillo et al. 2005). Moreover, these domain-specific antibodies have also been shown to be a powerful tool to explore possible changes in nucleoporin domain topology in a nuclear transport-dependent manner (Paulillo et al. 2005). In the present study, we have now used the domain specific antibodies against Nup153 and Nup214 to investigate nucleoporin domain topology with respect to NPC conformation. NPC conformation and topology have been shown by AFM and scanning EM (SEM) to be affected by chemical effectors, such as Ca^{2+} and ATP (Perez-Terzic et al. 1996; Stoffler et al. 1999; Wang and Clapham 1999; Goldberg et al. 2000; Jaggi et al. 2003). Our data suggest that gross structural changes at the level of the NPC as observed by AFM and SEM do not coincide with changes in the domain topology of the nucleoporins Nup153 and Nup214. However, the flexibility of the FG-repeat domains of both nucleoporins is affected by Ca^{2+} as well as ATP.

3.3.1 Calcium and nucleoporin domain topology

In isolated *Xenopus* oocyte nuclei, AFM studies have documented an opening and closing of the distal ring of the NPC's nuclear basket by 20-30 nm in the presence or absence of 100 µM Ca^{2+} in the surrounding buffer, respectively (Stoffler et al. 1999). Moreover, cryo-EM studies on isolated *Xenopus* nuclei in the presence or absence of 100 µM Ca^{2+} revealed significant differences in the radial mass density profiles of the central framework (Fig. 3.7). In calcium-free buffer, i.e. low salt buffer, the central framework appears more massive (Fig. 3.7 (a)) as compared to the central framework of NPCs treated with 100 µM Ca^{2+} (Fig. 3.7 (b)). Additionally, NPCs in the absence of Ca^{2+} yield more mass in the central pore, which might reflect cargo in transit, than NPCs that have been treated with calcium.

In the present immuno-EM study, we observed neither an effect by 100 µM Ca^{2+} on the topology and flexibility of the FG-repeat domains of Nup153 and Nup214 nor the location of the zinc-finger domain of Nup153, which resides at the distal ring of the nuclear basket (see Fig. 3.1). Nup153 and Nup214 are both peripheral nucleoporins that are anchored to the nuclear and cytoplasmic ring moiety, respectively, and do not contribute to the architecture of the central framework of the NPC (Walther et al. 2001; Walther et al. 2002). Our data therefore suggest that conformational changes on the level of the NPCs central framework do not correlate with changes in the topology of the FG-repeat domains of peripheral nucleoporins, indicating that their mobile character is not constrained by the

conformation of the central framework.

The presence of higher calcium concentrations, i.e. 2 mM Ca^{2+}, caused the redistribution of the FG-repeat domains of Nup153 and Nup214 within the NPC, whereas the location of the stationary zinc-finger domain of Nup153 remained unaffected (see Fig. 3.2). This effect on the spatial distribution of the FG-repeat domains, however, appears to be due to charge effects, since 2 mM Mg^{2+} had a similar effect on the location of the FG-repeat domains of Nup153 and Nup214, respectively (Fig. 3.3). FG-repeat domains are natively unfolded (Denning et al. 2002; Denning et al. 2003; Lim et al. 2006), and as such they are characterized by a large net charge and hence sensitivity to temperature, pH, and ionic strength (Uversky 2002). Under physiological temperature, pH and ionic strength, natively unfolded proteins are unstructured mainly because of electrostatic repulsion between non-compensated charges (Uversky 2002). This electrostatic repulsion, which, in turn, coincides with a partial folding of the protein, can be reduced by oppositely charged ions, as they are introduced by a shift in the pH or upon addition of salts (Uversky 2002). High concentrations of divalent cations, such as 2 mM Ca^{2+} or 2 mM Mg^{2+}, in the near-field of the FG-repeat domains therefore most likely cause their collapse, i.e. a partial folding which constrains their mobility.

Depletion of nuclear calcium stores by thapsigargin constrained the flexibility of the FG-repeat domains of both Nup153 and Nup214 (Fig. 3.5(a) and (b)), whereas calcium store depletion by EGTA had a milder effect on the FG-repeats (Fig. 3.S3). Thapsigargin is blocking the SERCA ATPase and, by this, is predicted to deplete lumenal calcium stores in the NE and the ER, since any leaking calcium ions cannot be replenished (Waldron et al. 1997). Similarly, the calcium chelator EGTA causes calcium store depletion (Kao and Fong 2004). Whereas thapsigargin causes a virtually irreversible depletion of the lumenal calcium stores, EGTA appears to not fully deplete calcium stores (Banhegyi et al. 1993). Hence the observed differences in the response of the FG-repeat domains of Nup153 and Nup214 to calcium depletion are therefore most likely due to these slight differences in the effect of EGTA and thapsigargin action on calcium stores. Nevertheless, our data suggest that such calcium store depletion can cause redistribution of nucleoporin FG-repeat regions within the NPC, which, in turn, might play a role in calcium signaling events to the nucleus.

3.3.2 ATP and nucleoporin domain topology

AFM studies have previously revealed that addition of 1 mM ATP to isolated *Xenopus* nuclei is inducing conformational changes on the cytoplasmic face of the NPC (Rakowska et al. 1998). Our data presented here show that these ATP-dependent conformational changes

do not correlate with changes within the topology of the FG-repeat domains of Nup153 and Nup214 (Fig. 3.S4), which most likely is due to the high flexibility of these nucleoporin domains. In contrast, ATP-depletion constrains the flexibility of the FG-repeat domains of both Nup153 and Nup214, indicating that FG-repeat flexibility is influenced by an active process that requires energy. Similar to our previous findings (Paulillo et al. 2005), limited FG-repeat flexibility under these conditions might be due to an arrest in nuclear transport, since nuclear transport is known to be ATP-dependent (Newmeyer and Forbes 1988).

Taken together, our findings suggest that the spatial distribution of flexible FG-repeat domains is not significantly influenced by gross conformational changes in the central framework or the central pore of the NPC, such as the appearance and movement of a central plug, mass redistribution within the central framework, or the opening and closing of the distal ring of the nuclear basket. However, increased levels in divalent cation concentrations as well as ATP-depletion, coincide with a constrained flexibility of the FG-repeat domains of Nup153 and Nup214, further strengthening the notion that FG-repeat domains are natively unfolded and that nucleoporin topology within the NPC architecture is influenced by energy-dependent processes.

These data underscore the multi-layered nature of NPCs dynamics and plasticity. Whereas gross changes in NPC architecture have been documented by atomic force to scanning electron microscopy studies (Perez-Terzic et al. 1996; Stoffler et al. 1999; Wang and Clapham 1999; Goldberg et al. 2000; Jaggi et al. 2003), dynamics in nucleoporin residence at the NPC have been revealed by real-time imaging (Griffis et al. 2004; Rabut et al. 2004), and changes in domain topology of Nup153 and Nup214 are reflected in this and other immuno-EM studies (Fahrenkrog et al. 2002; Paulillo et al. 2005). Here, we have shown that the local dynamics of FG-repeat domains can change in response to salts and energy-depletion. All these aspects of NPC dynamics and plasticity, although still poorly understood at the molecular level, are important to consider in the context of constitutive nuclear transport and its modulation in response to specific signaling and cell growth conditions essential for cell survival.

3.4 Material and Methods

All experimental procedures were performed at room temperature (rt) unless otherwise stated.

3.4.1 Immuno-EM of isolated nuclei from *Xenopus* oocytes and labelling at equilibrium state

Mature (stage 6) oocytes were surgically removed from female *Xenopus laevis*, and their nuclei were isolated as described (Panté et al. 1994). Colloidal gold particles, ~8-nm in diameter, were prepared by reduction of tetrachloroauric acid with sodium citrate in the presence of tannic acid and antibodies were conjugated to colloidal gold particles as described (Baschong and Wrigley 1990). Isolated nuclei were labelled with anti-Nup153 antibodies as described previously (Fahrenkrog et al. 2002). In case of Nup214, nuclei were incubated in a solution of anti-Nup214 antibodies diluted 1:1000 in PBS for 2 hours and washed twice in PBS. After washing, nuclei were incubated for 2 hours in an anti-rabbit IgG antibody conjugated to 10-nm colloidal gold (BBI International, Cardiff, UK). Labelled nuclei were fixed and processed for EM as described (Fahrenkrog et al. 2002; Paulillo et al. 2005).

3.4.2 Immunolocalization of FG-repeat domains in the presence of exogenous calcium

Freshly isolated nuclei from *Xenopus* oocytes were collected in low salt buffer (LSB) containing 1 mM KCl, 0.5 mM $MgCl_2$, 10 mM HEPES, pH 7.5, and incubated in LSB containing 100 µM Ca^{2+}, 2 mM Ca^{2+}, and 2 mM Mg^{2+}, respectively, for 30 minutes. Next the nuclei were fixed for 5 minutes in LSB containing 4% formaldehyde. The nuclei were washed twice in LSB for 5 minutes each, and incubated in anti-Nup153-C2 antibody directly conjugated to 8-nm gold (Fahrenkrog et al. 2002) for 2 hours to determine the localization of the FG-repeat domains of Nup153. For localization of the FG-repeat domain of Nup214, nuclei were incubated in anti-Nup214-D antibody and secondary anti-rabbit-IgG antibody conjugated to 10-nm colloidal gold as described above. After labelling the nuclei were prepared for EM as described.

3.4.3 Immunolocalization of FG-repeat domains after Ca^{2+}-depletion from calcium stores

Freshly isolated nuclei from *Xenopus* oocytes were collected in LSB and incubated in LSB containing 10 mM EGTA for 10 minutes, and 1 µM thapsigargin for 30 minutes, respectively. Next the nuclei were fixed for 5 minutes in LSB containing 4% formaldehyde. The nuclei were washed twice in LSB for 5 minutes each, and incubated in anti-Nup153-C2 antibody directly conjugated to 8-nm gold for 2 hours to determine the localization of the FG-repeat domains of Nup153. For localization of the FG-repeat domain of Nup214, nuclei were incubated in anti-Nup214-D antibody and secondary anti-rabbit-IgG antibody conjugated to 10-nm colloidal gold as described above. After labelling the nuclei were prepared for EM as described.

3.4.4 Immunolocalization of FG-repeat domains under different ATP concentrations

Freshly isolated nuclei from *Xenopus* oocytes were collected in LSB and incubated in LSB containing 1 mM ATP for various time points as indicated. To deplete ATP, isolated nuclei were incubated in LSB containing apyrase (2U/ml) for 30 minutes. Next the nuclei were fixed for 5 minutes in LSB containing 4% formaldehyde. The nuclei were washed twice in LSB for 5 minutes each, and incubated in anti-Nup153-C2 antibody directly conjugated to 8-nm gold (Fahrenkrog et al. 2002) for 2 hours to determine the localization of the FG-repeat domains of Nup153. For localization of the FG-repeat domain of Nup214, nuclei were incubated in anti-Nup214-D antibody and secondary anti-rabbit-IgG antibody conjugated to 10-nm colloidal gold as described above. After labelling the nuclei were prepared for EM as described.

3.4.5 Cryo-EM and 2-D image processing

Xenopus oocyte nuclei were isolated, opened manually and spread on an EM grid as described (Stoffler et al. 1999). After washing the grid with LSB, a 5 µl droplet of LSB containing 100 µM Ca^{2+} or a 5 µl droplet of fresh LSB were applied and allowed to equilibrate for 15 minutes at room temperature. Samples were prepared for rapid freezing and zero-loss filtered EM and image processing essentially as described (Stoffler et al. 2003). In brief, the images were recorded digitally with a slow-scan CCD camera (Proscan, Scheuring, Germany; 2 MHz read-out, 14 bit information depth, 1024×1024 pixel). The microscope and

the camera were controlled by a VIPS-1000 (Tietz Video and Image Processing Systems, Gauting, Germany. The sample thickness was determined on-line from a zero-loss filtered/unfiltered image pair by a macro routine applying the log/ratio method (Malis et al. 1988) combined with the experimentally determined partial inelastic mean free electron path (Feja and Aebi 1999). All images were recorded at 120 kV acceleration voltage. The magnification was 12,500× (15,600× on the camera), and the defocus was 15 µm. The electron dose ranged between 300 and 500 e^-/nm^2. 2-D image processing including was performed as described (Stoffler et al. 2003). The multivariate statistical analysis was performed with the Coran program package (Frank et al. 1988). From each image data set ~900 particles in 128×128 pixel subframes were extracted interactively and contrast-normalized.

Acknowledgements

The authors wish to thank Bernd Feja, Daniel Stoffler and Ueli Aebi for providing us with Figure 3.7. Thanks to Ursula Sauder and Vesna Oliveri for expert technical assistance. Ueli Aebi is greatly acknowledged for critically reading the manuscript and Melanie Börries for helpful discussions. This work was supported by research grants from the Swiss National Science Foundation (to B.F.) and the National Institutes of Health (grants GM59975 to M.A.P and GM61275 to K.S.U), by the Kanton Basel Stadt, and the M.E. Müller Foundation.

References

Akey, C. W. and M. Radermacher (1993). "Architecture of the *Xenopus* nuclear pore complex revealed by three-dimensional cryo-electron microscopy." J Cell Biol **122**(1): 1-19.

Assandri, R. and M. Mazzanti (1997). "Ionic permeability on isolated mouse liver nuclei: influence of ATP and Ca2+." J Membr Biol **157**(3): 301-9.

Banhegyi, G., G. Bellomo, et al. (1993). "Intraluminal calcium of the liver endoplasmic reticulum stimulates the glucuronidation of p-nitrophenol." Biochem J **292 (Pt 1)**: 99-104.

Baschong, W. and N. G. Wrigley (1990). "Small colloidal gold conjugated to Fab fragments or to immunoglobulin G as high-resolution labells for electron microscopy: a technical overview." J Electron Microsc Tech **14**(4): 313-23.

Bayliss, R., T. Littlewood, et al. (2000). "Structural basis for the interaction between FxFG nucleoporin repeats and importin-beta in nuclear trafficking." Cell **102**(1): 99-108.

Beck, M., F. Forster, et al. (2004). "Nuclear pore complex structure and dynamics revealed by cryoelectron tomography." Science **306**(5700): 1387-90.

Cronshaw, J. M., A. N. Krutchinsky, et al. (2002). "Proteomic analysis of the mammalian nuclear pore complex." J Cell Biol **158**(5): 915-27.

Denning, D. P., S. S. Patel, et al. (2003). "Disorder in the nuclear pore complex: the FG repeat regions of nucleoporins are natively unfolded." Proc Natl Acad Sci U S A **100**(5): 2450-5.

Denning, D. P., V. Uversky, et al. (2002). "The Saccharomyces cerevisiae nucleoporin Nup2p is a natively unfolded protein." J Biol Chem **277**(36): 33447-55.

Erickson, E. S., O. L. Mooren, et al. (2004). "Activation of ryanodine receptors in the nuclear envelope alters the conformation of the nuclear pore complex." Biophys Chem **112**(1): 1-7.

Fahrenkrog, B. and U. Aebi (2003). "The nuclear pore complex: nucleocytoplasmic transport and beyond." Nat Rev Mol Cell Biol **4**(10): 757-66.

Fahrenkrog, B., J. Koser, et al. (2004). "The nuclear pore complex: a jack of all trades?"

Trends Biochem Sci **29**(4): 175-82.

Fahrenkrog, B., B. Maco, et al. (2002). "Domain-specific antibodies reveal multiple-site topology of Nup153 within the nuclear pore complex." J Struct Biol **140**(1-3): 254-67.

Feja, B. and U. Aebi (1999). "Determination of the inelastic mean free path of electrons in vitrified ice layers for on-line thickness measurements by zero-loss imaging." J Microsc **193**(1): 15-19.

Frank, J., A. Verschoor, et al. (1988). "A new non-crystallographic image-processing technique reveals the architecture of ribosomes." Trends Biochem Sci **13**(4): 123-127.

Fried, H. and U. Kutay (2003). "Nucleocytoplasmic transport: taking an inventory." Cell Mol Life Sci **60**(8): 1659-88.

Gerasimenko, O. and J. Gerasimenko (2004). "New aspects of nuclear calcium signalling." J Cell Sci **117**(Pt 15): 3087-94.

Goldberg, M. W., S. A. Rutherford, et al. (2000). "Ran alters nuclear pore complex conformation." J Mol Biol **300**(3): 519-29.

Greber, U. F. and L. Gerace (1995). "Depletion of calcium from the lumen of endoplasmic reticulum reversibly inhibits passive diffusion and signal-mediated transport into the nucleus." J Cell Biol **128**(1-2): 5-14.

Griffis, E. R., B. Craige, et al. (2004). "Distinct functional domains within nucleoporins Nup153 and Nup98 mediate transcription-dependent mobility." Mol Biol Cell **15**(4): 1991-2002.

Hinshaw, J. E., B. O. Carragher, et al. (1992). "Architecture and design of the nuclear pore complex." Cell **69**(7): 1133-41.

Jaggi, R. D., A. Franco-Obregon, et al. (2003). "Modulation of nuclear pore topology by transport modifiers." Biophys J **84**(1): 665-70.

Kao, Y. S. and J. C. Fong (2004). "Thapsigargin and EGTA inhibit endothelin-1-induced glucose transport." J Biomed Sci **11**(2): 206-13.

Lim, R. Y., U. Aebi, et al. (2006). "From the trap to the basket: getting to the bottom of the nuclear pore complex." Chromosoma **115**(1): 15-26.

Malis, T., S. C. Cheng, et al. (1988). "EELS log-ratio technique for specimen-thickness measurement in the TEM." J Electron Microsc Tech **8**(2): 193-200.

Moore-Nichols, D., A. Arnott, et al. (2002). "Regulation of nuclear pore complex conformation by IP(3) receptor activation." Biophys J **83**(3): 1421-8.

Mooren, O. L., E. S. Erickson, et al. (2004). "Nuclear side conformational changes in the nuclear pore complex following calcium release from the nuclear membrane." Phys Biol **1**(1-2): 125-34.

Newmeyer, D. D., D. R. Finlay, et al. (1986). "In vitro transport of a fluorescent nuclear protein and exclusion of non-nuclear proteins." J Cell Biol **103**(6 Pt 1): 2091-102.

Newmeyer, D. D. and D. J. Forbes (1988). "Nuclear import can be separated into distinct steps in vitro: nuclear pore binding and translocation." Cell **52**(5): 641-53.

Panté, N., R. Bastos, et al. (1994). "Interactions and three-dimensional localization of a group of nuclear pore complex proteins." J Cell Biol **126**(3): 603-17.

Panté, N. and M. Kann (2002). "Nuclear pore complex is able to transport macromolecules with diameters of about 39 nm." Mol Biol Cell **13**(2): 425-34.

Paulillo, S. M., E. M. Phillips, et al. (2005). "Nucleoporin domain topology is linked to the transport status of the nuclear pore complex." J Mol Biol **351**(4): 784-98.

Pemberton, L. F. and B. M. Paschal (2005). "Mechanisms of receptor-mediated nuclear import and nuclear export." Traffic **6**(3): 187-98.

Perez-Terzic, C., J. Pyle, et al. (1996). "Conformational states of the nuclear pore complex induced by depletion of nuclear Ca^{2+} stores." Science **273**(5283): 1875-7.

Petersen, O. H., O. V. Gerasimenko, et al. (1998). "The calcium store in the nuclear envelope." Cell Calcium **23**(2-3): 87-90.

Rabut, G., V. Doye, et al. (2004). "Mapping the dynamic organization of the nuclear pore complex inside single living cells." Nat Cell Biol **6**(11): 1114-21.

Rakowska, A., T. Danker, et al. (1998). "ATP-Induced shape change of nuclear pores visualized with the atomic force microscope." J Membr Biol **163**(2): 129-36.

Reichelt, R., A. Holzenburg, et al. (1990). "Correlation between structure and mass distribution of the nuclear pore complex and of distinct pore complex components." J Cell Biol **110**(4): 883-94.

Stehno-Bittel, L., C. Perez-Terzic, et al. (1995). "Diffusion across the nuclear envelope inhibited by depletion of the nuclear Ca^{2+} store." Science **270**(5243): 1835-8.

Stoffler, D., B. Feja, et al. (2003). "Cryo-electron tomography provides novel insights into nuclear pore architecture: implications for nucleocytoplasmic transport." J Mol Biol **328**(1): 119-30.

Stoffler, D., K. N. Goldie, et al. (1999). "Calcium-mediated structural changes of native nuclear pore complexes monitored by time-lapse atomic force microscopy." J Mol Biol **287**(4): 741-52.

Strubing, C. and D. E. Clapham (1999). "Active nuclear import and export is independent of lumenal Ca^{2+} stores in intact mammalian cells." J Gen Physiol **113**(2): 239-48.

Uversky, V. N. (2002). "What does it mean to be natively unfolded?" Eur J Biochem **269**(1): 2-12.

Waldron, R. T., A. D. Short, et al. (1997). "Store-operated Ca^{2+} entry and coupling to Ca^{2+} pool depletion in thapsigargin-resistant cells." J Biol Chem **272**(10): 6440-7.

Walther, T. C., M. Fornerod, et al. (2001). "The nucleoporin Nup153 is required for nuclear pore basket formation, nuclear pore complex anchoring and import of a subset of nuclear proteins." Embo J **20**(20): 5703-14.

Walther, T. C., H. S. Pickersgill, et al. (2002). "The cytoplasmic filaments of the nuclear pore complex are dispensable for selective nuclear protein import." J Cell Biol **158**(1): 63-77.

Wang, H. and D. E. Clapham (1999). "Conformational changes of the in situ nuclear pore complex." Biophys J **77**(1): 241-7.

Yang, Q., M. P. Rout, et al. (1998). "Three-dimensional architecture of the isolated yeast nuclear pore complex: functional and evolutionary implications." Mol Cell **1**(2):

223-34.

Chapter 4

The Nucleoporin Nup214 Partially Localizes to Human Telomeres

The nucleoporin Nup214 partially localizes to human telomeres

Sara M. Paulillo and Birthe Fahrenkrog

M.E. Müller Institute for Structural Biology, Biozentrum, University of Basel, Klingelbergstrasse 70, 4056 Basel, Switzerland

Key words: Nuclear pore complex; Nup214; Tankyrase 1; TRF1 (isoform 2); telomeres

Summary

Nucleoporins constitute the building block of the nuclear pore complex (NPC) and mediate transport of proteins and RNA trafficking between the nucleus and cytoplasm of eukaryotic cells. Recent findings revealed that nucleoporins play a dynamic role in other cellular processes, such as chromosome segregation and kinetochore structure. Moreover, in yeast, nucleoporins tether telomeres to the NPC, which might play a role in the regulation of chromatin organization and gene expression. Here we show that the human nucleoporin Nup214 colocalizes in part with human telomeres. By performing pull-down assays to identify novel interacting partners of Nup214, we found a protein involved in telomere length regulation, named telomeric repeat-binding factor 1 (TFR1), isoform 2 as putative Nup214-interacting protein. By immunofluorescence we show that a fraction of Nup214 localizes to human telomeres and that Nup214 colocalizes with tankyrase 1, a binding partner of TRF1 (isoform 2) and which is known to localize to NPCs in interphase cells. However, we found no direct interaction between Nup214 and TRF1 (isoform 2), suggesting that Nup214 might form a trimeric complex with TRF1 (isoform 2) and tankyrase 1.

4.1 Introduction

Nuclear pore complexes (NPCs) perforate the nuclear envelope (NE) of eukaryotic cells and regulate the bidirectional transport of proteins, RNAs and ribonucleoprotein (RNP) particles between the nucleus and cytoplasm of eukaryotic cells (Gorlich and Kutay 1999; Fried and Kutay 2003). Proteomic analysis of the mammalian NPC revealed that it is composed of about ~30 different proteins called nucleoporins or Nups. About one-third of the nucleoporins are characterized by distinct phenylalanine-glycine (FG) sequence motifs (Cronshaw et al. 2002). FG-repeat nucleoporins interact specifically with the importin-β family of transport receptors (Radu et al. 1995), with NTF2 (Paschal and Gerace 1995; Clarkson et al. 1996) as well as factors involved in mRNA export (Bachi et al. 2000; Strasser et al. 2000), and thus play a crucial role in the translocation of cargoes through the NPC (Ryan and Wente 2000; Ribbeck and Gorlich 2001; Cronshaw et al. 2002).

Nup214 is a putative oncogenic nucleoporin that contains multiple FG-repeats which mediate interactions with a number of transport receptors, such as hCRM1, Xpo-t, Rev and TAP/NXF1 (Fornerod et al. 1997; Zolotukhin and Felber 1999; Bachi et al. 2000; Kuersten et al. 2002). Based on its primary amino acid sequence, Nup214 is organized into three different domains: (i) an N-terminal domain that forms an asymmetric seven-bladed beta-propeller structure (Weirich et al. 2004); (ii) a central domain that contains a leucine zipper motif and two predicted coiled-coil domains (von Lindern et al. 1992; Bastos et al. 1997); and (iii) a C-terminal domain that harbors a nuclear localization signal (NLS) and contains 36 FG dipeptid motifs and 6 FxFG motifs in the human isoform (Fornerod et al. 1995). Immuno-electron microscopy (EM) studies on the topology of Nup214's distinct domains revealed that Nup214 is anchored to the cytoplasmic side of the NPC by its N-terminal and central domain, whereas its C-terminal FG-repeat domain is able to shift from the cytoplasmic to the nuclear face of the NPC in a transport-dependent manner (Paulillo et al. 2005). This C-terminal FG-repeat domain of Nup214 mediates its interaction with several transport receptors and hence Nup214 plays an important role in different nuclear transport pathways, such as importin-β, CRM1, TAP and exportin-t-dependent/mediated transport (Fornerod et al. 1997; Zolotukhin and Felber 1999; Bachi et al. 2000; Kuersten et al. 2002; Rollenhagen et al. 2003). The central coiled-coil domain of Nup214 is critical for its incorporation into the NPC due to interaction with the coiled-coil domain of the nucleoporin Nup88 (Bastos et al. 1997). The functional role of the N-terminal domain of Nup214, however, has remained largely elusive, despite the fact that this domain has been shown to interact with the RNA helicase Dbp5 (Schmitt et al. 1999; Weirich et al. 2004).

The main function of NPCs is attributed to its role in nucleocytoplasmic transport. However, in the last few years, it has become evident that NPCs are involved in a number of other various cellular processes, for example, chromosome segregation, kinetochore

integrity, the secretory pathway and apoptosis (Fahrenkrog and Aebi 2003; Fahrenkrog et al. 2004). Amongst these processes, the association of NPCs with chromatin can play a role in genome regulation and integrity. The non-random distribution of heterochromatin in the close proximity to the NE and active genes localized to the nuclear periphery demonstrates that NPCs in particular play a critical role in activation of gene transcription. (Ishii et al. 2002; Casolari et al. 2004; Casolari et al. 2005; Dilworth et al. 2005; Schmid et al. 2006; Therizols et al. 2006). In yeast, an intriguing connection between NPCs and telomeres has been described (Therizols et al. 2006).

Telomeres are multifunctional structures that protect chromosome ends from end-to-end fusions and degradation, prevent activation of DNA damage checkpoints, and modulate the maintenance of telomeric DNA by telomerase (Chan and Blackburn 2002). Telomere regulation requires a minimal length of telomere repeats and telomere-binding proteins that protect the ends of human chromosomes, known as shelterin complex. This complex is composed by six telomere-specific proteins, which associates with the telomeric TTAGGG sequence. Three of these shelterin subunits, TRF1 (Telomeric Repeat Binding Factor 1), TRF2 (Telomeric Repeat Binding Factor 2), and POT1 (Protection Of Telomeres 1) directly recognize TTAGGG repeats, whereas TIN2 (TRF1-interacting nuclear factor 2), TPP1 (Tripeptidyl-Peptidase I Precursor), and Rap1 interconnect shelterin proteins (reviewed in (de Lange 2005)).

In yeast, telomeres are tethered to the nuclear periphery by an interaction with NPCs, which appears to be mediated by the Mlp (Myosin-like protein) proteins and yKu70p (Hediger et al. 2002). Mlp1p and Mlp2p have been shown to localize to the nuclear periphery and bind to nuclear pore proteins (Strambio-de-Castillia et al. 1999; Galy et al. 2000; Kosova et al. 2000). Additionally, Mlp2p is able to bind yKu70p, suggesting that telomere tethering to the nuclear periphery is mediated by an interaction of yKu with both Mlp proteins (Galy et al. 2000; Feuerbach et al. 2002). Disruption of Mlp proteins causes telomere clustering and releases telomeric gene repression (Hediger et al. 2002). Moreover, the Mlp proteins are interacting with NPCs via Nup145p, and consequently disruption of NPC architecture through mutation of Nup145p and Nup60p disrupted telomere anchoring to the nuclear periphery (Feuerbach et al. 2002). Moreover, Fabre and co-workers found that nucleoporins of the Nup84p complex anchor telomeres to the nuclear periphery and that the correct tethering of telomeres is critical for efficient double-strand DNA repair (Therizols et al. 2006).

In mammalian cells, the telomeric protein tankyrase 1 was found to localize at somatic telomeres and NPCs during interphase (Smith and de Lange 1999). Meiotic cells of certain plant and grasshopper species show an accumulation of NPCs near the membrane-attached telomeres (Loidl 1990; Zickler and Kleckner 1998) and during mammalian

meiosis, a small fraction of TRF1 was found to colocalize or partially overlap with NPC by immunofluorescence, although telomeres appear to be tethered to the nuclear envelope in areas that lack NPCs (Scherthan et al. 2000).

In order to better understand the functional role of the N-terminal domain in Nup214, we aimed to identify novel binding partners of this domain. By doing so, we identified TRF1 (isoform 2) as putative Nup214-interacting protein by performing pull-down assays. Transiently transfected TRF1 (isoform 2) localizes to telomeres of unsynchronized cells, and it colocalizes with tankyrase 1. We also show that Nup214 localizes partially to telomeres and colocalizes with tankyrase 1. Although Nup214 and TRF1 (isoform 2) were shown to colocalize with tankyrase 1, both proteins do not interact directly *in vitro*. Similarly to the localization of Nup214 N-terminal and central domain (Paulillo et al. 2005), tankyrase is known to localize to the cytoplasmic side of the NPC (Smith and de Lange 1999). Therefore, we speculate that these proteins form a heterotrimeric complex, which might confer a new functional role for Nup214 in either cell cycle control or telomere maintenance.

4.2 Results

4.2.1 Identification of novel Nup214-interacting protein

We have recently mapped the domain topology of the nucleoporin Nup214 and we found that Nup214-NTD, similar to its central domain is anchored to the cytoplasmic face of the NPC, whereas the FG-repeat domain of Nup214 is flexible, changing its location in a transport–dependent manner (Paulillo et al. 2005). Whereas it is known that Nup214 central domain mediates the incorporation of Nup214 to the NPC via interaction with Nup88 and that the C-terminal FG-repeat domain mediates the interaction with distinct nuclear transport factors, only little is know about the functional role of Nup214-NTD. Thus far, only the DEAD box helicase Dbp5 was found to interact with Nup214-NTD (Schmitt et al. 1999). We therefore aimed to identify novel interaction partners of this domain in order to better understand its functional role.

To do so, we first expressed residues 1-430 of Nup214-NTD in *E.coli* and purified the protein by affinity chromatography (see Materials and Methods). To identify proteins that bind to Nup214-NTD, the recombinantly expressed domain was immobilized on Ni-NTA beads and incubated with HeLa nuclear extract. Proteins that bind to the immobilized Nup214-NTD were analyzed by SDS-PAGE, and proteins that bound specifically to Nup214-NTD but not to Ni-NTA were identified by mass spectrometry.

As shown in Fig. 4.1, three proteins bind specifically to Nup214-NTD but not to the Ni-NTA beads. These proteins had molecular masses of approximately 65 kDa, 55 kDa and 35 kDa, and were identified as anti-Hepatitis C Virus E2 antibody, mitocondrial C1-tetrahydrofolate synthetase, and TRF1 (isoform 2), respectively.

The observed band for TRF1 (isoform 2) corresponds to ~35 kDa (Fig. 4.1) most probably due to cleavage during the experiment, since the molecular weight of the unprocessed precursor is ~50 kDa.

TRF1 is a double-stranded DNA binding protein involved in telomere length regulation via negative feedback mechanism, probably by inhibiting the activity of telomerase at the ends of individual telomeres (van Steensel and de Lange 1997). Moreover, TRF1 overexpression results in shortened telomeres, and mutation of its telobox domain causes elongated telomeres (van Steensel and de Lange 1997). Except for an internal deletion of 20 amino acids (296 to 316 in TRF1), TRF1 (isoform 2) is identical to TRF1, suggesting that these proteins may be generated by alternative splicing from the same gene, PIN2/TRF1 (Chong et al. 1995; Lu et al. 1996; Shen et al. 1997). Both TRF1 dimers were localized to telomeres, and no functional differences between these proteins have been demonstrated so

far. Additionally, Smith and de Lange have reported that tankyrase 1, an interacting partner from TRF1 localizes to the cytoplasmic face of the NPC during interphase (Smith and de Lange 1999). We therefore decided to analyze in more detail whether or not TRF1 (isoform 2) in fact interacts with Nup214, either directly or indirectly.

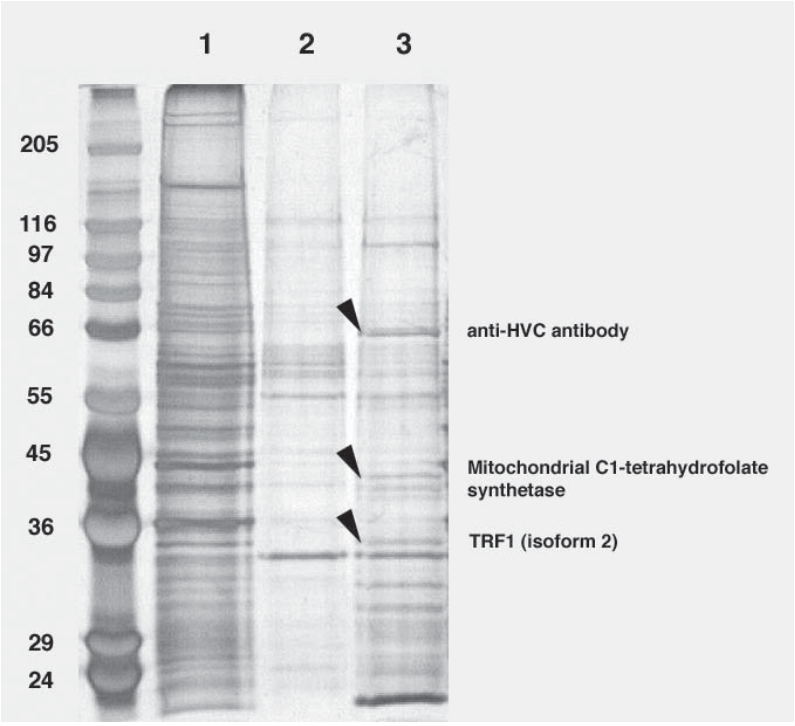

Figure 4.1: Silver-stained polyacrylamide gel showing proteins that interact with the N-terminal domain of Nup214. (1) HeLa S3 nuclei extract, (2) HeLa S3 nuclei extract bound to beads, (3) Nup214-NTD and bound fraction of HeLa S3 nuclei extracts.

4.2.2 Nup214 does not interact directly with TRF1 (isoform 2)

To further elucidate whether Nup214-NTD is able to directly interact with TRF1 (isoform 2), we performed solution-binding assays. For this purpose, we expressed Nup214-NTD by coupled *in vitro* transcription and translation as well as full-length His-tagged TRF1 (isoform 2) recombinantly in *E.coli*. Recombinant His-TRF1 (isoform 2) was immobilized on Ni-NTA beads and incubated with ^{35}S-labelled Nup214-NTD and the unbound and bound fractions were analyzed by SDS-PAGE and autoradiography. As shown in Fig. 4.2, Nup214-NTD does not directly interact with TRF1 (isoform 2) as Nup214-NTD was detected in the unbound fraction.

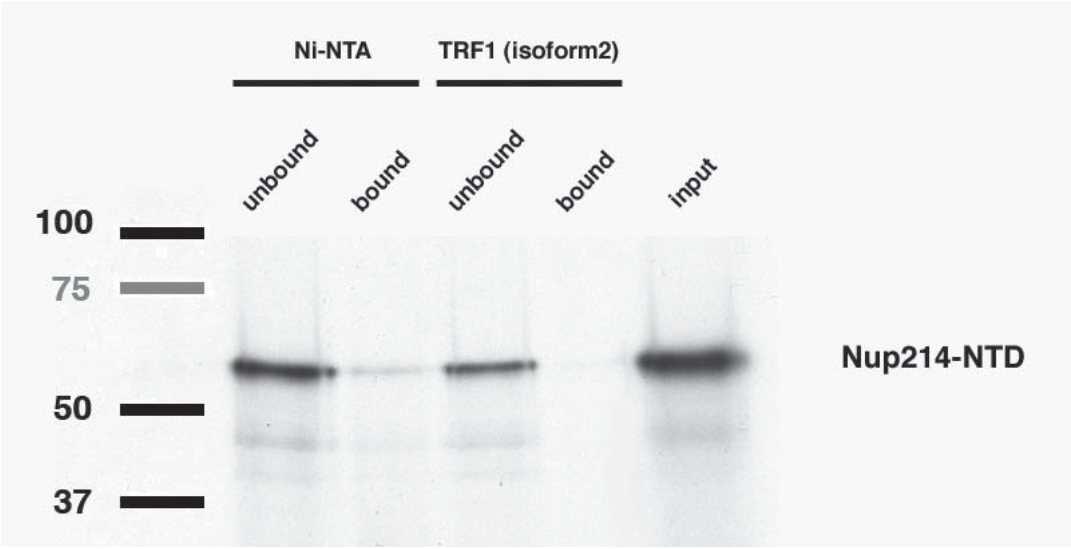

Figure 4.2: Solution-binding assay and autoradiography of protein-protein interaction between Nup214-NTD and TRF1 (isoform 2).

4.2.3 Cell cycle-dependent localization of Nup214

In a next step, since Nup214 does not appear to directly interact with TRF1 (isoform 2), we analyzed whether or not Nup214 and TRF1 (isoform 2) colocalize at any stage of the cell cycle. For this purpose, we first performed immunofluorescence detection of the Nup214-NTD epitope in a cell cycle-dependent manner. HeLa cells were arrested at the G_2/M boundary by treating the cells with nocodazole (40 ng/mL) or synchronized at the G_1/S boundary by mimosine arrest (400 μM), followed by an immunofluorescence assay. As shown in Figs. 4.3A and 4.3B, the immunofluorescence signals for Nup214 show a punctated pattern similar to telomere staining both in nocodazole and mimosine treated cells, but it is also dispersed throughout the nucleus, suggesting that Nup214 partially colocalizes with human telomeres.

4.2.4 Nup214 colocalizes with telomeres

In order to confirm that Nup214 in fact localizes to telomeres, we next performed co-localization immunofluorescence experiments. Tankyrase 1 is a known telomeric protein, and we therefore decided to use an anti-tankyrase 1 antibody as telomeric marker. Moreover,

tankyrase 1 is known to localize to the cytoplasm, while a minor portion is also found at the NPCs, and around the perinuclear matrix of mitotic centromeres (Smith and de Lange 1999). During interphase a small fraction of tankyrase 1 is found in the nucleus, associated with TRF1 (Smith and de Lange 1999).

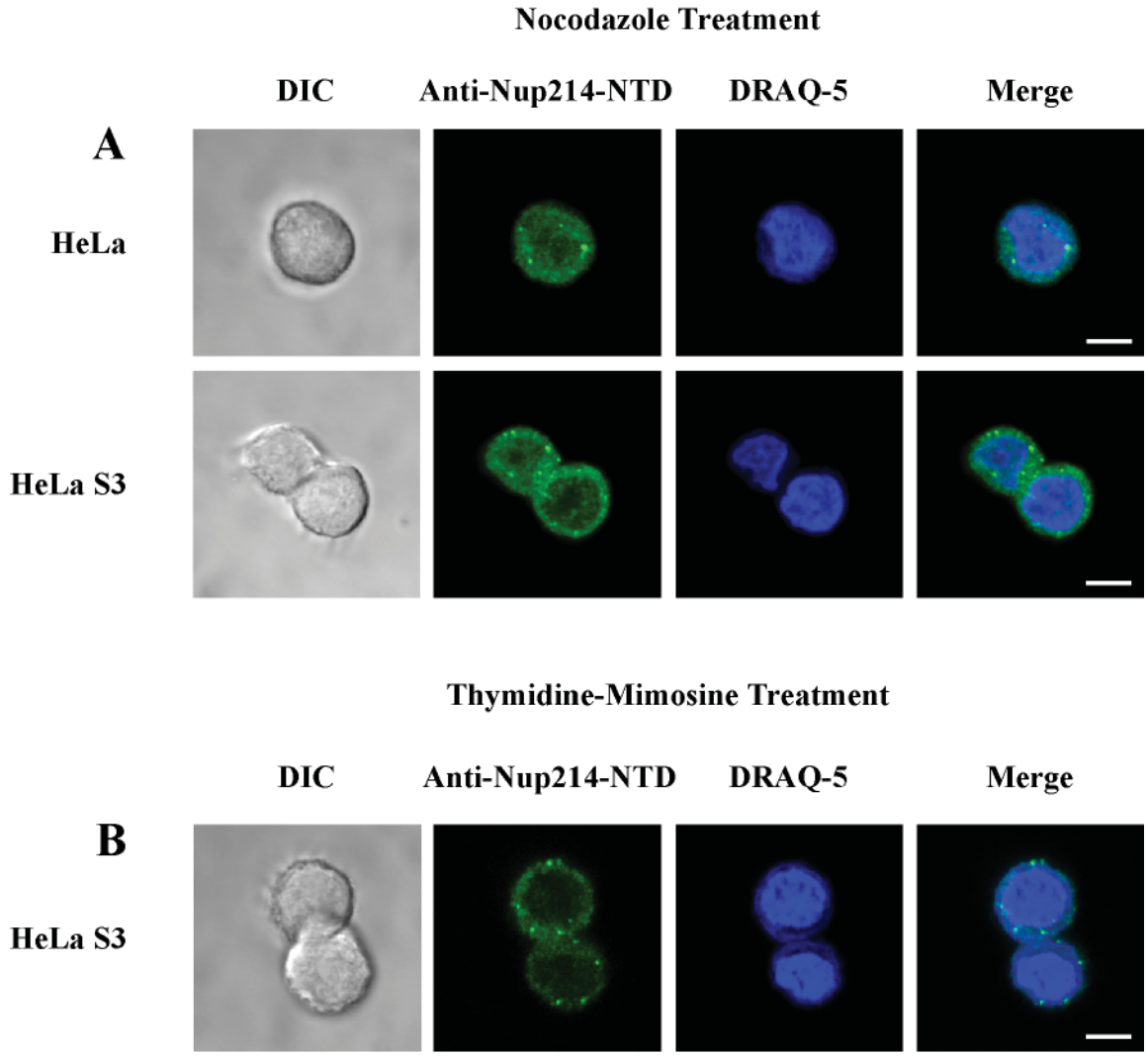

Figure 4.3: (A) HeLa or HeLa S3 cells synchronized with nocodazole at the G_2/M phase were immunostained with anti-Nup214-NTD and DRAQ-5 for DNA labeling, (B) Hela S3 cells arrested by thymidine-mimosine treatment at the G_1/S border and subsequently labeled with anti-Nup214-NTD and DRAQ-5 to detect DNA. Scale bar: 20 µm

As described in Materials and Methods, HeLa or HeLa S3 cells were synchronized at the G_1/S boundary and at the G_2/M boundary by mimosine and nocodazole treatment, respectively, and cells were first stained with anti-tankyrase 1 antibody and subsequently with anti-Nup214-NTD.

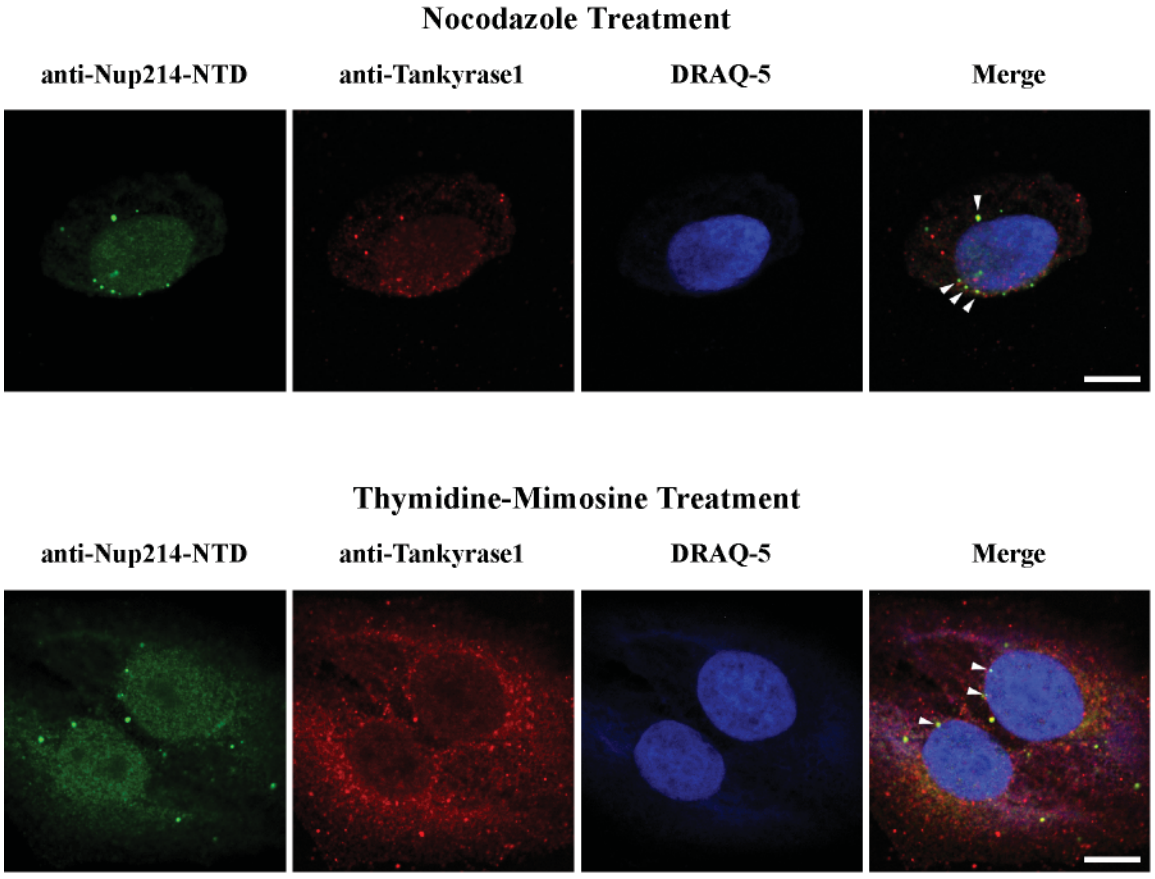

Figure 4.4: Immunofluorescence co-localization between Nup214 and tankyrase 1. HeLa cells were synchronized by thymidine-mimosine arrest at the G_1/S boundary; similarly, HeLa cells were arrested by nocodazole treatment at the G_2/M boundary and stained with anti-tankyrase 1 antibody and subsequently with anti-Nup214-NTD. Scale bar: 20 μm

As shown in Fig. 4.4, in both nocodazole and mimosine treated HeLa cells, we found a partial co-localization of Nup214 and tankyrase 1, suggesting that, in fact, a fraction of Nup214 localizes to telomeres.

4.2.5 TRF1 (isoform 2) exclusively localizes to human telomeres

Next, we wanted to analyze the subcellular localization of TRF1 (isoform 2), in particular whether or not TRF1 (isoform 2) colocalizes with NPCs. To to so, we transiently transfected TRF1 (isoform 2) into HEK-293 cells. The TRF1 (isoform 2) construct consists of an N-terminal GFP tag that was introduced to the full-length protein. GFP-TRF1 (isoform 2) shows telomeric signal pattern (Fig. 4.5A), but no colocalization with NPCs. However, a soluble pool within the nucleus may exist.

Next, we studied if TRF1 (isoform 2) in fact colocalizes with known telomeric proteins.

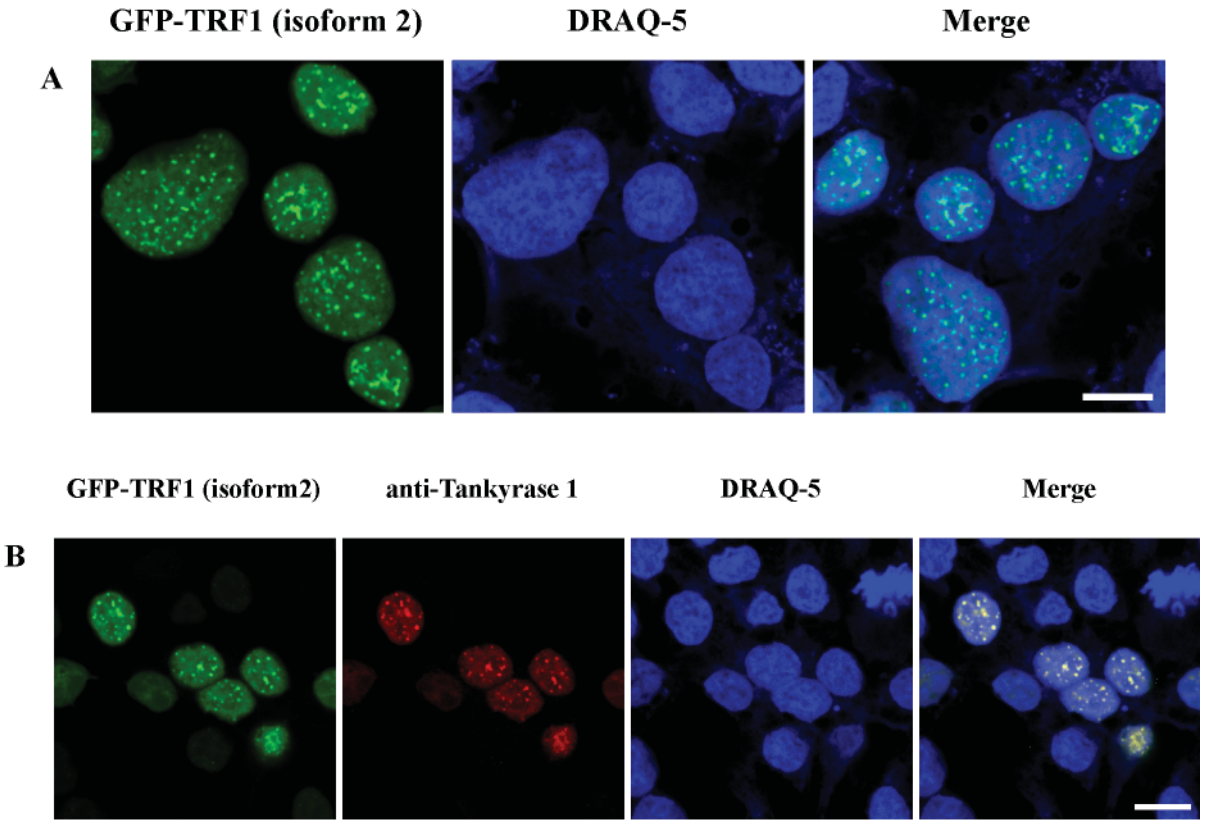

Figure 4.5: A. HEK-293 cells transfected with GFP-TRF1 (isoform 2) and DNA stained with DRAQ-5. According to previous studies, TRF1 (isoform 2) localizes to telomeres of mammalian chromosomes (Lages et al. 2004). **B.** HEK-293 cells transiently transfected with GFP-TRF1 (isoform 2) and immunostained with anti-tankyrase 1. The immunofluorescence pattern of TRF1 (isoform 2) and tankyrase 1 strongly indicated that tankyrase 1 co-localizes with TRF1 (isoform 2) at telomeres. Scale bar: 20 µm.

We therefore performed co-localization experiments using HEK-293 cells transiently transfected with GFP-TRF1 (isoform 2) and an anti-tankyrase 1 antibody. As shown in Fig. 4.5B, TRF1 (isoform 2) and tankyrase 1 in fact colocalize at human telomeres.

Taken together, our data suggest that TRF1 (isoform 2) exclusively localizes to telomeres, but not to NPCs. This, in turn, indicates that Nup214 interacts with telomeric proteins at telomeres and not at NPCs.

4.3 Discussion

Our search for novel binding partners of the Nup214-NTD has returned three putative candidates, from which we decided to investigate the telomeric protein TRF1 (isoform 2) more closely. Even though our pull-down assay is a strong indication for an interaction between Nup214 and TRF1 (isoform 2), we could not observe a direct interaction between the two proteins in solution binding assays.

Although Nup214 does not interact directly with TRF1 (isoform 2), both proteins were found to localize at telomeres on immunofluorescence level. It has been observed by us (Paulillo et al. 2005) and others (Kraemer et al. 1994) that unsynchronized cells show a nucleoporin characteristic nuclear rim-staining pattern for Nup214. However, in cells treated with nocodazole or mimosine, a punctated telomeric immunofluorescence signal was detected for Nup214 (Fig. 4.3). While Nup214 shows a partial telomeric localizaton, we found a GFP-TRF1 (isoform 2) fusion protein exclusively at telomeres. Interestingly, Schertan et al. by using immunofluorescence, found TRF1 at telomeres, partially co-localizing or overlaping with NPCs in spermatocyte nuclei (Scherthan et al. 2000). These data together suggest that in somatic cells a minor pool of TRF1 (isoform 2) may localize to NPCs, which is not detectable by immunofluorescence, but by electron microscopy. We found Nup214 and TRF1 (isoform 2) localized at telomeres but no direct interaction between both proteins could be detected *in vitro*. This paradoxical result led us to investigate a third protein, tankyrase 1. Tankyrase 1 is localized at human telomeres through its interaction with TRF1 (Smith and de Lange 1999). In addition to its telomeric localization, tankyrase 1 localizes to interphase NPCs (Smith and de Lange 1999). However, the interaction partner of tankyrase 1 at the NPC is still unknown. Tankyrase 1 was found to localize to the cytoplasmic face of the NPC, close to the cytoplasmic ring moiety of the NPC (Smith and de Lange 1999). Nup214-NTD is anchored to this cytoplasmic ring moiety (Paulillo et al. 2005), suggesting that Nup214 might be the docking site for tankyrase 1 at the NPC.

We show here, by immunofluorescence, that Nup214 and tankyrase 1 colocalize in interphase HeLa cells. Further double immuno-EM localization studies of Nup214 and tankyrase 1 are required to more precisely analyze the colocalization of both proteins at the nuclear envelope. Moreover, our immunofluorescence experiments confirmed the localization of TRF1 (isoform 2) and tankyrase 1 in unsynchronized HEK-293 cells (see Fig. 4.5). This is in agreement with previous studies, which have shown that tankyrase 1 localizes to mammalian telomeres through interaction with both TRF1 (isoform 2) and TRF1 (Smith et al. 1998; Smith and de Lange 1999; Lages et al. 2004). Taken together, the known interaction of TRF1 (isoform 2) with tankyrase 1 (Lages et al. 2004) and the observed colocalization of Nup214 with tankyrase 1 suggest that tankyrase 1 might be the binding factor between Nup214 and TRF1 (isoform 2).

This highly interesting link between Nup214 and telomeric proteins lead to questions about the functional roles of this putative complex. The first obvious speculation would be that Nup214 plays an unknown role in telomere regulation by controlling the entry of TRF1 (isoform 2) into the nucleus that, in turn, negatively regulates telomere length. Secondly, this Nup214-TRF1 (isoform 2) complex might play a role in cell cycle regulation/ progress. Van Deursen et al. showed that *NUP214-/-* mouse embryonic stem (ES) cells are not viable and that *NUP214-/-* embryos die in the utero (van Deursen et al. 1996). Although progressive depletion of Nup214 leads to cell cycle arrest, no morphological influence on the nuclear envelope or NPCs could be detected (van Deursen et al. 1996). Similarly, the depletion of *TERF1*, the TRF1 gene, first exon results in embryonic death, suggesting that TRF1 function is not limited to telomere length regulation, in particular since telomeres and telomerase activity are unaffected in this knock-out mice (van Steensel and de Lange 1997; Smogorzewska et al. 2000; Karlseder et al. 2002; Karlseder et al. 2003).

In summary, TRF1 (isoform 2) is a putative binding partner for Nup214, although both proteins do not appear to interact directly. Colocalization experiments, however, suggest that binding between Nup214 and TRF1 (isoform 2) might be mediated by tankyrase 1. Further analysis of the putative function of this novel Nup214 complex will require additional EM, cell biology and biochemistry studies to unravel its function, for example in cell cycle progression and/or telomere function.

4.4 Materials and Methods

4.4.1 DNA Constructs.

Full-length human Nup214 cloned in a Bluescript vector was a kind gift from Dr. Maureen A. Powers. The Nup214 N-terminal domain (Nup214-NTD) construct compraising residues 1-430 was PCR amplified from the Bluescript vector, cloned in a pETM-11 vector, and the correct DNA sequence was confirmed by sequencing. The nucleotide sequence of the forward primer was 5'-CATGCCATGGTATGGGAGACGAGATGGATGCC with NcoI restriction site.The reverse primer was 5'-ATAAGAATGCGGCCGCTCAT GACTTGGGCTGTCGCTCTCCTTC-3' with a NotI restriction site.

TRF1 (isoform 2) (IRAUp969A0289D, RZPD Deutsches Ressourcenzentrum für Genomforschung GmbH. Berlin, Germany) construct comprising the full-length sequence was PCR amplified from pDNR-LIB vector, cloned in a pETM-11 vector, and the construct was confirmed by sequencing. The nucleotide sequence of the forward primer was 5'-CATGCCATGGCGGAGGATGTTTCCTCA with *NcoI* restriction site. The reverse primer was 5'- GGGGTACCTCAGTCTTCGCTGTCTGAGGA-3' with a *KpnI* restriction site.

The pETM-11 expression vector (kindly provided by Dr. Olga Mayans, Biozentrum, Basel) is a modified version of the pET24d (Novagen, Madison, WI, USA) with an upstream sequence coding for a hexahistidine-tag (His_6-tag) plus a TEV protease cleavage site followed by the non-essential gene of a protein called MAD. For all constructs design, the MAD insert was excised and replaced with the gene encoding the protein of interest.

The Nup214-NTD construct comprising residues 1-455 was PCR amplified from pBluescript vector and cloned into a modified pBluescript vector (Stratagene, La Jolla, CA, USA) into which the multiple cloning site of the vector pALTER (Promega, Madison, WI, USA) was introduced (kind gift of Dr. D. Sitterlin, Université de Versailles St. Quentin en Yveline, France), and the correct sequence was confirmed by sequencing. The nucleotide sequence of the forward primer was 5'-CCGGAATTCATGGGAGACGAGATGGATGCC with an EcoRI restriction site. The reverse primer was 5'-AAGGAAAAAAGCGGCCGCTAAAGGGGCTGCAGCTGCAGAAG-3' with a NotI restriction site.

The full length TRF1 was amplified by PCR from pDNR-LIB vector, digested with KpnI and BamHI and ligated into pEGFP-C1 (Clontech Laboratories, Inc. Mountain View, USA), and the correct sequence was confirmed by sequencing. The nucleotide sequence of the forward primer was 5'-GGGGTACCATGGCGGAGGATGTTTCCTCA with *KpnI* restriction site. The reverse primer was 5'-GCGGATCCGTCAGTCTTCGCTGTCTGAGG-

3' with a *BamHI* restriction site.

4.4.2 Protein expression

Recombinant His_6-fusion proteins were expressed in *E.coli* Rosetta (DE3) strain (Novagen, Madison, WI, USA). Cells were grown in LB medium supplemented with 34 µg/ml chloramphenicol and 25 µg/ml kanamycin at 37°C. At an optical density (OD) of 0.3 at 600 nm for Nup214-NTD and OD_{600} of 0.4 for TRF1 (isoform 2), expression was induced by addition of 0.5 mM isopropyl-β-D-thiogalactopyranoside (IPTG) and cells were incubated at 20°C for 16-18 h. The cells were harvested by centrifugation at 8000 g, for 30 minutes at 4°C, and stored at -80°C or immediately used.

4.4.3 Protein purification

For purification of recombinantly expressed TRF1 (isoform2), cells were resuspended in lysis buffer containing of 50 mM HEPES pH 7.5, 800 mM KCl, 10% glycerol, 5 mM ß-mercaptoethanol, 10 mM imidazole, 5 µg/ml DNase I, 1 mM phenylmethylsulphonylfluoride (PMSF), 0.2 mg/ml lysozyme and protease inhibitor cocktail (Complete EDTA free; Roche Diagnostics GmbH, Mannheim, Germany).

Cell lysis was performed by sonication on ice (Branson Digital Sonifier, Branson Ultrasonics Corporation, Danbury, CT, USA) using 20 short pulses (5 seconds) with pauses (10 seconds).

The lysate was centrifuged at 40'000 g for 45 min at 4°C, the clarified supernatant was purified by affinity chromatography on a His-trap chelating column (GE Healthcare, Upsala, Sweden) pre-equilibrated with lysis buffer. A salt gradient wash was employed to discard contaminant proteins, and the protein was eluted with 200 mM imidazole. The elution product was dialyzed overnight in lysis buffer lacking imidazole. The protein was analyzed by SDS-PAGE and protein identity confirmed by mass spectrometry.

The same above described procedure was utilized for purification of the expressed Nup214-NTD, except that cell lysis was performed by using a French press (3 X 1000 pounds per square inch).

4.4.4 Isolation of HeLa nuclei

Nuclei from HeLa S3 cells were prepared by a method employing hypotonic swelling and Dounce homogenization (Spector, D., Cells, A laboratory manual, vol. 1, 43.7-43.11, 1998, CSHL press). Briefly, swollen cells were lysed in hypotonic buffer (0.01M NaCl, 1.5 mM $MgCl_2$, 0.01 M Tris-HCl, pH 7.4) by tight-fitting Dounce homogenization, and nuclear fractions were collected by low spin centrifugation. Isolated nuclei were stored at -70°C.

4.4.5 Pull-down assays with His-tagged protein

Recombinantly expressed Nup214-NTD (amino acids 1-430) was immobilized on 40 µL Ni-NTA beads (QIAGEN Inc, Valencia, CA, USA) in binding buffer and incubated at 4°C overnight. The beads were washed three times with wash buffer (50 mM Tris-HCl, pH 7.5, 200 mM NaCl, and 40 mM imidazole). HeLa S3 cell nuclei were lysed by hypotonic lysis with 450 µL of 50 mM Tris-HCl, pH 7.5, 150 mM potassium acetate, 5 mM magnesium acetate and homogenized with a tight fitting Dounce homogenizer. Next, beads were loaded with HeLa nuclei extract, incubated overnight at 4°C and subsequently washed three times with wash buffer. Bound proteins were eluted by boiling in 3X gel sample buffer (5 min, 95°C). Proteins that bound specifically to Nup214-NTD as well as unbound fractions were analyzed by 10% SDS-PAGE and visualized by silver staining. Proteins of interest were identified by mass spectrometry.

4.4.6 *In vitro* transcription and translation

Nup214-NTD (amino acids 1-455) was expressed by coupled *in vitro* transcription and translation following the manufacturer's protocol (TnT quick coupled transcription/ translation systems, Promega Corporation, Madison, USA). Briefly, Nup214-NTD (amino acids 1-455) cloned into a pBluescript modified vector containing a T7 promoter was added to the master mix and labelled with [^{35}S] methionine. The reaction was incubated at 30°C for 60-90min. The reaction mix was loaded onto a 10% SDS-PAGE gel and visualized by autoradiography.

4.4.7 Solution binding assay

Recombinant His-tagged Nup214-NTD was prebound to 40µL Ni-NTA beads for 8 h at 4°C with gentle agitation. The beads were washed three times with a washing buffer (50 mM HEPES, pH 7.5, 400 mM KCl, and 40 mM imidazole), and subsequently beads were loaded with 10 µl *in vitro* transcribed/translated TRF1 (isoform 2) for 24 h at 4°C with gentle agitation in a final volume of 200 µL of binding buffer. The beads were next washed for three times with wash buffer and bound proteins were eluted by heating in 3X gel sample buffer (5 min, 95°C). Unbound and bound protein fractions were separated by 10% SDS-PAGE gels and visualized by autoradiography.

4.4.8 Cell culture and cell synchronization

HeLa cells were grown in monolayer on coverslips in DMEM (Sigma-Aldrich, St. Louis, MO, USA) supplemented with 10% fetal calf serum (FCS), 2 mM L-glutamine and antibiotics at 37°C with 5% CO_2. Synchronous population of HeLa cells was obtained by nocodazole treatment. Briefly, exponentially growing cells (cell density 2 X 10^5 to 6 X 10^5) were treated with 40 ng/mL nocodazole (Sigma-Aldrich, St. Louis, MO, USA) for 12-16 h, mitotic cells were detached from the flask and prepared for immunofluorescence.

Alternatively, cells were arrested at the G_1/S border by mimosine (Sigma-Aldrich, St. Louis, MO, USA) treatment. Exponentially growing cells were treated for 12 h with 2 mM thymidine, released in DMEM medium for 9 h, and retreated with 400 µM of mimosine for 12 h and prepared for immunofluorescence.

4.4.9 Transient transfection assays

HEK-293 cells were cultured on coverslips coated with 0.01% poly-L-lysine (Sigma-Aldrich, St. Louis, MO, USA) in a 24-well plate in DMEM supplemented with 10% fetal bovine serum at 37°C in a 5% CO_2 atmosphere incubator. On the day of transfection, DMEM was removed and replaced with Opti-MEM® reduced serum medium (Life Technologies, Gaithersburg, MD, USA). Transfection was performed using Lipofectamine™ 2000 reagent (Invitrogen, Carlsbad, CA, USA) according to the manufacturer's protocol. Briefly, a mixture of Lipofectamine™ 2000 and Opti-MEM was incubated for 5 minutes at room temperature. This solution was then combined with plasmid DNA mixed with Opti-MEM and incubated for further 20-25 minutes and the reaction mixture was added to the cells. After 21 hours, the

cells were rinsed with PBS and prepared for immunofluorescence.

4.4.10 Immunofluorescence microscopy

HeLa cells were cultured on coverslips or HeLa S3 non-adherent cells were grown and seeded on poly-L-lysine coated coverslips. Cells were fixed in PBS containing 4% paraformaldehyde and permeabilized in PBS containing 0.2% Triton X-100. The permeabilized cells were washed and incubated with the corresponding primary antibodies in PBS for 1 h, followed by a wash step and 45 minutes incubation with a secondary antibody containing DRAQ-5 cell permeable DNA fluorescence dye (1:250, ALEXIS, San Diego, USA).

The following antibodies were used: anti-Nup214-NTD (1:100; (Paulillo et al. 2005)), anti-tankyrase1 (1:30 , Calbiochem, Darmstadt, Germany), anti-rabbit Alexa 488 (1:800, Molecular Probes, Eugene, OR, USA) and Cy3-anti-mouse IgG (1:2000; Jackson ImmunoResearch Europe Ltd., Cambridgeshire, UK).

The immunostained cells then were next mounted in Mowiol and visualized by using a confocal laser-scanning microscope (Leica TCS NT/SP1, Leica, Vienna, Austria). Images were recorded using the microscope-system software and processed with Adobe Photoshop (Adobe Systems, Mountain View, CA, USA).

Acknowledgements

The authors thank Dr. Maureen Powers (Department of Cell Biology, Emory University School of Medicine, Atlanta, USA) and Dr. Olga Mayans (Biozentrum, University of Basel) for providing the clones of human Nup214 and the vector pETM-11, respectively. Ueli Aebi is greatly acknowledged for critically reading of the manuscript. This work was supported by research grants from the Swiss National Science Foundation (to B.F.), by the Kanton Basel Stadt, and the M.E. Müller Foundation.

References

Bachi, A., I. C. Braun, et al. (2000). "The C-terminal domain of TAP interacts with the nuclear pore complex and promotes export of specific CTE-bearing RNA substrates." Rna **6**(1): 136-58.

Bastos, R., L. Ribas de Pouplana, et al. (1997). "Nup84, a novel nucleoporin that is associated with CAN/Nup214 on the cytoplasmic face of the nuclear pore complex." J Cell Biol **137**(5): 989-1000.

Casolari, J. M., C. R. Brown, et al. (2005). "Developmentally induced changes in transcriptional program alter spatial organization across chromosomes." Genes Dev **19**(10): 1188-98.

Casolari, J. M., C. R. Brown, et al. (2004). "Genome-wide localization of the nuclear transport machinery couples transcriptional status and nuclear organization." Cell **117**(4): 427-39.

Chan, S. W. and E. H. Blackburn (2002). "New ways not to make ends meet: telomerase, DNA damage proteins and heterochromatin." Oncogene **21**(4): 553-63.

Chong, L., B. van Steensel, et al. (1995). "A human telomeric protein." Science **270**(5242): 1663-7.

Clarkson, W. D., H. M. Kent, et al. (1996). "Separate binding sites on nuclear transport factor 2 (NTF2) for GDP-Ran and the phenylalanine-rich repeat regions of nucleoporins p62 and Nsp1p." J Mol Biol **263**(4): 517-24.

Cronshaw, J. M., A. N. Krutchinsky, et al. (2002). "Proteomic analysis of the mammalian nuclear pore complex." J Cell Biol **158**(5): 915-27.

de Lange, T. (2005). "Shelterin: the protein complex that shapes and safeguards human telomeres." Genes Dev **19**(18): 2100-10.

Dilworth, D. J., A. J. Tackett, et al. (2005). "The mobile nucleoporin Nup2p and chromatin-bound Prp20p function in endogenous NPC-mediated transcriptional control." J Cell Biol **171**(6): 955 - 65.

Fahrenkrog, B. and U. Aebi (2003). "The nuclear pore complex: nucleocytoplasmic transport and beyond." Nat Rev Mol Cell Biol **4**(10): 757-66.

Fahrenkrog, B., J. Koser, et al. (2004). "The nuclear pore complex: a jack of all trades?" Trends Biochem Sci **29**(4): 175-82.

Feuerbach, F., V. Galy, et al. (2002). "Nuclear architecture and spatial positioning help establish transcriptional states of telomeres in yeast." Nat Cell Biol **4**(3): 214-21.

Fornerod, M., J. Boer, et al. (1995). "Relocation of the carboxyterminal part of CAN from the nuclear envelope to the nucleus as a result of leukemia-specific chromosome rearrangements." Oncogene **10**(9): 1739-48.

Fornerod, M., J. van Deursen, et al. (1997). "The human homologue of yeast CRM1 is in a dynamic subcomplex with CAN/Nup214 and a novel nuclear pore component Nup88." Embo J **16**(4): 807-16.

Fried, H. and U. Kutay (2003). "Nucleocytoplasmic transport: taking an inventory." Cell Mol Life Sci **60**(8): 1659-88.

Galy, V., J. C. Olivo-Marin, et al. (2000). "Nuclear pore complexes in the organization of silent telomeric chromatin." Nature **403**(6765): 108-12.

Gorlich, D. and U. Kutay (1999). "Transport between the cell nucleus and the cytoplasm." Annu Rev Cell Dev Biol **15**: 607-60.

Hediger, F., K. Dubrana, et al. (2002). "Myosin-like proteins 1 and 2 are not required for silencing or telomere anchoring, but act in the Tel1 pathway of telomere length control." J Struct Biol **140**(1-3): 79-91.

Ishii, K., G. Arib, et al. (2002). "Chromatin boundaries in budding yeast: the nuclear pore connection." Cell **109**(5): 551-62.

Karlseder, J., L. Kachatrian, et al. (2003). "Targeted deletion reveals an essential function for the telomere length regulator Trf1." Mol Cell Biol **23**(18): 6533-41.

Karlseder, J., A. Smogorzewska, et al. (2002). "Senescence induced by altered telomere state, not telomere loss." Science **295**(5564): 2446-9.

Kosova, B., N. Pante, et al. (2000). "Mlp2p, a component of nuclear pore attached intranuclear filaments, associates with nic96p." J Biol Chem **275**(1): 343-50.

Kraemer, D., R. W. Wozniak, et al. (1994). "The human CAN protein, a putative oncogene

product associated with myeloid leukemogenesis, is a nuclear pore complex protein that faces the cytoplasm." Proc Natl Acad Sci U S A **91**(4): 1519-23.

Kuersten, S., G. J. Arts, et al. (2002). "Steady-state nuclear localization of exportin-t involves RanGTP binding and two distinct nuclear pore complex interaction domains." Mol Cell Biol **22**(16): 5708-20.

Lages, C. S., O. Etienne, et al. (2004). "Identification of alternative transcripts of the TRF1/Pin2 gene." J Cell Biochem **93**(5): 968-79.

Loidl, J. (1990). "The initiation of meiotic chromosome pairing: the cytological view." Genome **33**(6): 759-78.

Lu, K. P., S. D. Hanes, et al. (1996). "A human peptidyl-prolyl isomerase essential for regulation of mitosis." Nature **380**(6574): 544-7.

Paschal, B. M. and L. Gerace (1995). "Identification of NTF2, a cytosolic factor for nuclear import that interacts with nuclear pore complex protein p62." J Cell Biol **129**(4): 925-37.

Paulillo, S. M., E. M. Phillips, et al. (2005). "Nucleoporin domain topology is linked to the transport status of the nuclear pore complex." J Mol Biol **351**(4): 784-98.

Radu, A., G. Blobel, et al. (1995). "Identification of a protein complex that is required for nuclear protein import and mediates docking of import substrate to distinct nucleoporins." Proc Natl Acad Sci U S A **92**(5): 1769-73.

Ribbeck, K. and D. Gorlich (2001). "Kinetic analysis of translocation through nuclear pore complexes." Embo J **20**(6): 1320-30.

Rollenhagen, C., P. Muhlhausser, et al. (2003). "Importin beta-depending nuclear import pathways: role of the adapter proteins in the docking and releasing steps." Mol Biol Cell **14**(5): 2104-15.

Ryan, K. J. and S. R. Wente (2000). "The nuclear pore complex: a protein machine bridging the nucleus and cytoplasm." Curr Opin Cell Biol **12**(3): 361-71.

Scherthan, H., M. Jerratsch, et al. (2000). "Mammalian meiotic telomeres: protein composition and redistribution in relation to nuclear pores." Mol Biol Cell **11**(12): 4189-203.

Schmid, M., G. Arib, et al. (2006). "Nup-PI: the nucleopore-promoter interaction of genes in yeast." Mol Cell **21**(3): 379-91.

Schmitt, C., C. von Kobbe, et al. (1999). "Dbp5, a DEAD-box protein required for mRNA export, is recruited to the cytoplasmic fibrils of nuclear pore complex via a conserved interaction with CAN/Nup159p." Embo J **18**(15): 4332-47.

Shen, M., C. Haggblom, et al. (1997). "Characterization and cell cycle regulation of the related human telomeric proteins Pin2 and TRF1 suggest a role in mitosis." Proc Natl Acad Sci U S A **94**(25): 13618-23.

Smith, S. and T. de Lange (1999). "Cell cycle dependent localization of the telomeric PARP, tankyrase, to nuclear pore complexes and centrosomes." J Cell Sci **112 (Pt 21)**: 3649-56.

Smith, S., I. Giriat, et al. (1998). "Tankyrase, a poly(ADP-ribose) polymerase at human telomeres." Science **282**(5393): 1484-7.

Smogorzewska, A., B. van Steensel, et al. (2000). "Control of human telomere length by TRF1 and TRF2." Mol Cell Biol **20**(5): 1659-68.

Strambio-de-Castillia, C., G. Blobel, et al. (1999). "Proteins connecting the nuclear pore complex with the nuclear interior." J Cell Biol **144**(5): 839-55.

Strasser, K., J. Bassler, et al. (2000). "Binding of the Mex67p/Mtr2p heterodimer to FXFG, GLFG, and FG repeat nucleoporins is essential for nuclear mRNA export." J Cell Biol **150**(4): 695-706.

Therizols, P., C. Fairhead, et al. (2006). "Telomere tethering at the nuclear periphery is essential for efficient DNA double strand break repair in subtelomeric region." J Cell Biol **172**(2): 189-99.

van Deursen, J., J. Boer, et al. (1996). "G2 arrest and impaired nucleocytoplasmic transport in mouse embryos lacking the proto-oncogene CAN/Nup214." Embo J **15**(20): 5574-83.

van Steensel, B. and T. de Lange (1997). "Control of telomere length by the human telomeric protein TRF1." Nature **385**(6618): 740-3.

von Lindern, M., M. Fornerod, et al. (1992). "The translocation (6;9), associated with a

specific subtype of acute myeloid leukemia, results in the fusion of two genes, dek and can, and the expression of a chimeric, leukemia-specific dek-can mRNA." Mol Cell Biol **12**(4): 1687-97.

Weirich, C. S., J. P. Erzberger, et al. (2004). "The N-terminal domain of Nup159 forms a beta-propeller that functions in mRNA export by tethering the helicase Dbp5 to the nuclear pore." Mol Cell **16**(5): 749-60.

Zickler, D. and N. Kleckner (1998). "The leptotene-zygotene transition of meiosis." Annu Rev Genet **32**: 619-97.

Zolotukhin, A. S. and B. K. Felber (1999). "Nucleoporins nup98 and nup214 participate in nuclear export of human immunodeficiency virus type 1 Rev." J Virol **73**(1): 120-7.

Chapter 5

Conclusions and Future Prospects

5.1 FG-repeats: the chaperones of nucleocytoplasmic transport

In the last years, a consensus model of the 3-D architecture of the NPC has evolved from extensive EM studies, such as immuno-EM, cryo-EM, cryo-electron tomography, as well as AFM studies (Fahrenkrog et al. 2002; Stoffler et al. 2003; Beck et al. 2004; Lim et al. 2006). These studies led to a better understanding of the organization of individual nucleoporins within the NPC, how they assemble into subcomplexes, and how individual nucleoporins and subcomplexes act in nucleocytoplasmic transport (for review see (Tran and Wente 2006)).

In order to better understand the spatial organization of the nucleoporin Nup214, we used immuno-EM to determine the position of the three distinct domains of Nup214 within the 3-D architecture of the NPC. For this purpose, we used domain-specific antibodies in human somatic cells as well as in *Xenopus* oocyte nuclei in combination with the expression of epitope-tagged Nup214 in *Xenopus* oocytes. These studies revealed that the Nup214 N-terminal domain and central domain are located to the cytoplasmic face of the NPC, while the C-terminal FG-repeat domain localizes to both its cytoplasmic and the nuclear face. These results are in agreement with previous studies that showed that the N-terminal and central domain of Nup214 localized to the cytoplasmic face (Kraemer et al. 1994; Pante et al. 1994; Walther et al. 2002), whereas the C-terminal FG-repeat domain had thus far not been localized by immuno-EM.

FG-repeat domains have been previously described to be natively unfolded, i.e. they lack ordered secondary structures (α-helix and β-sheet) (Denning et al. 2002; Denning et al. 2003). Natively unfolded proteins exhibit features that assure simultaneous interactions with different binding partners and fast association-dissociation molecular rates (Denning et al. 2003), suggesting that the disordered nature of FG-repeat domains is intimately related to the mechanism of nuclear transport.

To further elucidate the functional role of FG-repeat domains in nucleocytoplasmic transport, we aimed to localize the domain topology of Nup214 and Nup153 FG-repeat domains in *Xenopus* oocyte nuclei. We found that in the presence of the excessive import cargo nucleoplasmin or in the presence of excessive poly(A^+) RNA isolated from HeLa cells, the localization of the FG-repeat domains of both, Nup214 and Nup153, shifted with regard to occurring import or export events. Moreover, an arrest of nucleocytoplasmic transport at 4°C constrains the mobility of the FG-repeat domains of Nup214 and Nup153 to their anchoring site within the NPC (Paulillo et al. 2005).

Our data therefore clearly underline the flexible and mobile character of FG-repeat domains, which, in turn, will have a high impact on the efficiency of nucleocytoplasmic

transport. Our data are supported by the finding that FG-repeat domains act as an entropic barrier at the periphery of the NPC and at the same time serve as selective gate by "trapping" transport complexes (Lim et al. 2006). Because of the natively unfolded nature of FG-repeat domains, even a small number of FG-repeat domains are sufficient to keep the entropic barrier, although probably less optimal (Lim et al. 2006). This, in turn, could explain why Wente and co-workers did not observe major effects on nucleocytoplasmic transport and cell viability when yeast cells were depleted for more than half of their FG-repeat domains (Strawn et al. 2004).

The notion that FG-repeat domains act as entropic barrier (see also (Lim et al. 2006)) is further supported by the finding that FG-repeat domains of Nup153 "collapse" upon binding of importin-β and that this collapse is reversible upon RanGTP binding, both *in vivo* and *in vitro* (R. Y. H. Lim, personal communication).

Our studies have revealed that the FG-repeat domains of Nup214 and Nup153 are both extended, flexible domains, which react to changes in their chemical environment, although slightly different (Paulillo et al. 2005; Paulillo et al. 2006).

In this context, it would be interesting to analyze if importin-β affects the FG-repeats of Nup214 in a similar way as described for Nup153. Also, it is known that Nup214 plays a critical role in CRM1-mediated nuclear export (Fornerod et al. 1997; Kehlenbach et al. 1999; Kehlenbach et al. 2001) and it would therefore be interesting to study the effect of importin-β versus CRM1 on both Nup214 and Nup153 FG-repeat domains.

5.2. Nup214 and nuclear export

Nup214 is anchored at the cytoplasmic face of the NPC and it is known to interact with the nuclear export receptor CRM1 (Kehlenbach et al. 1999; Kehlenbach and Gerace 2000). When CMR1 is depleted from HeLa cells, CRM1-mediated export is inhibited, whereas nuclear import appears to be unaffected (Hutten and Kehlenbach 2006). Fornerod and co-workers, in contrast, found nuclear import to be inhibited upon Nup214 depletion in mouse embryos, whereas a CRM1-dependent nuclear export was not studied (Fornerod et al. 1997). Both reports consistently show that Nup214 depletion results in an impaired mRNA export. Additional data from the Kehlenbach lab implies that Nup214 serves as a terminal binding for nuclear export complexes (Hutten and Kehlenbach 2006). RanGTP was shown to be required for the high-affinity complex containing Nup214, CRM1, RanGTP, and an export substrate (Hutten and Kehlenbach 2006). The complex formation between Nup214 and CRM1 at the nuclear face of the NPC is further supported by our immuno-EM data. We

performed co-localization experiments in *Xenopus* oocytes and found ~17% of the Nup214 and CRM1 gold particles co-localizing at the nuclear face of the NPC, whereas ~83% of the co-localization particles where found at the NPC cytoplasmic face. Interestingly, these particles were found exclusively at the distal ring of the basket or at the cytoplasmic ring of the NPC, possibly due to fast complex translocation through the NPC (unpublished data, Figure 5.1).

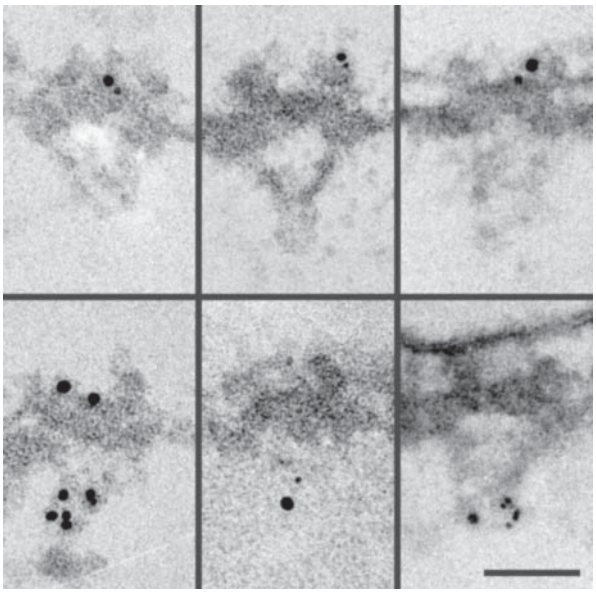

Fig. 5.1: Immuno-colocalization between Nup214 FG-repeats and CRM1. Intact isolated *Xenopus* nuclei were incubated with anti-Nup214-FG-repeats and to a secondary anti-rabbit IgG antibody conjugated to 10 nm colloidal gold. Subsequently the nuclei were incubated to anti-CRM1 direct conjugated to 5 nm colloidal gold. Scale bars represent 100 nm.

5.3 Chemical effectors and nucleoporin topology

Changes in levels of cellular calcium and ATP, respectively, are known to induce conformational changes in the NPC architecture, especially at the cytoplasmic face, but also at the nuclear basket and to affect nuclear transport (Greber and Gerace 1995; Rakowska et al. 1998; Stoffler et al. 1999; Wang and Clapham 1999). However, no direct link between these changes and nuclear transport has been demonstrated so far, although it has been suggested that NPC conformational changes could alter the accessibility of FG-repeat sites within the NPC (Erickson et al. 2004).

We studied the influence of Ca^{2+} or ATP on the domain topology of Nup214 and Nup153 in *Xenopus* oocytes (Paulillo et al. 2006). Previous AFM studies have revealed a reversible opening and closing of the distal ring of the nuclear basket in the presence or absence of 100 µM Ca^{2+} (Stoffler et al. 1999) and we have shown previously that the zinc-finger domain of Nup153 resides at the distal ring of the nuclear basket (Fahrenkrog et al. 2002). However, we observed no effect on the location of Nup153's zinc-finger domain upon addition of 100 µM and 2 mM Ca^{2+}, respectively (Paulillo et al. 2006).

Similarly, the presence of 100 µM Ca^{2+} in the buffer does not influence the distribution of the FG-repeat domains of Nup214 and Nup153. The presence of 2 mM Ca^{2+} as well as calcium store depletion by thapsigargin, in contrast, causes a dramatic redistribution of the FG-repeat domains of Nup214 and Nup153. This, however, is not a calcium-specific effect, since 2 mM Mg^{2+} lead to a similar alteration in the FG-repeat domain distribution of Nup214 and Nup153, underlining the natively unfolded nature of these domains. Natively unfolded proteins are characterized by the presence of charged amino acids, and are unstructured mainly due to electrostatic repulsion between non-compensated charges (Uversky 2002). Oppositely charged ions can reduce this electrostatic repulsion, which leads to partial refolding of the molecule. Therefore, FG-repeat domains likely collapse in the presence of high salt concentration and their partial folding reduces their mobility.

Whereas the peripheral FG-repeat domains of Nup214 and Nup153 as well as the zinc finger domain of Nup153 are rather unaffected in the presence of 100 µM Ca^{2+}, by employing cryo-EM in *Xenopus* nuclei we observed significant alterations in the radial mass density of the central framework in the presence of 100 µM Ca^{2+} in the buffer environment (Paulillo et al. 2006). Together our data therefore suggest that chemical effectors, such as Ca^{2+}, can cause structural reorganization within the central framework, whereas the highly flexible cytoplasmic filaments and the nuclear basket are rather insensitive to these effectors. In this context, it would be therefore interesting to map the domain topology of nucleoporins known to be components of the central framework, such as the Nup107-160 complex, in a Ca^{2+} dependent manner.

5.4 Other roles for Nup214

Nuclear pore complexes and nucleoporins undoubtedly have their main function in promoting nucleocytoplasmic transport and NPC structure. In the past few years, however, it became evident that nucleoporins play import roles in other processes, such as gene expression, DNA repair and apoptosis (Fahrenkrog et al., 2004; Fahrenkrog and Aebi, 2003).

The nuclear architecture provides a framework on which chromosomes are non-randomly organized into territories and their location within the nucleus varies between cell types (Oliver and Misteli 2005). Correct positioning of chromosomes reflects efficient transcriptional activity and have important implications for the regulation of gene expression (Misteli 2004; Gilbert et al. 2005). Additional roles of the nuclear periphery in gene regulation is linked to the NPC, since several export factors and NPC components were identified to be essential for activation of a reporter gene (Feuerbach et al. 2002; Hediger et al. 2002; Ishii et al. 2002; Casolari et al. 2004; Drubin et al. 2006). Measurements of gene locus movements reinforced the model that genes are physically associated with the NPC (Drubin et al. 2006). Likely, very similar experiments have shown that telomeres are highly associated with the NPC and nuclear periphery (Laroche et al. 1998; Galy et al. 2000; Heun et al. 2001; Feuerbach et al. 2002).

Along this line, we proposed that Nup214 might be involved in cell cycle and/or telomere length regulation via its putative interaction with two telomere associated proteins, TRF1 (isoform 2) and tankyrase 1. In this context, Nup214-NTD, which localizes to the cytoplasmic face of the NPC (Paulillo et al. 2005), may act as a docking site for a TRF1 (isoform 2)/tankyrase 1 complex during their nuclear import. This suggests that Nup214 might control the entry of TRF1 (isoform 2) into the nucleus and this, in turn, negatively regulates telomere length.

Interestingly, recently TRF1, similar to Nup214, has also been described to be associated with leukemia (Bellon et al. 2006). Patients with T-cell leukemia (ATL) showed increased transcriptional and post-transcriptional expression of telomeric binding proteins, such as TRF1, TRF2 and TIN2 (Bellon et al. 2006). Moreover, overexpression of TRF1 could be detected in several types of cancer (Matsutani et al. 2001; Yokota et al. 2003). Bellon et al. suggested that the overexpression of TRF1, TRF2 and TIN2 may increase the progress of ATL to a late stage (Bellon et al. 2006). In addition, high concentrations of TRF1 and TIN2 might prevent apoptotic signals resulting from short telomeres (Bellon et al. 2006). Overexpression of Nup214, on the other hand, is also known to induce apoptosis (Boer et al. 1998). If this, however, is linked to a role of Nup214 in telomere regulation remains to be elucidated.

Alternatively, both proteins Nup214 and TRF1 might have different functions from their original ones. Nup214 depletion leads to cell cycle arrest in mouse embryonic cells although no NPC or NE defects were detected (van Deursen et al. 1996). Similarly, depletion of part of the TRF1 gene resulted in embryonic death, but not due to telomere or telomerase misfunction (van Steensel and de Lange 1997; Smogorzewska et al. 2000; Karlseder et al. 2002; Karlseder et al. 2003), suggesting that TRF1 depletion causes cell cycle defects. TRF1 was also reported to interact with other non-telomere-interacting partners, such as the human

nucleoside diphosphate kinase nm23-H2 and the transcriptional repressor Sall1 (Sal-like 1) involved in Townes-Brocks syndrome (Nosaka et al. 1998; Netzer et al. 2001), which indicate that TRF1's function is not confined to the telomere regulation process.

Together this might indicate an unknown function for the Nup214-TRF1 complex, for example in cell cycle regulation/progression.

References

Beck, M., F. Forster, et al. (2004). "Nuclear pore complex structure and dynamics revealed by cryoelectron tomography." Science **306**(5700): 1387 - 90.

Bellon, M., A. Datta, et al. (2006). "Increased expression of telomere length regulating factors TRF1, TRF2 and TIN2 in patients with adult T-cell leukemia." Int J Cancer **119**(9): 2090-7.

Boer, J., J. Bonten-Surtel, et al. (1998). "Overexpression of the nucleoporin CAN/NUP214 induces growth arrest, nucleocytoplasmic transport defects, and apoptosis." Mol Cell Biol **18**(3): 1236-47.

Casolari, J. M., C. R. Brown, et al. (2004). "Genome-wide localization of the nuclear transport machinery couples transcriptional status and nuclear organization." Cell **117**(4): 427-39.

Denning, D. P., S. S. Patel, et al. (2003). "Disorder in the nuclear pore complex: the FG repeat regions of nucleoporins are natively unfolded." Proc Natl Acad Sci U S A **100**(5): 2450-5.

Denning, D. P., V. Uversky, et al. (2002). "The Saccharomyces cerevisiae nucleoporin Nup2p is a natively unfolded protein." J Biol Chem **277**(36): 33447-55.

Drubin, D. A., A. M. Garakani, et al. (2006). "Motion as a phenotype: the use of live-cell imaging and machine visual screening to characterize transcription-dependent chromosome dynamics." BMC Cell Biol **7**: 19.

Erickson, E. S., O. L. Mooren, et al. (2004). "Activation of ryanodine receptors in the nuclear envelope alters the conformation of the nuclear pore complex." Biophys Chem **112**(1): 1-7.

Fahrenkrog, B., B. Maco, et al. (2002). "Domain-specific antibodies reveal multiple-site topology of Nup153 within the nuclear pore complex." J Struct Biol **140**(1-3): 254-67.

Fahrenkrog, B. and U. Aebi (2003). "The nuclear pore complex: nucleocytoplasmic transport and beyond." Nat Rev Mol Cell Biol **4**(10): 757-66.

Fahrenkrog, B., J. Koser, et al. (2004). "The nuclear pore complex: a jack of all trades?"

Trends Biochem Sci **29**(4): 175-82.

Feuerbach, F., V. Galy, et al. (2002). "Nuclear architecture and spatial positioning help establish transcriptional states of telomeres in yeast." Nat Cell Biol **4**(3): 214-21.

Fornerod, M., J. van Deursen, et al. (1997). "The human homologue of yeast CRM1 is in a dynamic subcomplex with CAN/Nup214 and a novel nuclear pore component Nup88." Embo J **16**(4): 807-16.

Galy, V., J. C. Olivo-Marin, et al. (2000). "Nuclear pore complexes in the organization of silent telomeric chromatin." Nature **403**(6765): 108-12.

Gilbert, N., S. Gilchrist, et al. (2005). "Chromatin organization in the mammalian nucleus." Int Rev Cytol **242**: 283-336.

Greber, U. F. and L. Gerace (1995). "Depletion of calcium from the lumen of endoplasmic reticulum reversibly inhibits passive diffusion and signal-mediated transport into the nucleus." J Cell Biol **128**(1-2): 5-14.

Hediger, F., K. Dubrana, et al. (2002). "Myosin-like proteins 1 and 2 are not required for silencing or telomere anchoring, but act in the Tel1 pathway of telomere length control." J Struct Biol **140**(1-3): 79-91.

Heun, P., T. Laroche, et al. (2001). "Chromosome dynamics in the yeast interphase nucleus." Science **294**(5549): 2181-6.

Hutten, S. and R. H. Kehlenbach (2006). "Nup214 is required for CRM1-dependent nuclear protein export in vivo." Mol Cell Biol **26**(18): 6772-85.

Ishii, K., G. Arib, et al. (2002). "Chromatin boundaries in budding yeast: the nuclear pore connection." Cell **109**(5): 551-62.

Karlseder, J., L. Kachatrian, et al. (2003). "Targeted deletion reveals an essential function for the telomere length regulator Trf1." Mol Cell Biol **23**(18): 6533-41.

Karlseder, J., A. Smogorzewska, et al. (2002). "Senescence induced by altered telomere state, not telomere loss." Science **295**(5564): 2446-9.

Kehlenbach, R. H., R. Assheuer, et al. (2001). "Stimulation of nuclear export and inhibition of nuclear import by a Ran mutant deficient in binding to Ran-binding protein 1." J

Biol Chem **276**(17): 14524-31.

Kehlenbach, R. H., A. Dickmanns, et al. (1999). "A role for RanBP1 in the release of CRM1 from the nuclear pore complex in a terminal step of nuclear export." J Cell Biol **145**(4): 645-57.

Kehlenbach, R. H. and L. Gerace (2000). "Phosphorylation of the nuclear transport machinery down-regulates nuclear protein import in vitro." J Biol Chem **275**(23): 17848-56.

Kraemer, D., R. W. Wozniak, et al. (1994). "The human CAN protein, a putative oncogene product associated with myeloid leukemogenesis, is a nuclear pore complex protein that faces the cytoplasm." Proc Natl Acad Sci U S A **91**(4): 1519-23.

Laroche, T., S. G. Martin, et al. (1998). "Mutation of yeast Ku genes disrupts the subnuclear organization of telomeres." Curr Biol **8**(11): 653-6.

Lim, R. Y., N. P. Huang, et al. (2006). "Flexible phenylalanine-glycine nucleoporins as entropic barriers to nucleocytoplasmic transport." Proc Natl Acad Sci U S A **103**(25): 9512-7.

Matsutani, N., H. Yokozaki, et al. (2001). "Expression of telomeric repeat binding factor 1 and 2 and TRF1-interacting nuclear protein 2 in human gastric carcinomas." Int J Oncol **19**(3): 507-12.

Misteli, T. (2004). "Spatial positioning; a new dimension in genome function." Cell **119**(2): 153-6.

Netzer, C., L. Rieger, et al. (2001). "SALL1, the gene mutated in Townes-Brocks syndrome, encodes a transcriptional repressor which interacts with TRF1/PIN2 and localizes to pericentromeric heterochromatin." Hum Mol Genet **10**(26): 3017-24.

Nosaka, K., M. Kawahara, et al. (1998). "Association of nucleoside diphosphate kinase nm23-H2 with human telomeres." Biochem Biophys Res Commun **243**(2): 342-8.

Oliver, B. and T. Misteli (2005). "A non-random walk through the genome." Genome Biol **6**(4): 214.

Pante, N., R. Bastos, et al. (1994). "Interactions and three-dimensional localization of a group of nuclear pore complex proteins." J Cell Biol **126**(3): 603-17.

Paulillo, S. M., E. M. Phillips, et al. (2005). "Nucleoporin domain topology is linked to the transport status of the nuclear pore complex." J Mol Biol **351**(4): 784-98.

Paulillo, S. M., M. A. Powers, et al. (2006). "Changes in nucleoporin domain topology in response to chemical effectors." J Mol Biol **363**(1): 39-50.

Rakowska, A., T. Danker, et al. (1998). "ATP-Induced shape change of nuclear pores visualized with the atomic force microscope." J Membr Biol **163**(2): 129-36.

Smogorzewska, A., B. van Steensel, et al. (2000). "Control of human telomere length by TRF1 and TRF2." Mol Cell Biol **20**(5): 1659-68.

Stoffler, D., B. Feja, et al. (2003). "Cryo-electron tomography provides novel insights into nuclear pore architecture: implications for nucleocytoplasmic transport." J Mol Biol **328**(1): 119-30.

Stoffler, D., K. N. Goldie, et al. (1999). "Calcium-mediated structural changes of native nuclear pore complexes monitored by time-lapse atomic force microscopy." J Mol Biol **287**(4): 741-52.

Strawn, L. A., T. Shen, et al. (2004). "Minimal nuclear pore complexes define FG repeat domains essential for transport." Nat Cell Biol **6**(3): 197-206.

Tran, E. J. and S. R. Wente (2006). "Dynamic nuclear pore complexes: life on the edge." Cell **125**(6): 1041-53.

Uversky, V. N. (2002). "What does it mean to be natively unfolded?" Eur J Biochem **269**(1): 2-12.

van Deursen, J., J. Boer, et al. (1996). "G2 arrest and impaired nucleocytoplasmic transport in mouse embryos lacking the proto-oncogene CAN/Nup214." Embo J **15**(20): 5574-83.

van Steensel, B. and T. de Lange (1997). "Control of telomere length by the human telomeric protein TRF1." Nature **385**(6618): 740-3.

Walther, T. C., H. S. Pickersgill, et al. (2002). "The cytoplasmic filaments of the nuclear pore complex are dispensable for selective nuclear protein import." J Cell Biol **158**(1): 63-77.

Wang, H. and D. E. Clapham (1999). “Conformational changes of the in situ nuclear pore complex.” Biophys J **77**(1): 241-7.

Yokota, T., T. Suda, et al. (2003). “Telomere length variation and maintenance in hepatocarcinogenesis.” Cancer **98**(1): 110-8.

Appendix 1

Supplementary Figures

Supplementary figures - Chapter 2

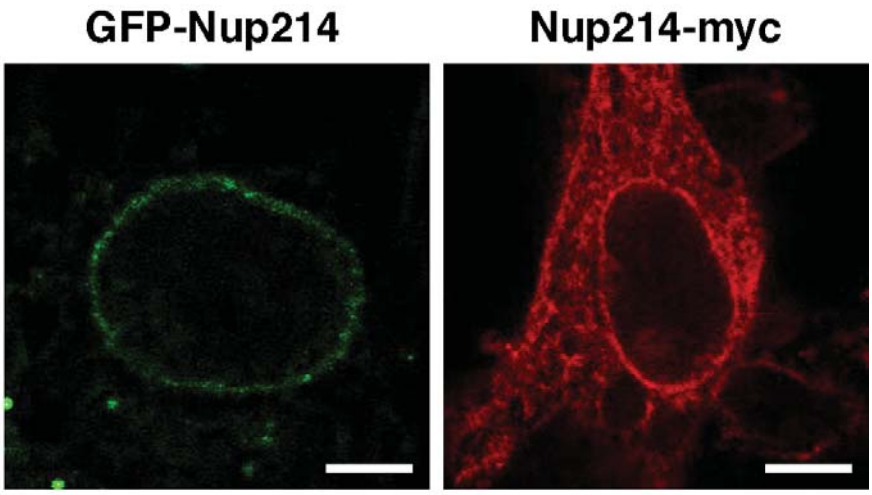

Figure S2.1: BHK cells transiently transfected with either pEGFP-Nup214 (left panel) or pCMV-Nup214-myc (right panel). GFP-Nup214 was visualized by direct immunofluorescence and Nup214-myc by using a primary monoclonal antibody against the myc-tag follwed by a secondary Cy3-labelled anti-mouse antibody. Scale bar, 5 μm.

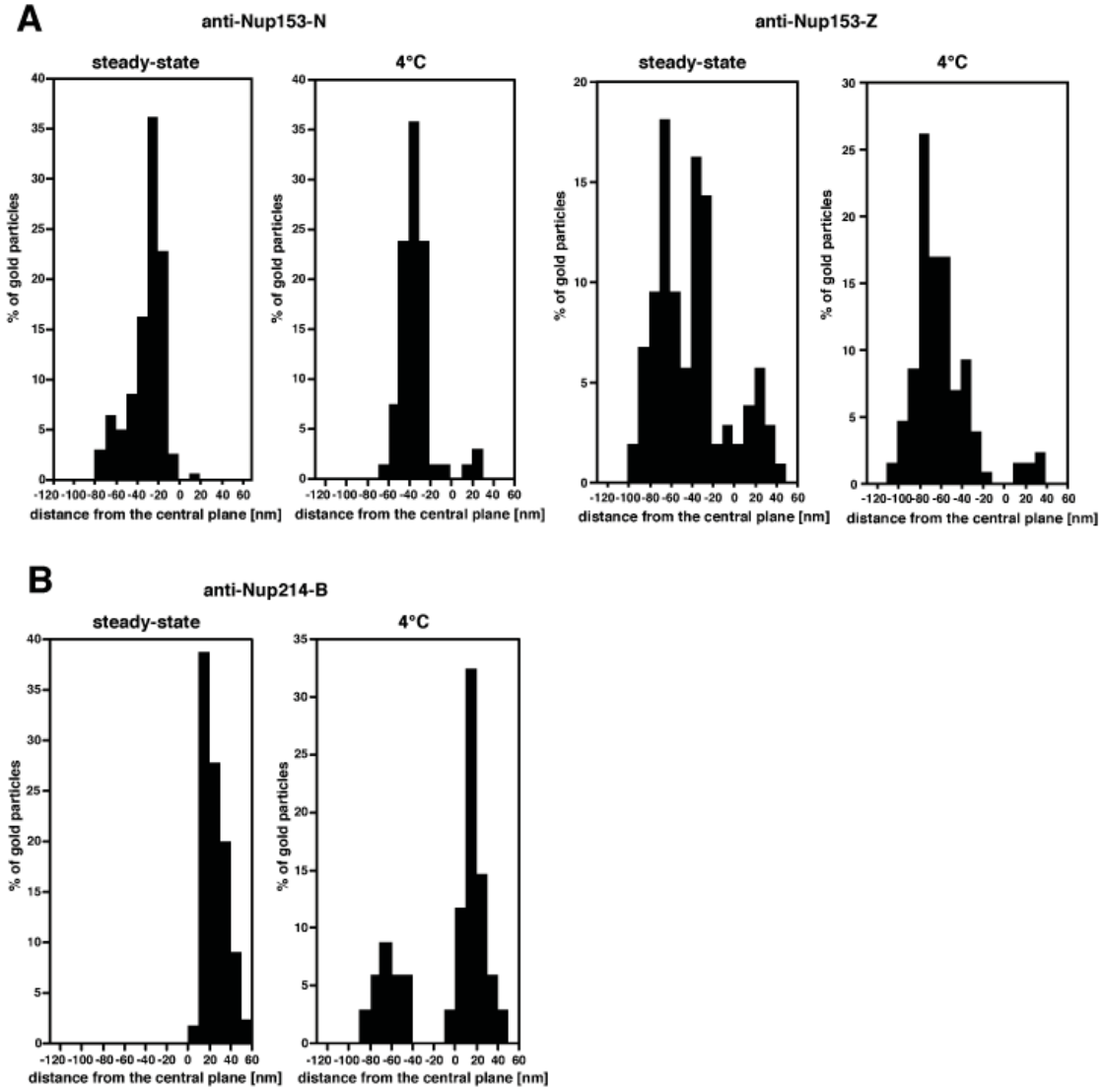

Figure S2.2: Attenuated nuclear transport does not influence the localization of the stationary domains Nup153 and Nup214. (A) Isolated *Xenopus* nuclei were incubated at 4°C prior labelling with an antibody against the N-terminal domain (anti-N-Nup153) and the central zinc-finger domain (anti-Z-Nup153) of Nup153, respectively, directly conjugated to 8-nm colloidal gold, and the gold particles associated with the NPC were quantitatively analyzed. The following numbers of gold particles were scored: two hundred three (anti-N-Nup153, steady-state), sixty-eight (anti-N-Nup153, 4°C), one hundred five (anti-Z-Nup153, steady-state), and one hundred thirty (anti-Z-Nup153, 4°C). (B) Immunolabelling of isolated *Xenopus* nuclei after incubation at 4°C with the anti-Nup214-B antibody and a secondary anti-rabbit IgG antibody conjugated to 10-nm colloidal and quantification of the gold particle distribution associated with the NPC. One hundred sixty-six (steady-state) and thirty-four (4°C) gold particles were scored, respectively. At 4°C, some cross-reactivity with the nuclear face of the NPC was observed as it has been seen in other sets of experiments at room temperature as well.

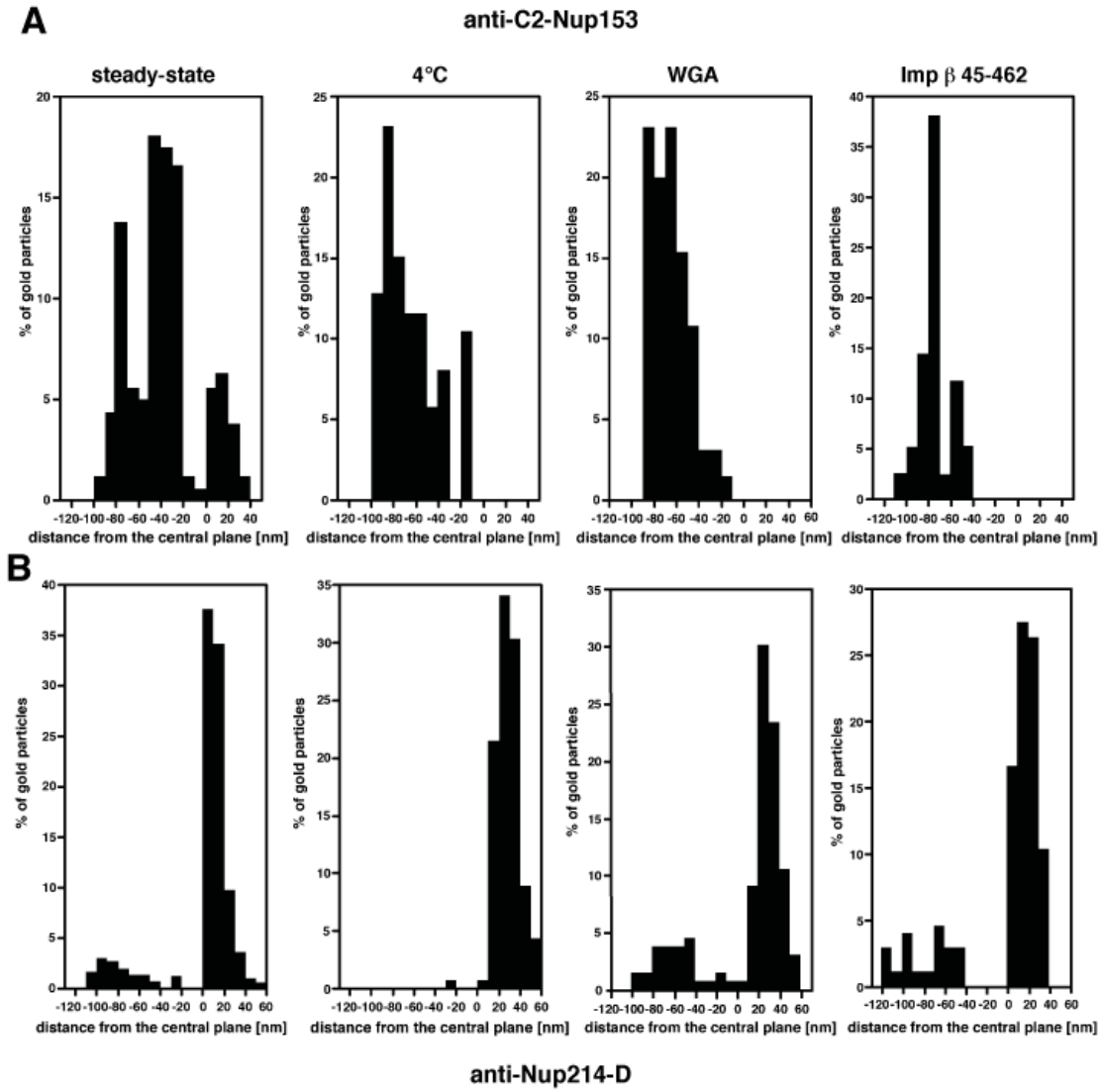

Figure S2.3: Influence of attenuating nuclear transport by WGA and importin-β 45-462 on the FG-repeat domains of Nup153 and Nup214. (A) Quantitative analysis of the gold particles associated with the NPC after labelling with the anti-C2-Nup153 antibody at 4°C, incubation with WGA or importin-β 45-462, respectively. The following numbers of gold particles were scored: one hundred sixty (steady-state), eighty-eight (4°C) sixty-five (WGA), and seventy-six (importin-β 45-462), respectively. (B) Quantification of the gold particle distribution associated with the NPC after labelling with the anti-Nup214-D antibody at 4°C, incubation with WGA or importin-β 45-462, respectively. Two hundred fifty-nine (steady-state), one hundred thirty-four (4°C), seventy-six (WGA), and one hundred seventy-five (importin-β 45-462) gold particles were scored, respectively.

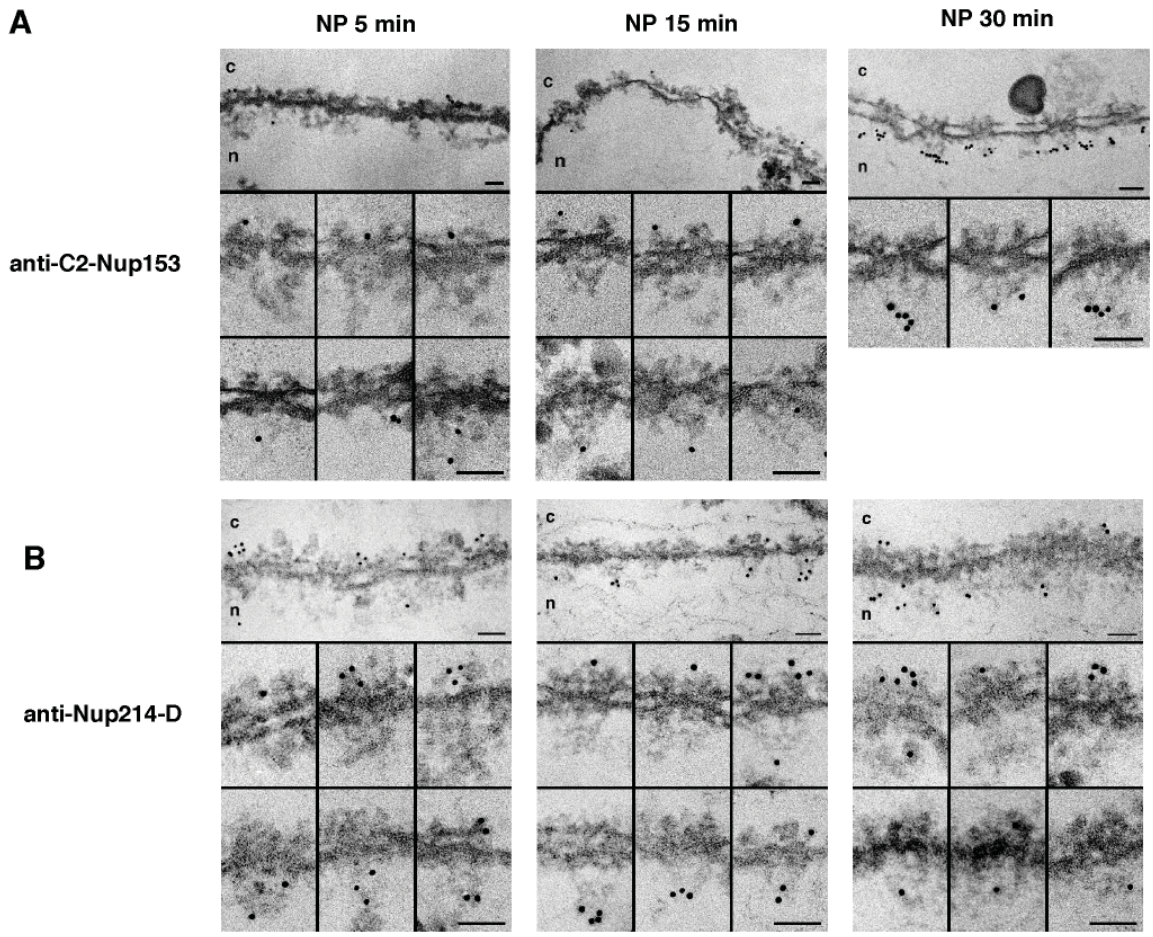

Figure S2.4: Immunolocalization of the FG-repeat domains of Nup153 and Nup214/CAN, respectively in the presence of excessive nucleoplasmin. *Xenopus* nuclei were isolated manually and incubated in nucleoplasmin-containing import mixture for the indicated time-points prior labelling with (A) the anti-C2-Nup153 antibody directly conjugated to 8-nm colloidal gold and (B) the anti-Nup214-D antibody and a secondary anti-rabbit IgG antibody conjugated to 10-nm colloidal gold, respectively. Shown ate stretches along the NE in cross sections (top panels) and selected examples of gold labelled NPCs in cross sections (middle and bottom panels). c, cytoplasm; n, nucleus. Scale bars, 100 nm.

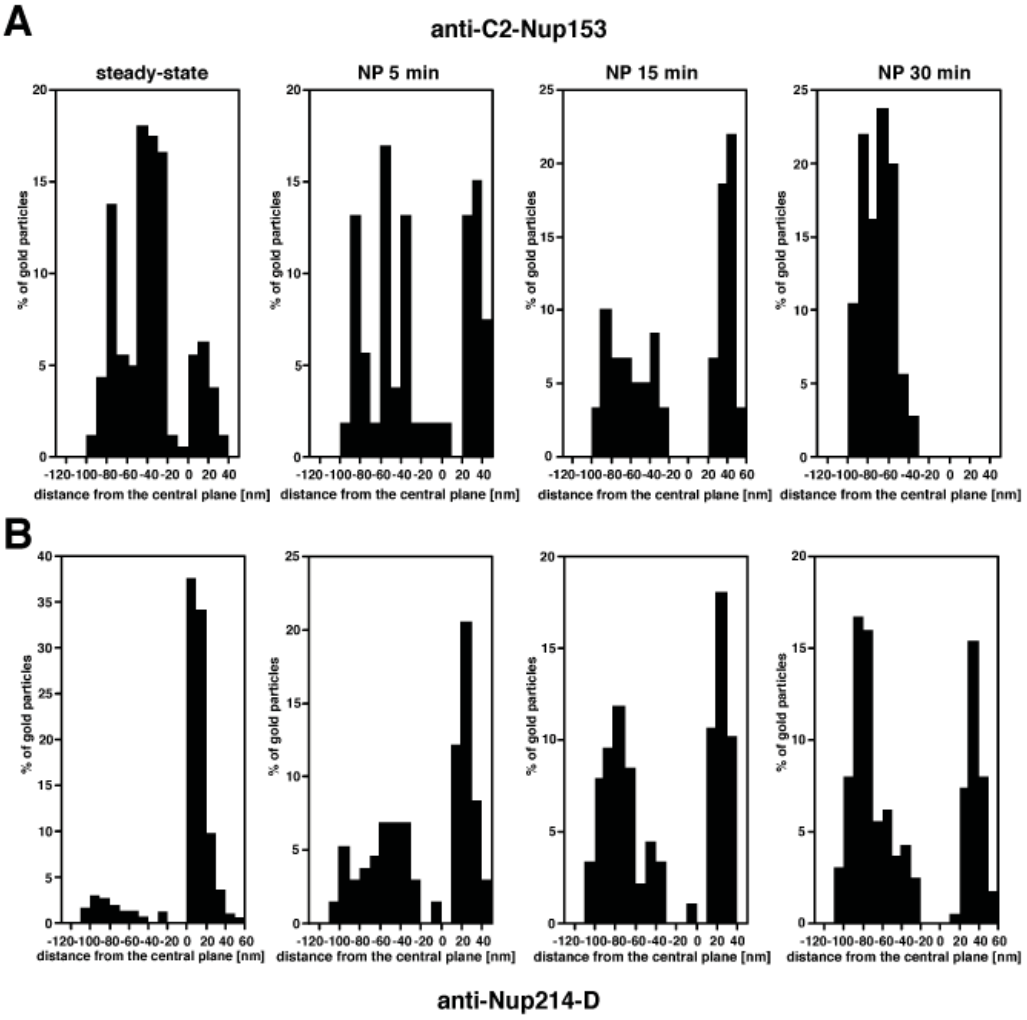

Figure S2.5: The location of the FG-repeat domain and the stationary domains of Nup153 in the presence of excess import cargo. (A) Quantitative analysis of the gold particles associated with the NPC after labelling with the anti-C2-Nup153 antibody in the presence of import mixture lacking additional cargo. One hundred sixty (steady-state) and one hundred twenty-seven (import mixture) gold particles were scored, respectively. (B) Quantitative analysis of the gold particles associated with the NPC after labelling with the anti-N-Nup153 and the anti-Z-Nup153 antibody, respectively, in the presence import mixture containing excess nucleoplasmin. Import of nucleoplasmin into isolated intact *Xenopus* oocytes nuclei was allowed for the indicated time-points before the nuclei were shortly prefixed in formaldehyde and pre-embedding labelled with the corresponding antibody. The following numbers of gold particles were scored for the individual experiments: not determined (anti-N-Nup153, 5 min), fifty-five (anti-N-Nup153, 15 min), fifty-eight (anti-N-Nup153, 30 min), fifty-five (anti-Z-Nup153, 5 min), forty-five (anti-Z-Nup153, 15 min), and fifty-five (anti-Z-Nup153, 30 min). Labelling with the anti-N-Nup153 antibody after 5 min incubation of the nuclei in the presence of excess nucleoplasmin could not be analyzed, since under these experimental conditions the nuclear face of the NPC repetitively appeared not accessible for the antibody.

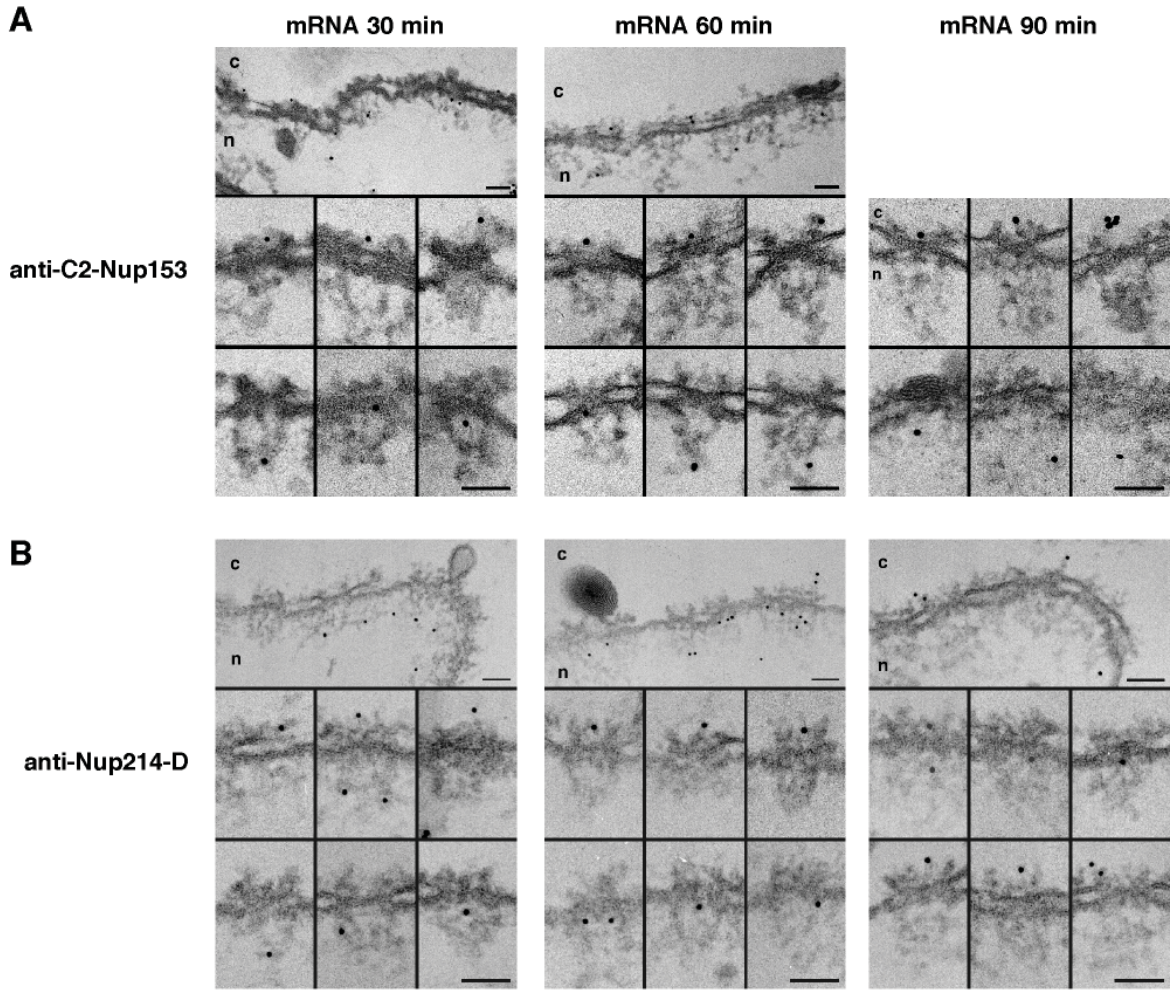

Figure S2.6: Immunolocalization of the FG-repeat domains of Nup153 and Nup214/CAN, respectively in the presence of excessive poly(A+) RNA. After microinjection of poly (A+) RNA into the nuclei of *Xenopus* oocytes, isolated nuclei were preembedding labelled with (A) the anti-C2-Nup153 antibody directly conjugated to 8-nm colloidal gold and (B) the anti-Nup214-D antibody and a secondary anti-rabbit IgG antibody conjugated to 10-nm colloidal gold, respectively. Cross section along the NE as well as selected examples of labelled NPCs are shown. c, cytoplasm; n, nucleus. Scale bars, 100 nm.

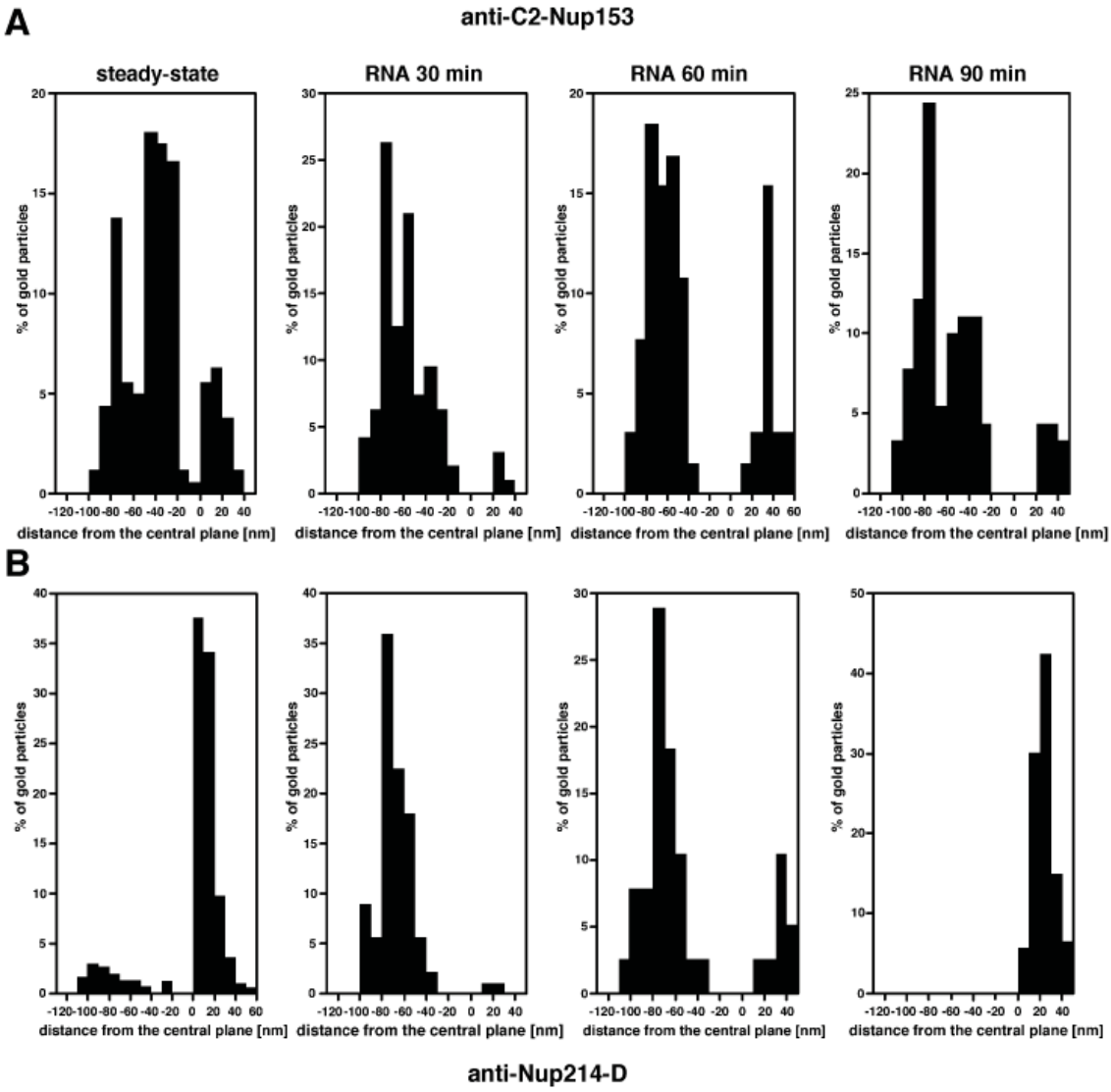

Figure S2.7: The influence of export cargo on the location of the FG-repeat domains of Nup153 and Nup214. Quantification of the gold particle distribution associated with the NPC after microinjection of total RNA into the nuclei of *Xenopus* oocytes and pre-embedding labelling with the (A) anti-C2-Nup153 and the (B) anti-Nup214-D antibody. The following numbers of gold particles were scored for the individual experiments: ninety-two (anti-C2-Nup153, 30 min), sixty-eight (anti-C2-Nup153, 60 min), ninety-three (anti-C2-Nup153, 90 min), ninety (anti-Nup214-D, 30 min), thirty-nine (anti-Nup214-D, 60 min), and one hundred fifty-four (anti-Nup214-D, 90 min).

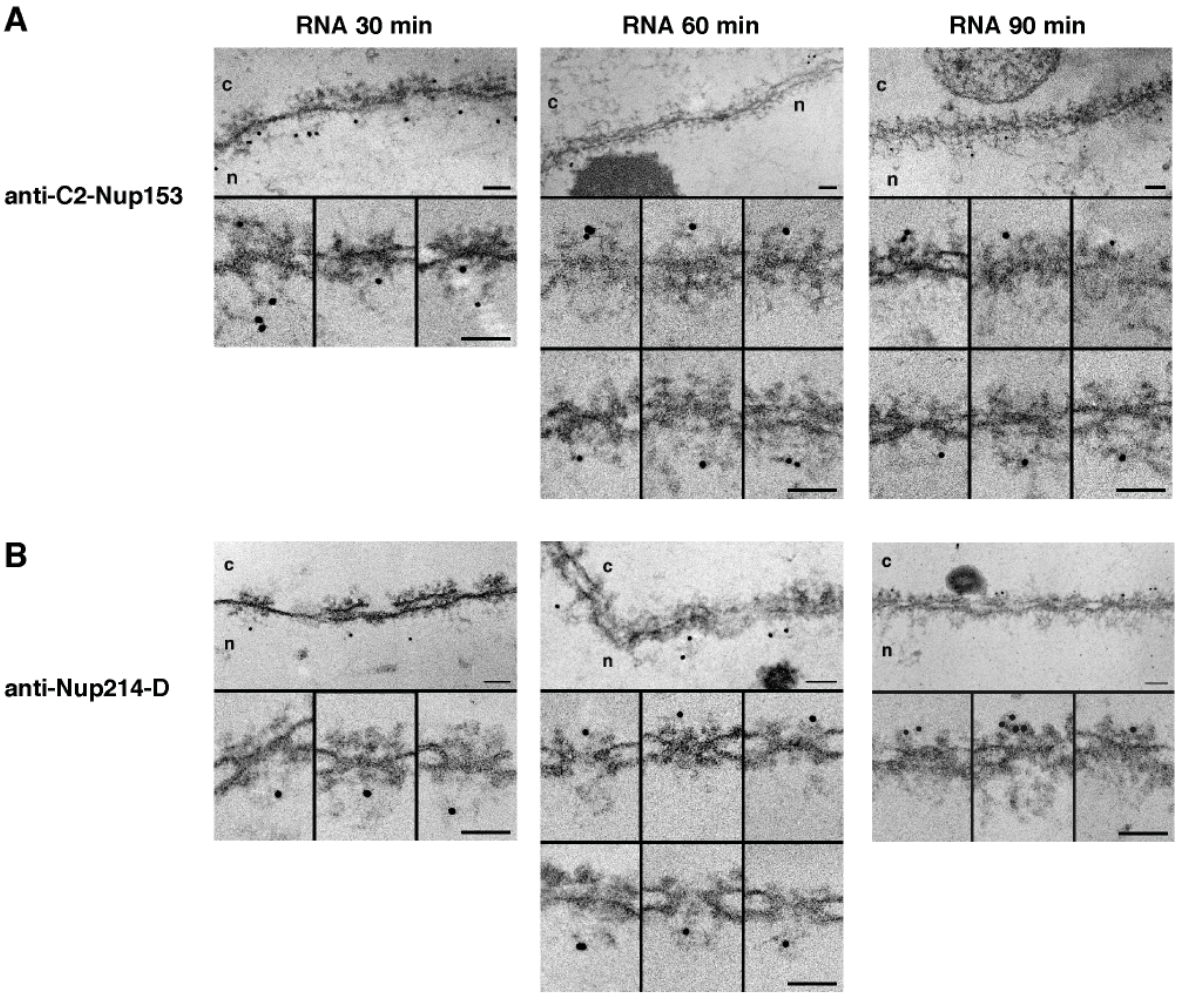

Figure S2.8: Immunolocalization of the FG-repeat domains of Nup153 and Nup214/CAN, respectively in the presence of excessive total RNA. After microinjection of RNA into the nuclei of *Xenopus* oocytes, isolated nuclei were preembedding labelled with (A) the anti-C2-Nup153 antibody directly conjugated to 8-nm colloidal gold and (B) the anti-Nup214-D antibody and a secondary anti-rabbit IgG antibody conjugated to 10-nm colloidal gold, respectively. Cross section along the NE as well as selected examples of labelled NPCs are shown. c, cytoplasm; n, nucleus. Scale bars, 100 nm.

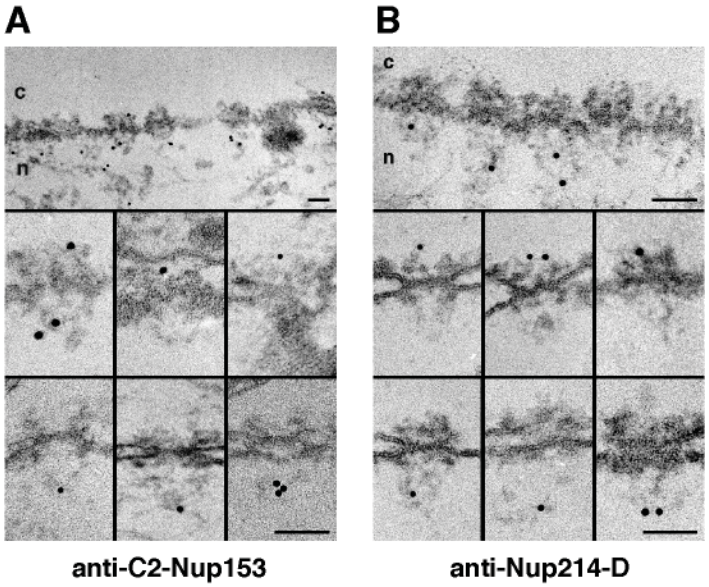

Figure S2.9: Localization of the FG-repeat domains of Nup153 and Nup214/CAN under influence of actinomycin D. A cross section along the NE and selected examples of NPCs in cross sections after labelling with (A) the anti-C2-Nup153 and (B) the anti-Nup214/CAN antibody are shown. c, cytoplasm; n, nucleus. Scale bars, 100 nm.

Supplementary figures - Chapter 3

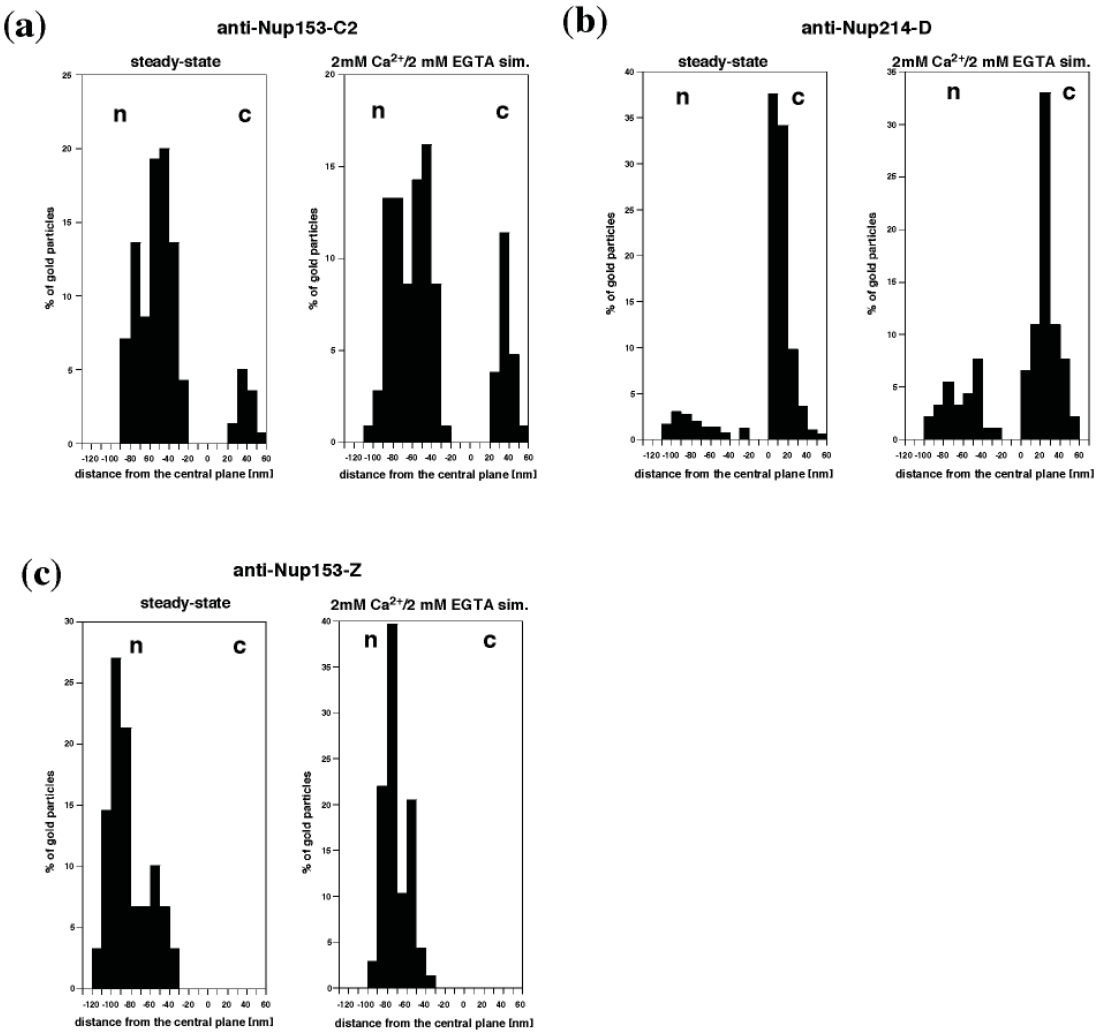

Figure S3.1: Quantification of the gold particle distribution associated with the NPC after isolated intact *Xenopus* nuclei were incubated in low salt buffer containing 2 mM Ca^{2+} and 2 mM EGTA for 10 minutes before nuclei were shortly fixed and pre-embedding labelled with (a) an antibody against the FG-repeat domain of Nup153 (anti-Nup153-C2), (b) an antibody against the FG-repeat domain of Nup214, and (c) the zinc-finger domain of Nup153. The following numbers of gold particles were scored for the individual experiments: 105 (anti-Nup153-C2, 2 mM Ca^{2+}/2 mM EGTA sim.), 165 (anti-Nup214-D, 2 mM Ca^{2+}/2 mM EGTA sim.), 65 (anti-Nup153-Z, 2 mM Ca^{2+}/2 mM EGTA sim.). Steady-state values are as shown in Figure 1 and are included here for reference.

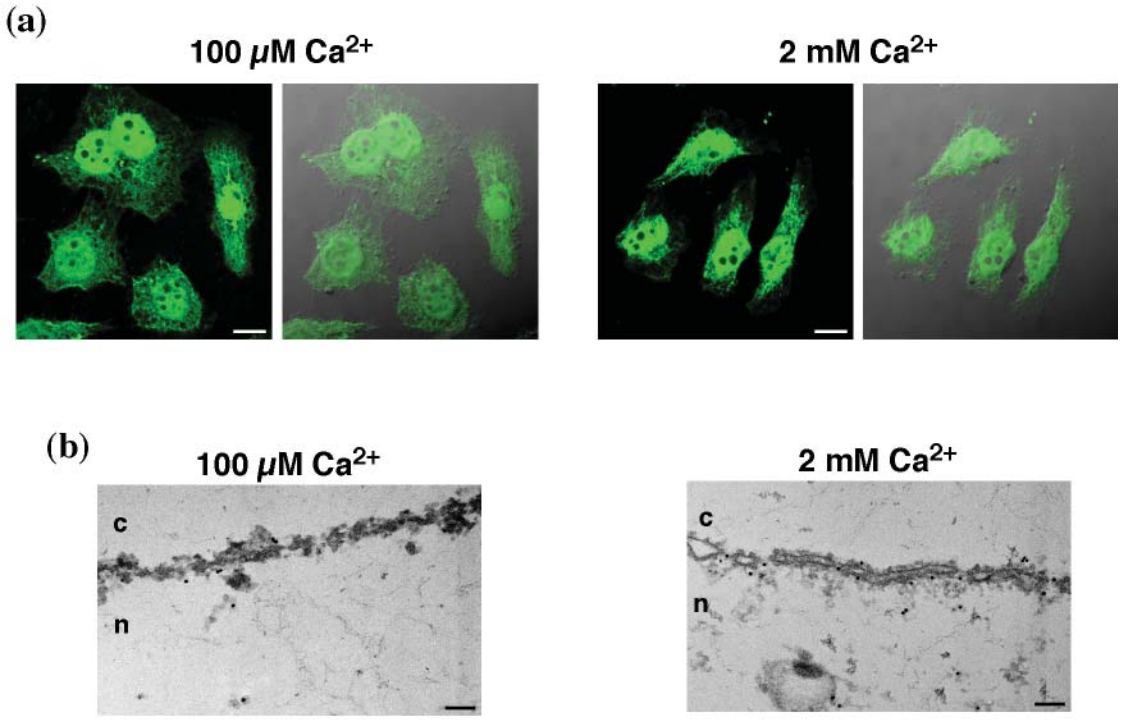

Figure S3.2: Influence of extranuclear calcium on the nuclear import of nucleoplasmin. (a) Digitonin permeabilized HeLa cells were incubated for 10 minutes with 100 µM Ca^{2+} and 2 mM Ca^{2+}, respectively, prior to incubation in an import-competent cytosolic mixture containing 100 nm nucleoplasmin-GFP for 30 minutes. Shown are confocal sections through the midplane of the nucleus as well as coincident fluorescence differential interference contrast images. (b) Isolated *Xenopus* oocyte nuclei were incubated for 10 minutes with 100 µM Ca^{2+} and 2 mM Ca^{2+}, respectively, prior to incubation in an import-competent cytosolic mixture containing nucleopplasmin-GFP conjugated to 8-nm colloidal gold for 30 minutes. Shown are stretches along the nuclear envelope. c, cytoplasm; n, nucleus. Scale bars, (a) 10 µm., (b) 100 nm.

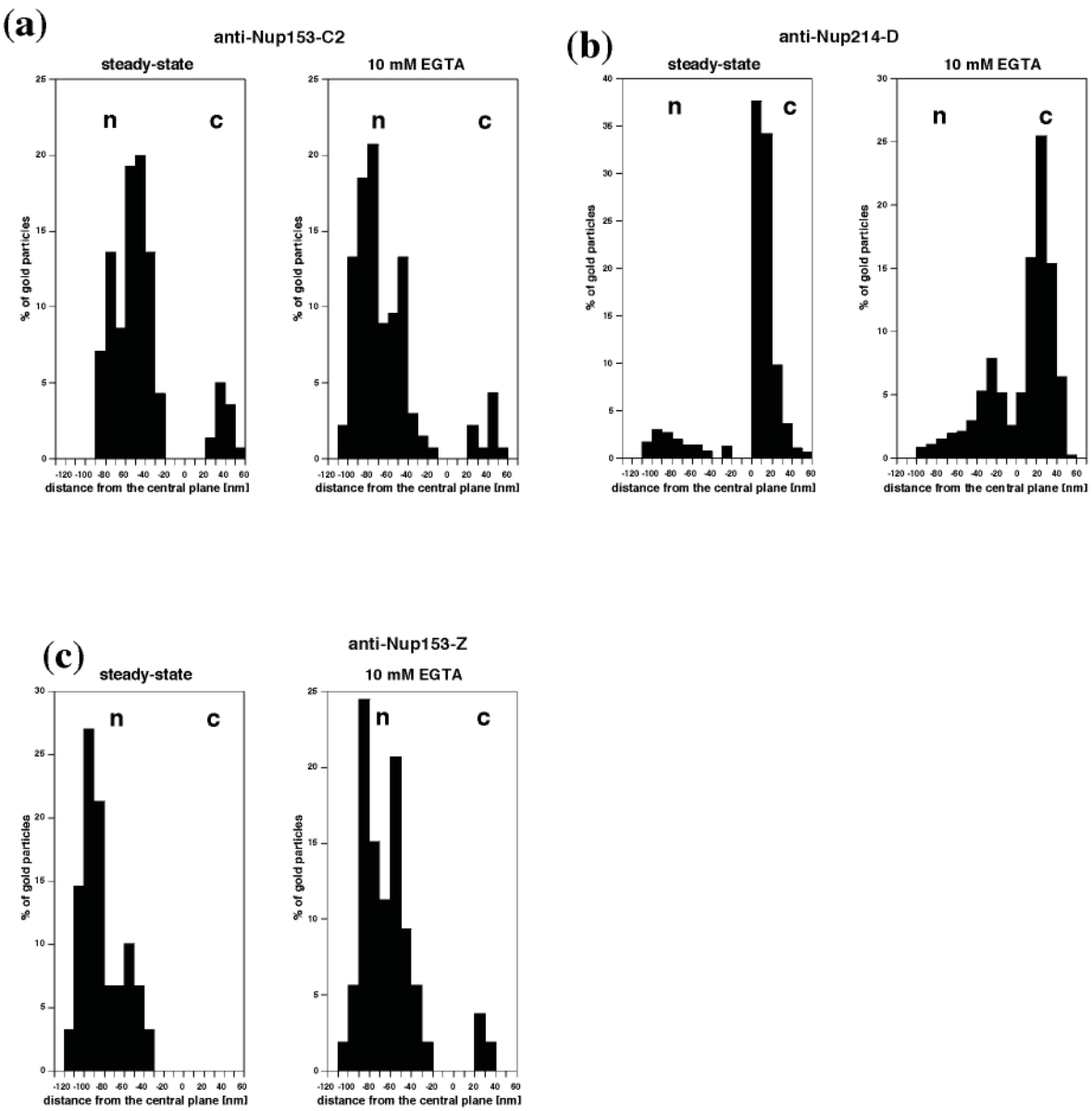

Figure S3.3: Quantification of the gold particle distribution associated with the NPC after incubation of isolated *Xenopus* oocyte nuclei in low salt buffer containing 10 mM EGTA to deplete luminal calcium stores and labelling with (a) an antibody against the FG-repeat domain of Nup153 (anti-Nup153-C2), (b) an antibody against the FG-repeat domain of Nup214, and (c) the zinc-finger domain of Nup153. The following numbers of gold particles were scored for the individual experiments: 135 (anti-Nup153-C2, 10 mM EGTA), 467 (anti-Nup214-D, 10 mM EGTA), 53 (anti-Nup153-Z, 10 mM EGTA). Steady-state values are as shown in Figure 1 and are included here for reference.

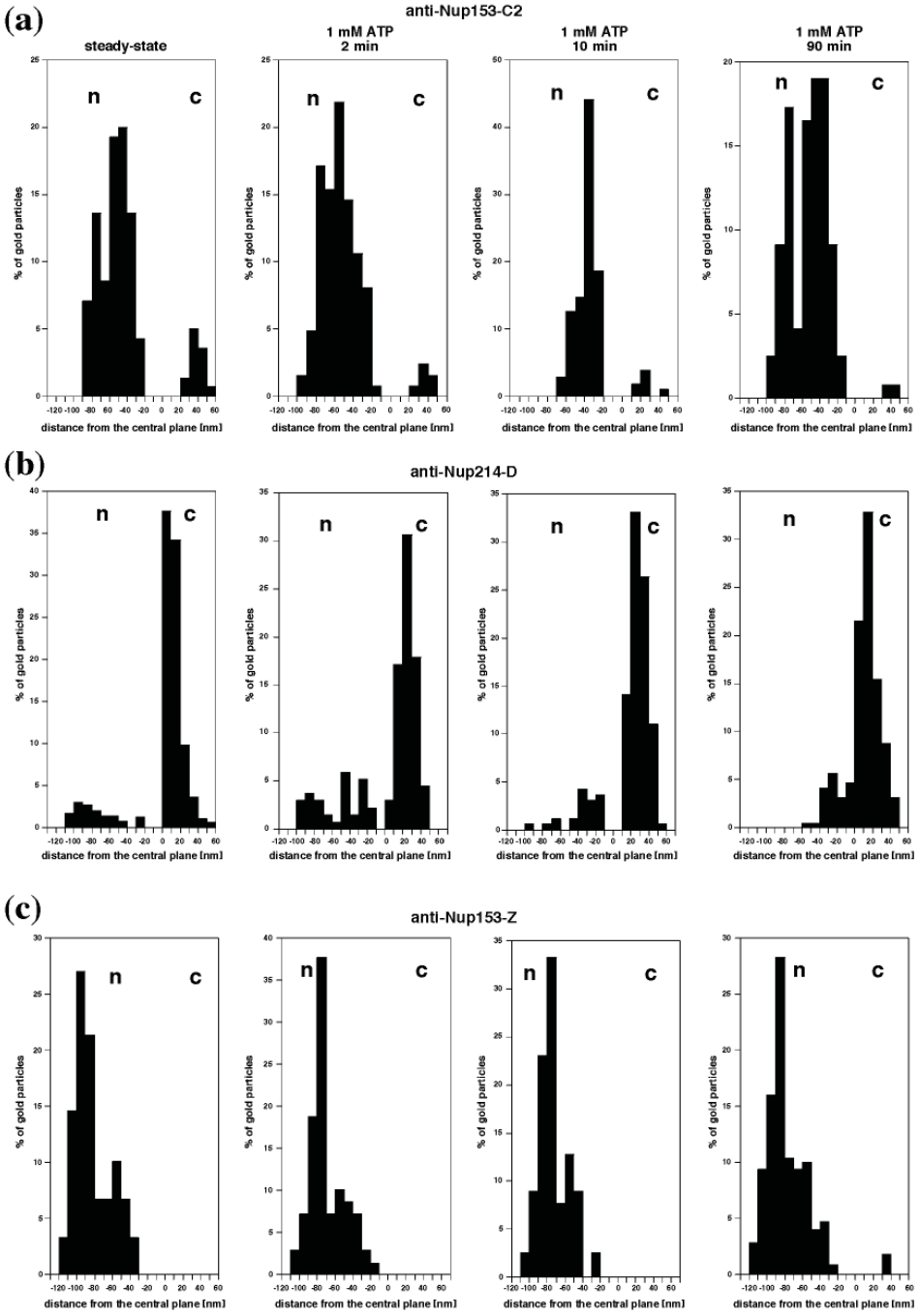

Figure S3.4: ATP and its influence on the domain topology of Nup153 and Nup214. Quantitative analysis of gold particles associated with the NPC after labelling with (a) the anti-Nup153-C2 antibody, (b) the anti-Nup214-D antibody, and (c) the anti-Nup153-Z antibody. Isolated intact *Xenopus* nuclei were incubated in low salt buffer containing 1 mM ATP for the indicated time-points before nuclei were shortly fixed and pre-embedding labelled with the corresponding antibodies. The following numbers of gold particles were scored for the individual experiments: 123 (anti-Nup153-C2, 2 minutes), 150 (anti-Nup153-C2, 10 minutes), 121 (anti-Nup153-C2, 90 minutes), 134 (anti-Nup214-D, 2 minutes), 163

(anti-Nup214-D, 10 minutes), 195 (anti-Nup214-D, 90 minutes), 69 (anti-Nup153-Z, 2 minutes), 78 (anti-Nup153-Z, 10 minutes), 106 (anti-Nup153-Z, 90 minutes). Steady-state values are as shown in Figure 1 and are included here for reference.

Appendix 2

Curriculum Vitae

SARA MARIA PAULILLO
Lothringerstrasse 23
4056 Basel, Switzerland
+41 79 5425250
sara.paulillo@unibas.ch

EDUCATION

Ph.D. student, Cell Biology, 2003-2006

Biozentrum – University of Basel, Basel, Switzerland

Oral examination: November 23, 2006.

Dissertation: "Analysis of the Functional Role of Nucleoporin Nup214 in Nuclear Transport and Other Cellular Processes"

Committee members: Chair Prof. Dr. Ueli Aebi, PD Dr. Birthe Fahrenkrog, Prof. Dr. Olga Mayans and Prof. Dr. Urs Greber

M.Sc. Chemistry, Department of Biological Chemistry, 1998

University of Campinas, Campinas, SP - Brazil

Thesis: "Biodegradation of Pesticides and soil remediation"

Committee members: Prof. Dr. Nelson Duran, Dr. Gilson P. Manfio, and Dr. Elisa Esposito.

PROFESSIONAL EXPERIENCE

Research

Ph.D. student, Biozentrum - University of Basel, Basel, Switzerland, 2003 – 2006

Supervisor: PD Dr. Birthe Fahrenkrog

Teaching

Fluorescence Microscopy Course – Microscopy Block Course for Biology and Nanosciences students, Biozentrum, University of Basel, Basel, 2003-2006.

Internships

"Development of new methods for identification of viscotoxins and triterpenes", Carl Gustav Carus Institut, Niefern-Öschelbronn, BW, Germany 1999-2000.

- Preparative and analytical high-performance liquid chromatographic (HPLC) methods in the resolution and analysis of organic compounds, enzymatic determination and protein purification.

"Organic synthesis of nonsteroidal anti-inflammatory drugs (NSAIDs) intermediates", Novartis Pharma AG (Chemical & Analytical Development), Basel, Switzerland, 1999

- Synthesis of COX-2 intermediates and confirmation of structure by TLC, GPC, HPLC, IR, NMR, MS.

Other Professional Experience

Research Associate, Novartis Pharma AG (Biotechnology Development), Basel, Switzerland, 2001-2002.

- Development of automated fluorescence microscopy software and hardware: microscope components, liquid handling and staining system.

Project Assistant, Pharmaplan AG, Basel, Switzerland, 2000-2001.

- Development of relational databases in Visual Basic, consulting project administration, notions in sterile process validation and qualification.

Quality Control Technician, Prodesa S.A., Campinas, SP, Brazil, 1992-1995.

- Chemical analysis from residual wastewater, chemical and microbiological control on yeast fermentation processes.

Microbiology Lab Technician, Fundação Tropical de Pesquisas e Tecnologia "André Tosello", Campinas, SP, Brazil, 1990-1992.

- Preservation of microorganisms, biochemical tests for the identification of bacteria.

Quality Control Technician, Pepsico & Cia, Itu, SP, Brazil, 1989

- Production line and chemical quality control.

Publications

1. **Paulillo SM** and Fahrenkrog B. "The Nuclear Pore Complex: From Higher Eukaryotes To Plants", *Book Running Title: "Current Research in Plant Cell Compartments"*, Editor: Schoefs, B., Research Signpost, 2006, Submitted.

2. **Paulillo SM**, Powers MA, Ullman KS, Fahrenkrog B. "Changes in nucleoporin domain topology in response to chemical effectors", *J Mol Biol. 2006 Oct 13;363(1):39-50*. PMID: 16962132.

3. Lill Y, Lill MA, Fahrenkrog B, Schwarz-Herion K, **Paulillo S**, Aebi U, Hecht B. "Single Hepatitis-B virus core capsid binding to individual nuclear pore complexes in HeLa cells", *Biophys J. 2006 Jul 28;* PMID: 16877503

4. **Paulillo SM**, Phillips EM, Koser J, Sauder U, Ullman KS, Powers MA, Fahrenkrog B. "Nucleoporin domain topology is linked to the transport status of the nuclear pore complex", *J Mol Biol. 2005 Aug 26;351(4):784-98*. PMID: 16045929.

5. Esposito E, **Paulillo SM**, Manfio GP. "Biodegradation of the herbicide Diuron in soil by indigenous actinomycetes", *Chemosphere. 1998 Aug;37(3):541-8*. PMID: 9661279

Posters

1. **"Structural Analysis of the Domain Topology of the Nucleoporin Nup214/CAN Depending on the Conformational State of the Nuclear Pore Complex"**, 45th Annual Meeting of the American Society for Cell Biology, San Francisco, USA, December 2005

2. **"Structural Analysis of the Domain Topology of the Nucleoporin Nup214/CAN with Respect to Conformational Changes of the Nuclear Pore Complex"**, EMBO/FEBS Conference on "Nuclear Structure and Dynamics", La Grande Motte, France, September 2005.

3. **"Structural Basis for Transport-Dependent Mobility of Nucleoporin FG-repeat domains"**, Cold Spring Harbor Meeting on "Dynamic Organization of Nuclear Function",

CSHL, USA, October 2004.

4. **"Structure Based Analysis of Nucleoporin FG Repeats and their Topology within the Nuclear Pore Complex"**, 4th Annual Congress ELSO, Nice, France, September 2004.

5. **"Structured-Based Analysis of Nucleoporin Function"**, 43rd Annual Meeting of the American Society for Cell Biology, San Francisco, USA, December 2003.

6. **"Structural Dissection of Nucleoporin Function"**, EMBO Workshop "Mechanisms of Nuclear Transport", Taormina, Italy, November 2003.

7. **"Potencial de um consórcio microbiano para degradação de 3-(3,4-Diclorofenil) 1,1-Dimetiluréia em solo"**. XXXVII Congresso Brasileiro de Química, Natal, RN, Brazil, 1997.

8. **"Herbicides biodegradation by endogenous bacteria"**, 1st National Meeting of Applied and Environmental Microbiology, Campinas, SP, Brazil, 1996.

9. **"Microbiological strategies on remediation of contaminated soil with organochlorides"**, 1st National Meeting of Applied and Environmental Microbiology Campinas, SP, Brazil, 1996.

Presentations

"Structural basis for transport-dependent mobility of nucleoporin FG-repeat domains", BioNano Workshop from the NCCR Nanoscale Science, Lenzerheide, Switzerland, January 2005.

Grants

Undergraduate Fellowship, ITI (Iniciação Tecnológica Industrial) CNPq-RHAE, Brazil, 1996-1997.

Memberships

Member, American Society for Cell Biology, 2005-2006.

Member, Swiss Society for Optics and Microscopy, 2005-2006.

Member, Swiss Society for Cell Biology, Molecular Biology and Genetics, 2005-2006.

Community Service

Youth Leader, Aliança Bíblica Universitária - International Fellowship of Evangelical Students, Campinas, SP, Brazil, 1996-1999.

Languages

Fluent: English, Spanish, and Portuguese (mother tongue).

Conversational: German, Italian.

Reading: German, Italian.

References

PD Dr. Birthe Fahrenkrog

Group Leader

University of Basel, Basel, Switzerland

+41 61 2671624

birthe.fahrenkrog@unibas.ch

Prof. Dr. Ueli Aebi

Director M. E. Mueller Institute for Structural Biology

University of Basel, Basel, Switzerland

+41 61 267

ueli.aebi@unibas.ch

Dr. Christian Leist

Group Head Biotechnology Development

Novartis Pharma AG, Basel, Switzerland

+41 61 6964651

christian.leist@pharma.novartis.com

Dr. Rainer Scheer

Head of Biotechnology Processes

Carl Gustav Carus Institute, Niefern-Öschelbronn, Germany

+49 7233 68418

rainer.scheer@carus-institut.de

Letters of recommendation are available upon request.

Appendix 3

Acknowledgements

Acknowledgements

I want to express my deepest gratitude to my supervisor Birthe Fahrenkrog for giving me more than a bench in the lab but the support and the understanding of what is to do serious research (as well as to write the serious research up…). “Meister” (BF) was always available, helpful and she always knew how to motivate and encourage me when I needed to get over the “straight-forward” experiments!! I also sincerely thank Ueli Aebi for giving me the chance to join the group; he is not only a great scientist but also a very generous person and an excellent boss. His advise for my future career has been of great help. I am also thankful to Dr. Urs Greber who promptly agreed to act as co-referee in my exam. Urs was very understanding during this process, specially regarding all my deadlines.

It has been lots fun to work with David Walter and Yvonne Lussi. The mix of David’s serenity and Yvonne’s joy (she is the one who makes me laugh) are a must for the progress of science in our lab. Anyway, about logistics… our side is the best side! Kyrill Schwarz-Herion is probably our lab’s most interested scientist in the diverse available techniques and subjects in cell biology. I learned with him to consider that the “new” can be applicable. I am also happy to add Esther Owsianowski. It has been so little time you joined us but it is really good to have you here.

When it comes to research, the need of new inspiring ideas is absolutely necessary. In addition, you need the right riverfront to hang out with the right people. The members of the “Cargobarverein” shared with me a bit of their ideas and knowledge. Special thanks to Joachim Koeser and Roderick Y. H. Lim for their help and to make me think about their questions. Jocheli patiently introduced to me the secrets and surprises of molecular and cell biology. He was “the answer giver” for most of the questions I had in biology (as for the other questions… hummm). Rod’s enthusiasm regarding science is remarkable! My best regards to Rod and Cindy as the birth of their baby is coming soon…

The excellent technical contribution of Ursula Sauder and Vesna Olivieri was much appreciated. Many times they had to use their imagination to see the *Xenopus* oocyte nuclei in the embedded sample. Thanks to Cora Schoenenberger’s help with immunofluorescence and cell culture. Many thanks go to Ulrich Schroeder for the partnership in organizing the fluorescence microscopy block course for the undergraduate students. Markus Dürrenberger (MaDü) was always prompt to help when I had problems with the confocal microscope. In addition, Marku’s sense of humor and patience are highly appreciated. Thanks!

I am deeply indebted to Laurent Kreplak and Eleonore von Castelmur for their friendship. Laurent’s multiple skills include metacognition, politeness but more importantly he has a

huge heart. Elli is the one who comforts others when life is getting “grey” to avoid them to get “lost”. Her care and empathy enormously supported me in difficult times. The time we spent together was not only quantity but quality time and it is a privilege to have her as a friend.

Another friend I would like to thank is Pilar Garcia. Her vivid temper and depth of passion were highly appreciated by me and many of us miss her a lot.

I would like to say a big “thank you” to the friends Bohumil Maco (Bohusli) and Miroslava Macová (Mirka). More precious are the ones that listen than the ones that actively make use of their verbosity!!

Two guys who always were cheering me up: Pernille Jensen and Sebastian Meier. The news was always updated and we had lots of good laughs! I wish you lots of success in Copenhagen.

The long hiking trips were more enjoyable in the company of Carmen Chan and Martin Allan. After 7 hours walking, suddenly we started to sing: “the hills are alive with the sound of music” or “wen-i nume wüsst, wo ds Vogu-Lisi wär. ds Vogu-Lisi chunnt vo Adelbode här”…

I am grateful to the excellent technical support from Robert Wyss (Mech-Röbbi), Robert Häring (El Röbbi), Rosmarie Suetterlin, Liselotte Walti, Debbie Meyer, Roland Buerki and Margrit Jenny. Our lives in the Biozentrum would be much more difficult if you were not there to help us.

I cannot forget to mention here the dynamic cleaning ladies Clara and Emilia, thanks also for helping me to acquire some Iberian Portuguese. Obrigada! I wish also to thank Barbara and Filomena for autoclaving my medium and biological waste. Thanks for helping me with that. Danke schön/Grazie mille! I want to include here the “Mayans”, “Schirmers”, “Grzesieks” and “Engels”: Zöhre and Dimi, Olga, Kitaru, Fabio, Navratna, Arnaud, Caroline, etc. Thank you for the good time at the Biozentrum’s 3rd floor! Thanks to all “Aebis” as well: Martin Stolz & Co., the intermediate filament guys and the crystallographers!

Additional strength and vitality for this research was acquired at the Tuesdays praying meetings from the Basel Christian Fellowship. I cannot express how grateful I am to Nils and Mary Blom for their constant expression of affection and respect towards me. I am also grateful to the Stampflis for their care! My friends from the Brazilian Baptist Church in Basel also encouraged me a lot, I am lucky to have you here.

Irene Montaño (Muchacha) and Marina Tavares are also part of this process. It is superb to have friends that challenge us with questions with don't come with easy answers.

My sincere thanks to my good friends Elizete Lima (Zazá) and Carla Avila. They always inspired me and shared with me their precious thoughts about fundamental questions in life such as "where do I belong?"

I wish God's blessings upon Aluísio and Aline as they start to raise a new family. Many thanks for giving me the opportunity to participate in this process. I greatly appreciated the period of time that Livia Miranda (Lili) and I had here in Basel. I also want to acknowledge Suely and Adolfo Sperling for the spectacular conversations we always had.

Many professors and friends from UNICAMP (Campinas State University, Brazil) could not be let out of this acknowledgement. However, I will limit my thanks to Prof. Marcia Ferreira, Prof. Renato Atilio, Carolina Gama, Sandra Krauchenco, Ataualpa A.C. Braga and the ABUB friends.

I am very grateful to Rainer and Regina Scheer for their sincere friendship all these years. Thanks so much for all your help and encouragement.

I felt very welcome in Switzerland and this is also my country now. I found here a spectacular family that cared and loved me during these years. My "mami" Christa Felix (Christeli) offered her love, care and support throughout these years. This is unforgettable! Thanks also to my Swiss "papi" Ernst Roggensinger and his wife Mariete, also thank you Marthe and Ruedi Frey.

Now, I feel indeed blessed to have a family like mine. My mom (*in memoriam*) was an example of strenght and persistence, I learned from her that one should never give up. My dad José Rivetto can be "a piece of art" as result of his simplicity! I love to chat with my sister Elza M.J. Rivetto Ferreira, despite the huge phone bill, we kept our intense relationship always alive. My brother-in-law Evaldo Ferreira is known for demonstrate his cheerfulness wherever he is. Elza and Evaldo's reverence and close fellowship with the Lord are awesome. Their love and support cannot be properly described here. My deepest and sincere gratitude! Amo vocês!

Finally, "To Him who sits on the throne and to the Lamb, be praise and honor and glory and power, forever and ever! (Revelation 5:13b)."